Associação Instituto Nacional de Matemática Pura e
Aplicada - IMPA-OS

ESCOAMENTOS FRICCIONAIS DO AR

Paul Krause

Tese apresentada para a obtenção do grau de
Doutor em Ciências

Rio de Janeiro
1º de Julho de 2002

RESUMO

Propomos um modelo para a previsão em baixa resolução da evolução de escoamentos na grande escala. O modelo representa um levantamento estatístico das equações de Euler em um mecanismo de equilíbrio local que satisfaz o princípio da conservação da energia total e é fenomenologicamente estendido para capturar efeitos viscosos de massa.

Propomos um modelo para a previsão em baixa resolução da evolução de escoamentos na grande escala. O modelo representa um levantamento estatístico das equações de Euler em um mecanismo de equilíbrio local que satisfaz o princípio da conservação da energia total e é fenomenologicamente estendido para descrever processos irreversíveis nas transformações de tempo finito de grandes massas de fluido. Testamos a descrição qualitativa unidimensional que o modelo faz dos escoamentos planares de Couette e Poiseuille, e dos escoamentos de Ekman.

Palavras-chave: dinâmica dos fluidos, multi-escalas, levantamento estatístico

Aos meus pais,

exímios em paciência, disposição e simpatia.

À minha esposa,

especialista em força, coragem e alegria.

FRICTIONAL AIR FLOWS

P. KRAUSE

Contents

1. Introduction

Due to incompleteness of initial data or to limitations in storage space and processing time, the smallest scales cannot be resolved in computer simulations of real flows. Since all involved scales interact, underresolved simulations of real flows frequently have poor predictive value. This is the case with frictional flows.

We are looking for a model that yields fair predictions of the large scale evolution of flows without the need to resolve the smallest scales, that is, a model for underresolved predictions of the large scale evolution of flows. Our approach is to "Reynolds

average" the Euler equations. Currently, "Reynolds averaging" is regarded as a modelling approach to describe the statistical mean values of the flow variables together with a finite subset of their joint central moments conveniently chosen in each problem. Here, instead, we regard it as a modelling approach to describe local balances of $\langle\rho\rangle\langle\phi\rangle$ and of $\langle\rho'\phi'\rangle$, for any flow variable ϕ built upon the fluid density ρ, so as to provide a statistical upscaling of $\rho\phi$ into $\langle\rho\phi\rangle = \langle\rho\rangle\langle\phi\rangle + \langle\rho'\phi'\rangle$. Therefore, we split each "Reynolds averaged" Euler equation into a pair of local statistical balance equations. By doing so we obtain two coupled mechanisms: a reversible "bulk" mechanism of large scales and an irreversible "turbulence" mechanism for the small scales effects on the large scales. Then, we close the turbulence mechanism so as to satisfy the total energy conservation principle in the upscaled description. Finally, we extend the reversible bulk mechanism to an irreversible bulk mechanism by means of molecular viscosities, following the linear thermodynamic phenomenological approach for irreversible processes ([7, 10]). This gives rise to the Extended Upscaled Euler model (EUE).

Among the features of EUE, we mention: it is an extension of the compressible Navier-Stokes model (see Eqs. (2.70)–(2.76) and Remark 6); it can be derived from the Euler equations either in material derivative or flux form (see Remark 1); the closure assumptions apply to both the enthalpy and the internal energy representations of heat balance (see Remark 2); its total energy is governed by a conservation law (see Eq. 3.18); the pressure gradient arises as an affinity ([7, 11]) of the entropy source term in the upscaled description (see Eq. (3.22)); the turbulence mechanism has a curl formulation (see Eq. 2.64); the model can be readily extended to comprise a compressible turbulent mixing mechanism for passive species (see Eqs. (5.1)–(5.2)).

Based on experimental studies of transition to turbulence in pipe flows, Reynolds (1883) proposed to describe such flows by superposing mean and perturbation fields. Considering the perturbation fields as unpredictable, he time-averaged the Navier-Stokes equations and arrived at the so called Reynolds averaged Navier-Stokes (RANS) equations. This view of turbulence encouraged further observations of flows under various averagings, leading to significant development in instrumentation (hot-wire anemometry, laser-Doppler velocimetry etc). Because the statistical average is appropriate, this view of turbulence is bolstered by the success of the statistical approach in several fields of theoretical physics, especially the statistical mechanics approach to the kinetic theory of gases. There is an extensive body of literature on turbulence within the statistical framework. The works of Taylor, von Karman, Heisenberg, Kolmogoroff, Loitsianskii and Kraichnan must be mentioned. The books of McComb ([14]) and Frisch ([9]) summarize the legacy of these works. We refer to [2, 15] for several current practical issues and models, to [20, 12] for several current physical issues and models, to [4, 5, 6] for current stochastic methods

in underresolved predictions.

The Large Eddy Simulation (LES), introduced by Deardorff, uses space or time-filtering to compute flow features down to a certain space or time scale. For an overview on LES, we refer to [18].

In Chapter 2 we derive the EUE model. In Chapter 3 we find the evolution laws for the total energy and the entropy in the upscaled description resulting from EUE. In Chapter 4, regarding ρ' as a thermodynamical quantity that vanishes identically only in a static state, we test the energy transfer mechanism of EUE in the context of stationary one-dimensional solutions for the Couette and Poiseuille frictional flows between planar plates, by checking the qualitative behavior of the resulting profiles and the qualitative behavior of the entropy source term in the upscaled description. The Ekman frictional flows are examined briefly in Appendix A. In Chapter 5 we draw the conclusions.

2. REYNOLDS MODELLING

2.1. **The open Upscaled Euler model.** Under a gravitational field $\mathbf{g}_0$ and in a coordinate system rotating with constant angular velocity $\mathbf{\Omega}$, the Euler model reads:

$$\text{enthalpy:} \qquad \rho d_t h = d_t p, \qquad (2.1)$$

$$\text{momentum:} \qquad \rho d_t \mathbf{u} = \rho \mathbf{u} \times 2\mathbf{\Omega} + \rho \mathbf{g} - \nabla p, \qquad (2.2)$$

$$\text{mass:} \qquad d_t \rho = -\rho \nabla \cdot \mathbf{u}, \qquad (2.3)$$

$$\text{state:} \qquad \kappa \rho h = p, \qquad (2.4)$$

where h is the enthalpy per unit mass, $\mathbf{u} \times 2\mathbf{\Omega}$ is the Coriolis acceleration, $\mathbf{g} \equiv \mathbf{g}_0 + \mathbf{\Omega} \times (\mathbf{\Omega} \times \mathbf{x})$ is the apparent gravitational field and $d_t \equiv \partial_t + (\mathbf{u} \cdot \nabla)$ is the material derivative. We adopt the ideal gas state equation with constant c_p, therefore $h = c_\mathrm{p} T$ ([21]). In (2.4), κ denotes $R/c_\mathrm{p} = (c_\mathrm{p} - c_\mathrm{v})/c_\mathrm{p} = 1 - 1/\gamma$.

We remind that the statistical average $\langle \cdot \rangle$ of random functions is a linear transformation possessing the properties:

$$\langle 1 \rangle = 1, \qquad (2.5)$$

$$\langle \partial_s f \rangle = \partial_s \langle f \rangle \quad \text{for} \quad s = x, y, z, t, \qquad (2.6)$$

$$\langle f_1 \langle f_2 \rangle \rangle = \langle f_1 \rangle \langle f_2 \rangle. \qquad (2.7)$$

The following relations follow from (2.5)–(2.7) together with linearity:

$$\langle \langle f \rangle \rangle = \langle f \rangle, \qquad (2.8)$$

$$\langle f' \rangle = 0, \qquad (2.9)$$

$$\langle f_1 f_2 \rangle = \langle f_1 \rangle \langle f_2 \rangle + \langle f_1' f_2' \rangle, \qquad (2.10)$$

where

$$f' \equiv f - \langle f \rangle \text{ is the deviation of } f \text{ with respect to its bulk value } \langle f \rangle. \qquad (2.11)$$

Here, (2.8) comes from (2.5) and (2.7); (2.9) comes from (2.8), the definition of f' and the linearity of $\langle \cdot \rangle$; (2.10) comes from (2.5), (2.7), (2.8), (2.9) and the linearity of $\langle \cdot \rangle$.

In the following sections, we split each statistically averaged Euler equation into a pair of local statistical balance equations.

2.1.1. *The local statistical balance equations of enthalpy.* Applying $\langle \cdot \rangle$ on Eq. (2.1), we use the linearity of this operator to write $\langle \rho d_t h \rangle$ as $\langle \rho d_t \langle h \rangle \rangle + \langle \rho d_t h' \rangle$ and $\langle d_t p \rangle$ as $\langle d_t \langle p \rangle \rangle + \langle d_t p' \rangle$. Then, we split the statistically averaged enthalpy equation into the following two local balance equations:

$$\langle \rho d_t \langle h \rangle \rangle = \langle d_t \langle p \rangle \rangle, \qquad (2.12)$$

$$\langle \rho d_t h' \rangle = \langle d_t p' \rangle. \qquad (2.13)$$

Next, we use the mass conservation equation (2.3) and the properties of $\langle \cdot \rangle$ to transform Eqs. (2.12)–(2.13) into evolution laws. The flux version of (2.3) yields

$$\langle \langle h \rangle (\partial_t \rho + \nabla \cdot (\mathbf{u} \rho)) \rangle = 0, \qquad (2.14)$$

$$\langle h' (\partial_t \rho + \nabla \cdot (\mathbf{u} \rho)) \rangle = 0. \qquad (2.15)$$

Adding (2.14) to (2.12) and (2.15) to (2.13), we use the linearity of $\langle \cdot \rangle$ to write:

$$\langle \rho d_t \langle h \rangle \rangle = \langle \rho d_t \langle h \rangle \rangle + \langle \langle h \rangle (\partial_t \rho + \nabla \cdot (\mathbf{u} \rho)) \rangle = \langle \partial_t (\rho \langle h \rangle) + \nabla \cdot (\mathbf{u} \rho \langle h \rangle) \rangle,$$

$$\langle \rho d_t h' \rangle = \langle \rho d_t h' \rangle + \langle h' (\partial_t \rho + \nabla \cdot (\mathbf{u} \rho)) \rangle = \langle \partial_t (\rho h') + \nabla \cdot (\mathbf{u} \rho h') \rangle.$$

Then, by applying properties (2.5)–(2.10) on each right hand side we obtain the identities:

$$\langle \rho d_t \langle h \rangle \rangle = \partial_t (\langle \rho \rangle \langle h \rangle) + \nabla \cdot (\langle \mathbf{u} \rangle \langle \rho \rangle \langle h \rangle + \langle \rho' \mathbf{u}' \rangle \langle h \rangle), \qquad (2.16)$$

$$\langle \rho d_t h' \rangle = \partial_t \langle \rho' h' \rangle + \nabla \cdot (\langle \mathbf{u} \rangle \langle \rho' h' \rangle + \langle \rho \mathbf{u}' h' \rangle). \qquad (2.17)$$

Properties (2.5)–(2.10) also yield the identities:

$$\langle d_t \langle p \rangle \rangle = \partial_t \langle p \rangle + \langle \mathbf{u} \rangle \cdot \nabla \langle p \rangle, \qquad (2.18)$$

$$\langle d_t p' \rangle = \langle \mathbf{u}' \cdot \nabla p' \rangle. \qquad (2.19)$$

Therefore, taking (2.16)–(2.19) into account, Eqs. (2.12)–(2.13) read:

$$\partial_t (\langle \rho \rangle \langle h \rangle - \langle p \rangle) + \nabla \cdot (\langle \mathbf{u} \rangle (\langle \rho \rangle \langle h \rangle - \langle p \rangle) + \langle \rho' \mathbf{u}' \rangle \langle h \rangle) = -\langle p \rangle \nabla \cdot \langle \mathbf{u} \rangle, \qquad (2.20)$$

$$\partial_t \langle \rho' h' \rangle + \nabla \cdot (\langle \mathbf{u} \rangle \langle \rho' h' \rangle + \langle \rho \mathbf{u}' h' \rangle) = \langle \mathbf{u}' \cdot \nabla p' \rangle. \qquad (2.21)$$

2.1.2. *The local statistical balance equations of momentum.* Applying $\langle\,\cdot\,\rangle$ on Eq. (2.2), we write $\langle\rho d_t\mathbf{u}\rangle$ as $\langle\rho d_t\langle\mathbf{u}\rangle\rangle + \langle\rho d_t\mathbf{u}'\rangle$, expand $\langle\rho\mathbf{u}\times 2\mathbf{\Omega}\rangle$ into $\langle\rho\rangle\langle\mathbf{u}\rangle\times 2\mathbf{\Omega} + \langle\rho'\mathbf{u}'\rangle\times 2\mathbf{\Omega}$ and expand $\langle\rho\mathbf{g}-\nabla p\rangle$ into $\langle\rho\rangle\mathbf{g}-\nabla\langle p\rangle$. Then, we split the statistically averaged momentum equation into the following two local balance equations:

$$\langle\rho d_t\langle\mathbf{u}\rangle\rangle = \langle\rho\rangle\langle\mathbf{u}\rangle\times 2\mathbf{\Omega} + \langle\rho\rangle\mathbf{g}-\nabla\langle p\rangle, \tag{2.22}$$

$$\langle\rho d_t\mathbf{u}'\rangle = \langle\rho'\mathbf{u}'\rangle\times 2\mathbf{\Omega}. \tag{2.23}$$

Next, by using the mass conservation equation (2.3) and the properties of $\langle\,\cdot\,\rangle$ we transform Eqs. (2.22)–(2.23) into evolution laws:

$$\partial_t(\langle\rho\rangle\langle\mathbf{u}\rangle) + \partial_j(\langle u_j\rangle\langle\rho\rangle\langle\mathbf{u}\rangle + \langle\rho'u_j'\rangle\langle\mathbf{u}\rangle) = \langle\rho\rangle\langle\mathbf{u}\rangle\times 2\mathbf{\Omega} + \langle\rho\rangle\mathbf{g}-\nabla\langle p\rangle, \tag{2.24}$$

$$\partial_t\langle\rho'\mathbf{u}'\rangle + \partial_j(\langle u_j\rangle\langle\rho'\mathbf{u}'\rangle + \langle\rho u_j'\mathbf{u}'\rangle) = \langle\rho'\mathbf{u}'\rangle\times 2\mathbf{\Omega}. \tag{2.25}$$

2.1.3. *The local statistical mass conservation equations.* Applying $\langle\,\cdot\,\rangle$ on Eq. (2.3), we write $\langle d_t\rho\rangle$ as $\langle d_t\langle\rho\rangle\rangle + \langle d_t\rho'\rangle$ and expand $\langle\rho\nabla\cdot\mathbf{u}\rangle$ into $\langle\rho\rangle\nabla\cdot\langle\mathbf{u}\rangle + \langle\rho'\nabla\cdot\mathbf{u}'\rangle$. Then, we split the statistically averaged mass conservation equation into the following two local balance equations:

$$\langle d_t\langle\rho\rangle\rangle = -\langle\rho\rangle\nabla\cdot\langle\mathbf{u}\rangle, \tag{2.26}$$

$$\langle d_t\rho'\rangle = -\langle\rho'\nabla\cdot\mathbf{u}'\rangle. \tag{2.27}$$

Next, we expand $\langle d_t\langle\rho\rangle\rangle$ and $\langle d_t\rho'\rangle$ to obtain:

$$\partial_t\langle\rho\rangle + \nabla\cdot(\langle\mathbf{u}\rangle\langle\rho\rangle) = 0, \tag{2.28}$$

$$\nabla\cdot\langle\rho'\mathbf{u}'\rangle = 0. \tag{2.29}$$

2.1.4. *The open Upscaled Euler model.* Collecting Eqs. (2.20)–(2.21), (2.24)–(2.25) and (2.28)–(2.29), we are led to the open Upscaled Euler model:

bulk mechanism

$$\partial_t(\rho h - p) + \nabla\cdot(\mathbf{u}(\rho h - p) + \boldsymbol{\chi}\rho h) = -p\nabla\cdot\mathbf{u}, \tag{2.30}$$

$$\partial_t(\rho\mathbf{u}) + \partial_j(u_j\rho\mathbf{u} + \chi_j\rho\mathbf{u}) = \rho\mathbf{u}\times 2\mathbf{\Omega} + \rho\mathbf{g}-\nabla p, \tag{2.31}$$

$$\partial_t\rho + \nabla\cdot(\mathbf{u}\rho) = 0; \tag{2.32}$$

turbulence mechanism

$$\partial_t(\rho\zeta) + \nabla\cdot(\mathbf{u}\rho\zeta + \langle\rho\mathbf{u}'h'\rangle) = \langle\mathbf{u}'\cdot\nabla p'\rangle, \tag{2.33}$$

$$\partial_t(\rho\boldsymbol{\chi}) + \partial_j(u_j\rho\boldsymbol{\chi} + \langle\rho u_j'\mathbf{u}'\rangle) = \rho\boldsymbol{\chi}\times 2\mathbf{\Omega}, \tag{2.34}$$

$$\nabla\cdot(\boldsymbol{\chi}\rho) = 0; \tag{2.35}$$

state equation

$$\kappa\rho(h+\zeta) = p. \tag{2.36}$$

where

$$\zeta \equiv \langle \rho' h' \rangle / \langle \rho \rangle, \tag{2.37}$$

$$\boldsymbol{\chi} \equiv \langle \rho' \mathbf{u}' \rangle / \langle \rho \rangle, \tag{2.38}$$

$$\langle \, \cdot \, \rangle \text{ is omitted from } \langle h \rangle, \langle \mathbf{u} \rangle, \langle \rho \rangle, \langle p \rangle. \tag{2.39}$$

Remark 1. *The open Upscaled Euler model can also be derived from the Euler equations in flux form: one uses the linearity of $\langle \, \cdot \, \rangle$ to write*

$$\langle \partial_t(\rho h) + \nabla \cdot (\mathbf{u}\rho h) \rangle \quad as \quad \langle \partial_t(\rho \langle h \rangle) + \nabla \cdot (\mathbf{u}\rho \langle h \rangle) \rangle + \langle \partial_t(\rho h') + \nabla \cdot (\mathbf{u}\rho h') \rangle,$$

$$\langle \partial_t(\rho \mathbf{u}) + \partial_j(u_j \rho \mathbf{u}) \rangle \quad as \quad \langle \partial_t(\rho \langle \mathbf{u} \rangle) + \partial_j(u_j \rho \langle \mathbf{u} \rangle) \rangle + \langle \partial_t(\rho \mathbf{u}') + \partial_j(u_j \rho \mathbf{u}') \rangle,$$

$$and \quad \langle \partial_t \rho + \nabla \cdot (\mathbf{u}\rho) \rangle \quad as \quad \langle \partial_t \langle \rho \rangle + \nabla \cdot (\mathbf{u}\langle \rho \rangle) \rangle + \langle \partial_t \rho' + \nabla \cdot (\mathbf{u}\rho') \rangle$$

before splitting the averaged equations.

2.2. **The closed Upscaled Euler model.** The terms $\langle \mathbf{u}' \cdot \nabla p' \rangle$, $\langle \rho \mathbf{u}' h' \rangle$ and $\langle \rho u_j' \mathbf{u}' \rangle$ in the turbulence mechanism (2.33)–(2.35) require closure.

The ideal gas state equation (2.4) yields $\langle \mathbf{u}' \kappa \rho h \rangle = \langle \mathbf{u}' p \rangle$. Applying the properties of $\langle \, \cdot \, \rangle$, this equation becomes $\kappa(\langle h \rangle \langle \rho' \mathbf{u}' \rangle + \langle \rho \mathbf{u}' h' \rangle) = \langle \mathbf{u}' p' \rangle$. Therefore, we have:

$$\langle \rho \mathbf{u}' h' \rangle = -\langle \rho' \mathbf{u}' \rangle \langle h \rangle + \langle \mathbf{u}' p' \rangle / \kappa. \tag{2.40}$$

The flux terms $\langle \rho \mathbf{u}' h' \rangle$ and $\langle \rho \mathbf{u}' u_i' \rangle$ refer to enthalpy and momentum transfers by the turbulence mechanism. According to (2.40), this transfer mechanism involves $\langle \rho' \mathbf{u}' \rangle$. Therefore, we write

$$\langle \rho \mathbf{u}' u_i' \rangle \equiv -\langle \rho' \mathbf{u}' \rangle \langle u_i \rangle + \mathrm{P}_i, \tag{2.41}$$

for some tensor $\mathrm{P} \equiv (p_{ji})$.

According to the statistical identity $\langle \rho \phi \rangle = \langle \rho \rangle \langle \phi \rangle + \langle \rho' \phi' \rangle$, the variables in the upscaled description are obtained by superposing corresponding bulk and turbulence variables. Then, taking into account (2.40)–(2.41), the evolution law for the total energy in the upscaled description resulting from Eqs. (2.30)–(2.36) is:

$$\partial_t(\rho \tfrac{1}{2}\mathbf{v}^2 + \rho \epsilon + \rho \phi) + \nabla \cdot (\mathbf{u}(\rho \tfrac{1}{2}\mathbf{v}^2 + \rho \omega) + \mathbf{v}(\rho \phi) + \mathrm{P}\mathbf{v} + \langle \mathbf{u}' p' \rangle / \kappa) = \langle \mathbf{u}' \cdot \nabla p' \rangle - \tilde{\Phi} - \boldsymbol{\chi} \cdot \nabla p,$$

where the definitions (2.37)–(2.39) are employed, and

$$\mathbf{v} \equiv \mathbf{u} + \boldsymbol{\chi}, \; \omega \equiv h + \zeta, \; \epsilon \equiv \omega - p/\rho, \; \nabla(-\phi) \equiv \mathbf{g}, \tag{2.42}$$

$$\tilde{\Phi} \equiv (\mu_c \nabla \chi_i) \cdot \nabla(u_i + \chi_i). \tag{2.43}$$

We omit the derivation of this equation because the steps are analogous to those in Section 3.1 to derive the evolution law for the total energy in the upscaled description resulting from the final model.

We want the total energy conservation principle to be satisfied in the upscaled description. Therefore, we take:

$$\langle \mathbf{u}' \cdot \nabla p' \rangle \equiv \tilde{\Phi} + \boldsymbol{\chi} \cdot \nabla p. \tag{2.44}$$

Now we consider the turbulent flux terms $\langle \mathbf{u}'p' \rangle / \kappa$ and P_i appearing in Eqs. (2.40) and (2.41). Assuming that the turbulence mechanism (2.33)–(2.35) is dissipative, we take:

$$\langle \mathbf{u}'p' \rangle / \kappa \equiv -\lambda_c \nabla \Theta, \tag{2.45}$$
$$\mathrm{P}_i \equiv -\mu_c \nabla \chi_i, \tag{2.46}$$

where

$$\Theta \equiv \langle \rho'T' \rangle / \langle \rho \rangle. \tag{2.47}$$

After closure, Eqs. (2.33)–(2.34) become:

$$\partial_t(\rho\zeta) + \nabla \cdot (\mathbf{u}\rho\zeta - \boldsymbol{\chi}\rho h - \lambda_c \nabla \Theta) = \tilde{\Phi} + \boldsymbol{\chi} \cdot \nabla p, \tag{2.48}$$
$$\partial_t(\rho\boldsymbol{\chi}) + \partial_j(u_j \rho\boldsymbol{\chi} - \chi_j \rho \mathbf{u} - \mu_c \partial_j \boldsymbol{\chi}) = \rho\boldsymbol{\chi} \times 2\boldsymbol{\Omega}. \tag{2.49}$$

Substituting Eqs. (2.33)–(2.34) by Eqs. (2.48)–(2.49), we are led to the closed Upscaled Euler (UE) model:

bulk mechanism

$$\partial_t(\rho h - p) + \nabla \cdot (\mathbf{u}(\rho h - p) + \boldsymbol{\chi}\rho h) = -p\nabla \cdot \mathbf{u}, \tag{2.50}$$
$$\partial_t(\rho\mathbf{u}) + \partial_j(u_j \rho\mathbf{u} + \chi_j \rho\mathbf{u}) = \rho\mathbf{u} \times 2\boldsymbol{\Omega} + \rho\mathbf{g} - \nabla p, \tag{2.51}$$
$$\partial_t\rho + \nabla \cdot (\mathbf{u}\rho) = 0; \tag{2.52}$$

turbulence mechanism

$$\partial_t(\rho\zeta) + \nabla \cdot (\mathbf{u}\rho\zeta - \boldsymbol{\chi}\rho h - \lambda_c \nabla \Theta) = \tilde{\Phi} + \boldsymbol{\chi} \cdot \nabla p, \tag{2.53}$$
$$\partial_t(\rho\boldsymbol{\chi}) + \partial_j(u_j \rho\boldsymbol{\chi} - \chi_j \rho \mathbf{u} - \mu_c \partial_j \boldsymbol{\chi}) = \rho\boldsymbol{\chi} \times 2\boldsymbol{\Omega}, \tag{2.54}$$
$$\nabla \cdot (\boldsymbol{\chi}\rho) = 0; \tag{2.55}$$

state equation

$$\kappa\rho(h + \zeta) = p, \tag{2.56}$$

where the definitions (2.37)–(2.39), (2.43) and (2.47) are employed.

Remark 2. *The internal energy versions of Eqs.* (2.50) *and* (2.53) *are:*

$$\partial_t(\rho e) + \nabla \cdot (\mathbf{u}\rho e + \boldsymbol{\chi}\rho e) = -p\nabla \cdot \mathbf{u}, \tag{2.57}$$
$$\partial_t(\rho\varepsilon) + \nabla \cdot (\mathbf{u}\rho\varepsilon - \boldsymbol{\chi}\rho e - \lambda_c \nabla \Theta) = \tilde{\Phi} + \boldsymbol{\chi} \cdot \nabla p. \tag{2.58}$$

Here, $\varepsilon \equiv \langle \rho' e' \rangle / \langle \rho \rangle$ (where e is the internal energy per unit mass) and $\langle \cdot \rangle$ is omitted from $\langle e \rangle$. Indeed, after applying $\langle \cdot \rangle$ on the internal energy balance equation $\rho d_t e = -p \nabla \cdot \mathbf{u}$, we split the resulting statistically averaged internal energy equation into the following two local balance equations:

$$\langle \rho d_t \langle e \rangle \rangle = -\langle p \rangle \nabla \cdot \langle \mathbf{u} \rangle, \qquad (2.59)$$

$$\langle \rho d_t e' \rangle = -\langle p' \nabla \cdot \mathbf{u}' \rangle. \qquad (2.60)$$

Then, by using the mass conservation equation (2.3) and the properties of $\langle \cdot \rangle$ we transform Eqs. (2.59)–(2.60) into the evolution laws:

$$\partial_t (\langle \rho \rangle \langle e \rangle) + \nabla \cdot (\langle \mathbf{u} \rangle \langle \rho \rangle \langle e \rangle + \langle \rho' \mathbf{u}' \rangle \langle e \rangle) = -\langle p \rangle \nabla \cdot \langle \mathbf{u} \rangle, \qquad (2.61)$$

$$\partial_t \langle \rho' e' \rangle + \nabla \cdot (\langle \mathbf{u} \rangle \langle \rho' e' \rangle + \langle \rho \mathbf{u}' e' \rangle) = -\langle p' \nabla \cdot \mathbf{u}' \rangle. \qquad (2.62)$$

Given that $\kappa \equiv R/c_{\mathrm{p}} = (c_{\mathrm{p}} - c_{\mathrm{v}})/c_{\mathrm{p}} = 1 - 1/\gamma$, $h = c_{\mathrm{p}} T$ and $e = c_{\mathrm{v}} T$, one has $p = \kappa \rho h = (\gamma - 1)\rho e$. Consequently $\langle \mathbf{u} p \rangle = \langle \mathbf{u}'(\gamma - 1)\rho e \rangle$, that is $\langle \mathbf{u}' p' \rangle = (\gamma - 1)(\langle e \rangle \langle \rho' \mathbf{u}' \rangle + \langle \rho \mathbf{u}' e' \rangle)$. Then $\langle \rho \mathbf{u}' e' \rangle = -\langle e \rangle \langle \rho' \mathbf{u}' \rangle + \langle \mathbf{u}' p' \rangle/(\gamma - 1)$. Substituting $\langle \rho \mathbf{u}' e' \rangle$ and $\langle p' \nabla \cdot \mathbf{u}' \rangle = \nabla \cdot \langle \mathbf{u}' p' \rangle - \langle \mathbf{u}' \cdot \nabla p' \rangle$ in Eq. (2.62), we obtain

$$\partial_t \langle \rho' e' \rangle + \nabla \cdot (\langle \mathbf{u} \rangle \langle \rho' e' \rangle - \langle \rho' \mathbf{u}' \rangle \langle e \rangle + \langle \mathbf{u}' p' \rangle / \kappa) = \langle \mathbf{u}' \cdot \nabla p' \rangle. \qquad (2.63)$$

Under the closure assumptions used for Eq. (2.33), equation (2.63) becomes (2.58).

Remark 3. Using the vector identity $\partial_j (u_j \rho \boldsymbol{\chi} - \chi_j \rho \mathbf{u}) = \nabla \times (\rho \boldsymbol{\chi} \times \mathbf{u})$, Eq. (2.54) also reads:

$$\partial_t (\rho \boldsymbol{\chi}) + \nabla \times (\rho \boldsymbol{\chi} \times \mathbf{u}) = \rho \boldsymbol{\chi} \times 2\boldsymbol{\Omega} + \partial_j (\mu_c \partial_j \boldsymbol{\chi}). \qquad (2.64)$$

Remark 4. For $\boldsymbol{\chi} = \mathbf{0}$ and $\Theta = 0$ identically, the Upscaled Euler model (2.50)–(2.56) reduces to the Euler model (2.1)–(2.4).

Remark 5. Landau's words ([13], §33) on L. Richardson's description (1922) of the energy transfer process in frictional flows are:

"The energy passes from large eddies to smaller ones, practically no dissipation occurring in this process. (...) This flow of energy is dissipated in the smallest eddies, where the kinetic energy is transformed into heat."

In the Upscaled Euler model (2.50)–(2.56), we interpret that the opposite sign terms $+\boldsymbol{\chi} \rho h$ and $-\boldsymbol{\chi} \rho h$ appearing in Eqs. (2.50) and (2.53) as well as $+\chi_j \rho \mathbf{u}$ and $-\chi_j \rho \mathbf{u}$ appearing in Eqs. (2.51) and (2.54) model the enthalpy and the momentum transfers between bulk and fluctuation scales; we interpret that the terms $(-\lambda_c \nabla \Theta)$, $(-\mu_c \nabla \chi_i)$ and $\tilde{\Phi}$ model mixing and dissipation at fluctuation scales.

2.3. **The Extended Upscaled Euler model.** We follow the linear thermodynamic phenomenological approach for irreversible processes ([7, 10]) to extend the

reversible bulk mechanism (2.50)–(2.52) to describing irreversible processes in finite-time transformations of bulk elements of fluid. Thus, we model the molecular conduction of bulk heat and bulk momentum by introducing the flux term $J_h \equiv -\lambda\nabla T$ in Eq. (2.50) and the flux term $J_{u_i} \equiv -\mu\nabla u_i$ in Eq. (2.51); we model the molecular dissipation of bulk kinetic energy into bulk heat by introducing a source term $\bar{\Phi}$ in Eq. (2.50). In the phenomenological approach, the dissipation term is modelled in such a way that the total energy is conserved. Here, we take $\bar{\Phi}$ in such a way that the total energy is conserved in the upscaled description.

Extending Eqs. (2.50)–(2.51) to

$$\partial_t(\rho h - p) + \nabla \cdot (\mathbf{u}(\rho h - p) + \boldsymbol{\chi}\rho h - \lambda\nabla T) = \bar{\Phi} - p\nabla \cdot \mathbf{u}, \qquad (2.65)$$
$$\partial_t(\rho\mathbf{u}) + \partial_j(u_j\rho\mathbf{u} + \chi_j\rho\mathbf{u} - \mu\partial_j\mathbf{u}) = \rho\mathbf{u} \times 2\boldsymbol{\Omega} + \rho\mathbf{g} - \nabla p, \qquad (2.66)$$

the evolution law for the total energy in the upscaled description resulting from Eqs. (2.65)–(2.66) together with Eqs. (2.52)–(2.56) is:

$$\partial_t(\rho\tfrac{1}{2}\mathbf{v}^2 + \rho\epsilon + \rho\phi) + \nabla \cdot (\mathbf{u}(\rho\tfrac{1}{2}\mathbf{v}^2 + \rho\omega) + \mathbf{v}(\rho\phi) + \mathrm{P}\mathbf{v} - \lambda\nabla T - \lambda_c\nabla\Theta) = \bar{\Phi} + \tilde{\Phi} - \Phi,$$

where the definitions (2.37)–(2.39), (2.42)–(2.43) and (2.47) are employed, and

$$\mathrm{P} \equiv (p_{ji}) \equiv -\mu\partial_j u_i - \mu_c\partial_j\chi_i, \qquad (2.67)$$
$$\Phi \equiv (\mu\nabla u_i + \mu_c\nabla\chi_i) \cdot \nabla(u_i + \chi_i). \qquad (2.68)$$

We omit the derivation of this equation because the steps are analogous to those in Section 3.1 to derive the evolution law for the total energy in the upscaled description resulting from the final model.

Thus, we take

$$\bar{\Phi} \equiv \Phi - \tilde{\Phi} = (\mu\nabla u_i) \cdot \nabla(u_i + \chi_i), \qquad (2.69)$$

so that the total energy conservation principle is satisfied in the upscaled description.

Substituting Eqs. (2.50)–(2.51) by Eqs. (2.65)–(2.66), we are led to the Extended Upscaled Euler (EUE) model:

extended bulk mechanism

$$\partial_t(\rho h - p) + \nabla \cdot (\mathbf{u}(\rho h - p) + \boldsymbol{\chi}\rho h - \lambda\nabla T) = \bar{\Phi} - p\nabla \cdot \mathbf{u}, \tag{2.70}$$

$$\partial_t(\rho\mathbf{u}) + \partial_j(u_j\rho\mathbf{u} + \chi_j\rho\mathbf{u} - \mu\partial_j\mathbf{u}) = \rho\mathbf{u} \times 2\boldsymbol{\Omega} + \rho\mathbf{g} - \nabla p, \tag{2.71}$$

$$\partial_t\rho + \nabla \cdot (\mathbf{u}\rho) = 0; \tag{2.72}$$

turbulence mechanism

$$\partial_t(\rho\zeta) + \nabla \cdot (\mathbf{u}\rho\zeta - \boldsymbol{\chi}\rho h - \lambda_c\nabla\Theta) = \tilde{\Phi} + \boldsymbol{\chi} \cdot \nabla p, \tag{2.73}$$

$$\partial_t(\rho\boldsymbol{\chi}) + \partial_j(u_j\rho\boldsymbol{\chi} - \chi_j\rho\mathbf{u} - \mu_c\partial_j\boldsymbol{\chi}) = \rho\boldsymbol{\chi} \times 2\boldsymbol{\Omega}, \tag{2.74}$$

$$\nabla \cdot (\boldsymbol{\chi}\rho) = 0; \tag{2.75}$$

state equation

$$\kappa\rho(h + \zeta) = p, \tag{2.76}$$

where the definitions (2.37)–(2.39), (2.43), (2.47) and (2.69) are employed.

Remark 6. *For $\boldsymbol{\chi} = \mathbf{0}$ and $\Theta = 0$, identically,* EUE *reduces to the compressible Navier-Stokes model.*

3. Energy laws in the upscaled description

Let $e = c_\mathrm{v}T$ be the internal energy per unit mass and $\varepsilon \equiv \langle\rho'e'\rangle/\langle\rho\rangle$. We call "upscaled variables" the following variables of the upscaled description:

ρ		mass per unit volume,	(3.1)
p		pressure,	(3.2)
$\mathcal{T}$	$\equiv T + \Theta$	temperature,	(3.3)
$\mathbf{v}$	$\equiv \mathbf{u} + \boldsymbol{\chi}$	linear momentum per unit mass,	(3.4)
ω	$\equiv h + \zeta = c_\mathrm{p}\mathcal{T}$	enthalpy per unit mass,	(3.5)
ϵ	$\equiv e + \varepsilon = c_\mathrm{v}\mathcal{T}$	internal energy per unit mass,	(3.6)
$\nabla(-\phi) \equiv \mathbf{g}$		apparent grav. potential energy per unit mass,	(3.7)

where $\langle \cdot \rangle$ is omitted from $\langle\rho\rangle$, $\langle p\rangle$, $\langle T\rangle$, $\langle\mathbf{u}\rangle$, $\langle h\rangle$, $\langle e\rangle$.

Here, by applying $\langle \cdot \rangle$ on the thermodynamic relation $\rho h = \rho e + p$ one obtains $\langle\rho\rangle\langle h\rangle + \langle\rho'h'\rangle = \langle\rho\rangle\langle e\rangle + \langle\rho'e'\rangle + \langle p\rangle$, and the following relation between upscaled variables is found:

$$\omega = \epsilon + p/\rho, \tag{3.8}$$

where $\langle \,\cdot\, \rangle$ is omitted from $\langle p \rangle$, $\langle \rho \rangle$.

In the following sections, we find the evolution laws for the total energy $(\frac{1}{2}\mathbf{v}^2+\epsilon+\phi)$ and the entropy in the upscaled description resulting from EUE. Before doing so, let us write for future use the evolution laws for the upscaled enthalpy ω and the upscaled momentum $\mathbf{v}$: we add Eq. (2.70) to Eq. (2.73) and Eq. (2.71) to Eq. (2.74), to obtain

$$\partial_t(\rho\omega - p) + \nabla \cdot (\mathbf{u}(\rho\omega - p) - \lambda\nabla T - \lambda_c\nabla\Theta) = \Phi + \boldsymbol{\chi} \cdot \nabla p - p\nabla \cdot \mathbf{u}, \qquad (3.9)$$

$$\partial_t(\rho\mathbf{v}) + \partial_j(u_j\rho\mathbf{v} - \mu\partial_j\mathbf{u} - \mu_c\partial_j\boldsymbol{\chi}) = \rho\mathbf{v} \times 2\boldsymbol{\Omega} + \rho\mathbf{g} - \nabla p, \qquad (3.10)$$

or else, by using the mass conservation equation (2.72),

$$\rho d_t(\omega - p/\rho) = \Phi + \boldsymbol{\chi} \cdot \nabla p - p\nabla \cdot \mathbf{u} + \nabla \cdot (\lambda\nabla T + \lambda_c\nabla\Theta), \qquad (3.11)$$

$$\rho d_t\mathbf{v} = \rho\mathbf{v} \times 2\boldsymbol{\Omega} + \rho\mathbf{g} - \nabla p + \partial_j(\mu\partial_j\mathbf{u} + \mu_c\partial_j\boldsymbol{\chi}), \qquad (3.12)$$

where

$$d_t \equiv \partial_t + (\mathbf{u} \cdot \nabla) \quad \text{is the upscaled material derivative.} \qquad (3.13)$$

Here, $\langle \,\cdot\, \rangle$ is omitted from $\langle \mathbf{u} \rangle$.

Remark 7. *The evolution laws for the upscaled enthalpy and the upscaled momentum can be written in either flux or material derivative form.*

Remark 8. *The evolution law for the upscaled internal energy ϵ can be obtained in either flux or material derivative form, by substituting (3.8) in Eq. (3.9) or in Eq. (3.11).*

Remark 9. *Equation (2.72) may be written $\rho d_t(1/\rho) = \nabla \cdot \mathbf{u}$, for d_t as in (3.13). Then, we have $\rho d_t(p/\rho) = \rho(d_t p\,(1/\rho) + p\,d_t(1/\rho)) = d_t p + p\nabla \cdot \mathbf{u}$. Thus (3.11) may be written as:*

$$\rho d_t\omega - d_t p = \Phi + \boldsymbol{\chi} \cdot \nabla p + \nabla \cdot (\lambda\nabla T + \lambda_c\nabla\Theta). \qquad (3.14)$$

3.1. **The total energy law in the upscaled description.** Because the potential energy ϕ is time-independent, we have

$$\partial_t(\rho\tfrac{1}{2}\mathbf{v}^2 + \rho\epsilon + \rho\phi) = (\tfrac{1}{2}\mathbf{v}^2)\partial_t\rho + \rho\partial_t(\tfrac{1}{2}\mathbf{v}^2) + \partial_t(\rho\epsilon) + \phi\partial_t\rho. \qquad (3.15)$$

Let us obtain $\partial_t(\rho\epsilon)$ and $\partial_t(\frac{1}{2}\mathbf{v}^2)$. Substituting (3.8) in the time-derivative term of Eq. (3.9) and expanding $\nabla \cdot (\mathbf{u}p)$, one readily obtains:

$$\partial_t(\rho\epsilon) = -\nabla \cdot (\mathbf{u}\rho\omega - \lambda\nabla T - \lambda_c\nabla\Theta) + \mathbf{v} \cdot \nabla p + \Phi. \qquad (3.16)$$

Taking the inner product of $\mathbf{v}$ with each member of Eq. (3.12), one has:

$$\mathbf{v} \cdot \rho d_t\mathbf{v} = \mathbf{v} \cdot (\rho\mathbf{v} \times 2\boldsymbol{\Omega} + \rho\mathbf{g} - \nabla p + \partial_j(\mu\partial_j\mathbf{u} + \mu_c\partial_j\boldsymbol{\chi})), \text{ or}$$

$$\rho\mathbf{v} \cdot (\partial_t\mathbf{v} + (\mathbf{u} \cdot \nabla)\mathbf{v}) = \mathbf{v} \cdot (\rho\mathbf{g} - \nabla p + \partial_j(\mu\partial_j\mathbf{u} + \mu_c\partial_j\boldsymbol{\chi})), \text{ or}$$

$$\rho\partial_t(\tfrac{1}{2}\mathbf{v}^2) = -\rho\mathbf{v} \cdot ((\mathbf{u} \cdot \nabla)\mathbf{v}) + \mathbf{v} \cdot (\rho\mathbf{g} - \nabla p + \partial_j(\mu\partial_j\mathbf{u} + \mu_c\partial_j\boldsymbol{\chi})),$$

where

(i) $\quad -\rho\mathbf{v}\cdot((\mathbf{u}\cdot\nabla)\mathbf{v}) \quad \equiv -\rho\mathrm{v}_j(u_i\partial_i\mathrm{v}_j) = -\rho u_i(\mathrm{v}_j\partial_i\mathrm{v}_j)$
$\quad\quad\quad\quad\quad\quad\quad\quad\quad\quad\quad\quad = -\rho u_i\partial_i(\tfrac{1}{2}\mathbf{v}^2) \equiv -\rho\mathbf{u}\cdot\nabla(\tfrac{1}{2}\mathbf{v}^2),$

(ii) $\quad \mathbf{v}\cdot\partial_j(\mu\partial_j\mathbf{u}+\mu_c\partial_j\boldsymbol{\chi}) \quad \equiv \mathrm{v}_i\partial_j(\mu\partial_j u_i+\mu_c\partial_j\chi_i)$
$\quad\quad\quad\quad\quad\quad\quad\quad\quad\quad\quad\quad = \partial_j((\mu\partial_j u_i+\mu_c\partial_j\chi_i)\mathrm{v}_i) - (\mu\partial_j u_i+\mu_c\partial_j\chi_i)\partial_j\mathrm{v}_i$
$\quad\quad\quad\quad\quad\quad\quad\quad\quad\quad\quad\quad \equiv -\nabla\cdot(\mathrm{P}\mathbf{v}) - \Phi \text{ (see the definitions (2.67)–(2.68))},$

(iii) $\quad \mathbf{v}\cdot(\rho\mathbf{g}) = -\rho\mathbf{v}\cdot\nabla\phi.$

Thus, we obtain:

$$\rho\partial_t(\tfrac{1}{2}\mathbf{v}^2) = -\rho\mathbf{u}\cdot\nabla(\tfrac{1}{2}\mathbf{v}^2) - \rho\mathbf{v}\cdot\nabla\phi - \mathbf{v}\cdot\nabla p - \nabla\cdot(\mathrm{P}\mathbf{v}) - \Phi. \quad\quad (3.17)$$

Finally, we substitute Eqs. (3.16)–(3.17) in (3.15) and use Eq. (2.72) and Eq. (2.75) to obtain the evolution law for the total energy in the upscaled description resulting from EUE:

$$\partial_t(\rho\tfrac{1}{2}\mathbf{v}^2+\rho\epsilon+\rho\phi) + \nabla\cdot(\mathbf{u}(\rho\tfrac{1}{2}\mathbf{v}^2+\rho\omega)+\mathbf{v}(\rho\phi)+\mathrm{P}\mathbf{v}-\lambda\nabla T-\lambda_c\nabla\Theta) = 0. \quad\quad (3.18)$$

Remark 10. *The total energy in the upscaled description is governed by a conservation law.*

3.2. **The entropy law in the upscaled description.** In Gas Dynamics, the flow domain is supposed to be continuously covered at unobserved scales by near-equilibrium mass elements undergoing finite-time transformations of their state (the slower transformations the closer to equilibrium mass elements are). This is the "local equilibrium assumption", which accounts for intensive thermodynamic variables and densities of extensive variables to be well defined smooth functions of space and time in non-equilibrium flows, and thus for the ideal gas state equation (2.4) as well as for the Gibbs relation $Tds = de + pd(1/\rho) - \sum_k \mu_k dc_k$ to apply to non-equilibrium flows ([7, 11]). We assume that EUE describes transformations of mass element ensembles, making up larger particles, that are subject to the state equation (2.76) (which reads $\kappa\rho\omega = p$). That is, we assume that EUE stands for a local equilibrium mechanism at larger scales. Therefore, we define the entropy rate of change per unit mass in the upscaled description by:

$$\mathcal{T}d\sigma = d\epsilon + pd(1/\rho), \quad\quad (3.19)$$

where d represents the upscaled material derivative d_t and $\langle\,\cdot\,\rangle$ is omitted from $\langle p\rangle$ and $\langle\rho\rangle$.

Applying d_t on Eq. (3.8), the identity $d_t\epsilon + pd_t(1/\rho) = d_t\omega - (1/\rho)d_tp$ follows. Thus, the upscaled enthalpy version of Eq. (3.19) is:

$$\mathcal{T}d\sigma = d\omega - (1/\rho)dp. \quad\quad (3.20)$$

We substitute Eq. (3.8) in Eq. (3.11), apply Eq. (3.19) and use the mass conservation equation $\rho d_t(1/\rho) = \nabla\cdot\mathbf{u}$, or else we substitute Eq. (3.20) in Eq. (3.14), to

obtain:

$$\mathcal{T}\rho d_t\sigma = \Phi + \boldsymbol{\chi} \cdot \nabla p + \nabla \cdot (\lambda\nabla T + \lambda_c\nabla\Theta). \tag{3.21}$$

Then, we use the vector identity $f\nabla \cdot \mathbf{G} = \nabla \cdot (\mathbf{G}f) - \mathbf{G} \cdot \nabla f$ in Eq. (3.21), with $f \equiv 1/\mathcal{T}$ and $\mathbf{G} \equiv \lambda\nabla T + \lambda_c\nabla\Theta$, to obtain the evolution law for the entropy in the upscaled description:

$$\rho d_t\sigma = \frac{\Phi}{\mathcal{T}} + \boldsymbol{\chi} \cdot \frac{\nabla p}{\mathcal{T}} + \frac{\Psi}{\mathcal{T}^2} + \nabla \cdot \big(\frac{\lambda\nabla T + \lambda_c\nabla\Theta}{\mathcal{T}}\big), \tag{3.22}$$

where

$$\Psi \equiv (\lambda\nabla T + \lambda_c\nabla\Theta) \cdot \nabla\mathcal{T}. \tag{3.23}$$

For future reference, we indicate by Π the entropy source term in the upscaled description:

$$\Pi \equiv (\Phi/\rho)/\mathcal{T} + (\boldsymbol{\chi}/\rho) \cdot (\nabla p/\mathcal{T}) + (\Psi/\rho)/\mathcal{T}^2. \tag{3.24}$$

Remark 11. *The pressure gradient arises as an affinity ([7, 11]) of the entropy source term in the upscaled description.*

Remark 12. *The viscous dissipation functions in the upscaled description are sums of quadratic forms:*

$$\Phi \equiv (\mu\nabla u_i + \mu_c\nabla\chi_i) \cdot \nabla(u_i + \chi_i) = \mu(\nabla u_i)^2 + (\mu + \mu_c)\nabla u_i \cdot \nabla\chi_i + \mu_c(\nabla\chi_i)^2,$$
$$\Psi \equiv (\lambda\nabla T + \lambda_c\nabla\Theta) \cdot \nabla(T + \Theta) = \lambda(\nabla T)^2 + (\lambda + \lambda_c)\nabla T \cdot \nabla\Theta + \lambda_c(\nabla\Theta)^2.$$

For $0 < \lambda < \lambda_c$ and $0 < \mu < \mu_c$, they satisfy:

$$\Phi \geq 0 \quad if \quad \partial_j u_i/\partial_j\chi_i \notin (-\mu_c/\mu, -1) \quad i,j = 1,2,3, \tag{3.25}$$
$$\Psi \geq 0 \quad if \quad \partial_j T/\partial_j\Theta \notin (-\lambda_c/\lambda, -1) \quad j = 1,2,3. \tag{3.26}$$

4. Frictional air flows

We consider frictional air flows between two planar parallel plates, and describe them as stationary flows in the upscaled description that depend only on the direction z orthogonal to the plate. This includes describing the exact (that is, in all scales) stationary states of these flows, which occur in laminar regimes, given by the corresponding Navier-Stokes description.

When $\boldsymbol{\Omega} = \mathbf{0}$, we have $\mathbf{g} = \mathbf{g}_0$. In a sufficiently thin domain of fluid and for small gradients of temperature, one can assume that ρ is constant and gravitation effects are negligible. We employ the constant ρ thermodynamical limit, where p is treated as a dynamic pressure through the substitution of the state equation by $\nabla \cdot \mathbf{u} = 0$.

For solutions that vary only in the direction z orthogonal to the boundary, the EUE model (2.70)–(2.76) reads:

$$d_z(u_3(h - p/\rho) + \chi_3 h - \upsilon \, d_z T) = (\nu d_z u_i) d_z(u_i + \chi_i), \tag{4.1}$$

$$d_z(u_3 u_1 + \chi_3 u_1 - \nu \, d_z u_1) = -\partial_x(p/\rho), \tag{4.2}$$

$$d_z(u_3 u_2 + \chi_3 u_2 - \nu \, d_z u_2) = -\partial_y(p/\rho), \tag{4.3}$$

$$d_z(u_3 u_3 + \chi_3 u_3 - \nu \, d_z u_3) = -\partial_z(p/\rho), \tag{4.4}$$

$$d_z u_3 = 0, \tag{4.5}$$

$$d_z(u_3 \zeta - \chi_3 h - \upsilon_c \, d_z \Theta) = (\nu_c d_z \chi_i) d_z(u_i + \chi_i) + \chi_1 \partial_x(p/\rho) + \chi_3 \partial_z(p/\rho), \tag{4.6}$$

$$d_z(u_3 \chi_1 - \chi_3 u_1 - \nu_c \, d_z \chi_1) = 0, \tag{4.7}$$

$$d_z(u_3 \chi_2 - \chi_3 u_2 - \nu_c \, d_z \chi_2) = 0, \tag{4.8}$$

$$d_z(-\nu_c \, d_z \chi_3) = 0, \tag{4.9}$$

$$d_z \chi_3 = 0, \tag{4.10}$$

where d_z stands for the derivative of a function that depends only on z, and we define

$$\nu \equiv \mu/\rho, \quad \upsilon \equiv \lambda/\rho, \quad \nu_c \equiv \mu_c/\rho, \quad \upsilon_c \equiv \lambda_c/\rho. \tag{4.11}$$

Notice that we have applied $\nabla \cdot \mathbf{u} = 0$ in Eq. (2.70) to obtain Eq. (4.1), and abandoned the state equation (2.76).

From Eq. (4.5), u_3 is constant. Hence, $u_3 = 0$ for an impermeable boundary. In this case, Eq. (4.4) reduces to $\partial_z(p/\rho) = 0$. Consequently $\partial_z \partial_x(p/\rho) = \partial_x \partial_z(p/\rho) = 0$ and $\partial_z \partial_y(p/\rho) = \partial_y \partial_z(p/\rho) = 0$, that is $\partial_x(p/\rho)$ and $\partial_y(p/\rho)$ must be constant. From Eq. (4.10), χ_3 is constant. With $u_3 = 0$ and χ_3 constant, Eq. (4.3) and Eq. (4.8) become linear. Thus, for $\partial_y(p/\rho) = 0$ and for homogeneous boundary conditions on u_2 and χ_2 we obtain $u_2 = 0$ and $\chi_2 = 0$. Therefore, the system (4.1)–(4.10) reduces to:

$$\upsilon T'' - \xi c_{\mathrm{p}} T' = -(\nu u_1')(u_1' + \chi_1'), \tag{4.12}$$

$$\nu u_1'' - \xi u_1' = \eta_1, \tag{4.13}$$

$$\upsilon_c \Theta'' + \xi c_{\mathrm{p}} T' = -(\nu_c \chi_1')(u_1' + \chi_1') - \chi_1 \eta_1, \tag{4.14}$$

$$\nu_c \chi_1'' + \xi u_1' = 0, \tag{4.15}$$

where we substituted $h = c_{\mathrm{p}} T$ and $\zeta = c_{\mathrm{p}} \Theta$, and we define

$$f' \equiv d_z f, \tag{4.16}$$

$$\xi \equiv \chi_3, \tag{4.17}$$

$$\eta_1 \equiv \partial_x(p/\rho). \tag{4.18}$$

The definition (4.16) is not to be confused with the definition (2.11) employed in Chapters 2 and 3.

Remark 13. *For $\xi = 0$, the solution of Eqs. (4.14)–(4.15) with the homogeneous boundary conditions $\chi_1 = 0$ and $\Theta = 0$ at $z = -L$ and $z = +L$ is zero. This means that the turbulence mechanism (2.73)–(2.75) does not take place in one-dimensional frictional flows. Thus, the strictly one-dimensional approximation of* EUE *is inadequate to describe frictional flows. Therefore, in this study our goal will be limited to finding the* EUE *qualitative description of planar Couette and planar Poiseuille flows by providing some scaling for ξ.*

We show in Appendix B that the general solution of the system of ordinary differential equations (4.12)–(4.15) is given by polynomials in z and $\exp(z)$.

Remark 14. *In order to help exploring the role of Θ in the model (4.12)–(4.15), we examine the temperature profiles produced when Θ is neglected. In this case, the equation (2.73) reduces to:*

$$\nabla \cdot (-\boldsymbol{\chi}\rho h) = \tilde{\Phi} + \boldsymbol{\chi} \cdot \nabla p. \tag{4.19}$$

According to this equation, the flux term $(-\boldsymbol{\chi}\rho h)$ balances the source terms $\tilde{\Phi}$ and $\boldsymbol{\chi} \cdot \nabla p$ when $\Theta = 0$. Substituting $\nabla \cdot (\boldsymbol{\chi}\rho h)$ in (2.70), we obtain

$$\partial_t(\rho h) + \nabla \cdot (\mathbf{u}(\rho h - p) - \lambda \nabla T) = \Phi + \boldsymbol{\chi} \cdot \nabla p - p\nabla \cdot \mathbf{u}, \tag{4.20}$$

where Φ is defined in (2.68). The state equation (2.76) reduces to $\kappa\rho h = p$ when $\Theta = 0$. However, we are interested in the constant ρ thermodynamic limit, therefore we substitute this equation by $\nabla \cdot \mathbf{u} = 0$. Thus, for stationary one-dimensional solutions, Eq. (4.20) reads:

$$\upsilon T'' = -(\nu u_1' + \nu_c \chi_1')(u_1' + \chi_1') - \chi_1 \eta_1. \tag{4.21}$$

Notice that neither c_{p}, nor υ_c, appear in this formulation. Taking into account that u_1 and χ_1 are given by (B.10) and (B.12), we obtain:

$$
\begin{aligned}
T = {}& (1/(12\nu_c\upsilon))(\eta_1\xi a/2 - \xi^2 a^2)\, z^4 + (1/(6\upsilon))((\eta_1\xi A_1/\nu_c - \eta_1 B_1) \\
& + ((\nu a - \xi A_1 + \nu_c B_1)(\xi a/\nu_c) + \xi a(a - \xi A_1/\nu_c + B_1)))\, z^3 \\
& - (1/(2\upsilon))((\nu a - \xi A_1 + \nu_c B_1)(a - \xi A_1/\nu_c + B_1) + \eta_1 B_0)\, z^2 + E_2\, z + E_1 \\
& + (((\xi a/\upsilon)(A_2 r_2 - \xi A_2/\nu_c) + (\xi a/(\nu_c\upsilon))(\nu A_2 r_2 - \xi A_2))(z/r_2^2 - 1/r_2^3) \\
& - (1/r_2^3)((\xi a/\upsilon)(A_2 r_2 - \xi A_2/\nu_c) + (\xi a/(\nu_c\upsilon))(\nu A_2 r_2 - \xi A_2)) \\
& + \eta_1\xi A_2/(\nu_c r_2^3\upsilon) - (\nu a - \xi A_1 + \nu_c B_1)(A_2 r_2 - \xi A_2/\nu_c)/(\upsilon r_2^2) \\
& - (\nu A_2 r_2 - \xi A_2)(a - \xi A_1/\nu_c + B_1)/(\upsilon r_2^2))\, e^{r_2 z} \\
& - (1/(4\upsilon r_2^2))(\nu A_2 r_2 - \xi A_2)(A_2 r_2 - \xi A_2/\nu_c)\, e^{2r_2 z}, \tag{4.22}
\end{aligned}
$$

where E_1 and E_2 stand for the constants to be determined by the boundary conditions. For the boundary conditions

$$T(L) = T_0, \tag{4.23}$$

$$T'(0) = 0, \tag{4.24}$$

we obtain:

$$
\begin{aligned}
E_1 = &(-\eta_1 \xi a L^5 r_2^5 - 2\xi a^2 L^4 r_2^5 \nu_c - 12 L^3 r_2^5 \nu a^2 \nu_c - 2\xi a^2 L^4 r_2^5 \nu - 24 T_0 \nu_c r_2^5 \upsilon L \\
&+ 36 a^2 \xi^2 r_2 L - \xi^2 a^2 L^5 r_2^5 + 60 L^2 a^2 \xi^2 r_2^2 - 24 L r_2^2 \nu_c \xi a^2 - 24 L r_2^2 \nu a^2 \xi \\
&- 12 L^3 r_2^4 \xi a^2 \nu_c + 20 L^3 r_2^3 \xi^2 a^2 - 12 L^3 r_2^4 \nu a^2 \xi - 36 r_2^4 L^2 a^2 \nu \nu_c - 24 r_2^3 L^2 a^2 \nu \xi \\
&- 24 r_2^3 L^2 a^2 \xi \nu_c + 8 \eta_1 \xi a r_2^3 L^3 + 24 L^2 \eta_1 \xi a r_2^2 + (48 a^2 \xi \nu_c r_2^2 L + 24 a^2 \xi^2 L^2 r_2^2 \\
&+ 4 \eta_1 \xi a r_2^3 L^3 + 4 L^3 r_2^3 \xi^2 a^2 + 24 a^2 \nu \xi r_2 + 24 a^2 \nu_c \xi r_2 - 120 a^2 \xi^2 r_2 L \\
&+ 48 a^2 \nu \xi r_2^2 L - 24 \eta_1 \xi a r_2 L + 48 a^2 r_2^3 \nu \nu_c L - 48 a^2 \xi^2) \, e^{r_2 L} + (6 a^2 \nu \xi r_2^2 L \\
&+ 6 a^2 \xi \nu_c r_2^2 L - 18 a^2 \xi^2 r_2 L - 6 a^2 r_2^3 \nu \nu_c L - 24 a^2 \nu \xi r_2 - 24 a^2 \nu_c \xi r_2 + 48 a^2 \xi^2) \, e^{2 r_2 L}) \\
&/ (-24 r_2^5 L \nu_c \upsilon),
\end{aligned}
\tag{4.25}
$$

$$
\begin{aligned}
E_2 = &(2 \eta_1 \xi r_2 L - 3 r_2^3 \nu a \nu_c L - a r_2^3 \xi \nu_c L^2 + 2 \xi^2 a r_2^2 L^2 - 2 a r_2 \xi \nu_c + 4 \xi^2 a - a r_2^3 \nu \xi L^2 \\
&- 2 a r_2 \nu \xi - a r_2^2 \nu \xi L - a r_2^2 \xi \nu_c L + 5 \xi^2 a r_2 L + (2 a r_2 \xi \nu_c - 4 \xi^2 a + 2 a r_2 \nu \xi) \, e^{r_2 L}) \\
&/ (2 r_2^4 L \nu_c \upsilon / a).
\end{aligned}
\tag{4.26}
$$

4.1. The planar Couette flows.

We consider Couette flows between two planar parallel plates. These flows are driven by relative motion of the plates; no pressure gradient is imposed. We place the frame of reference at mid-distance between the plates.
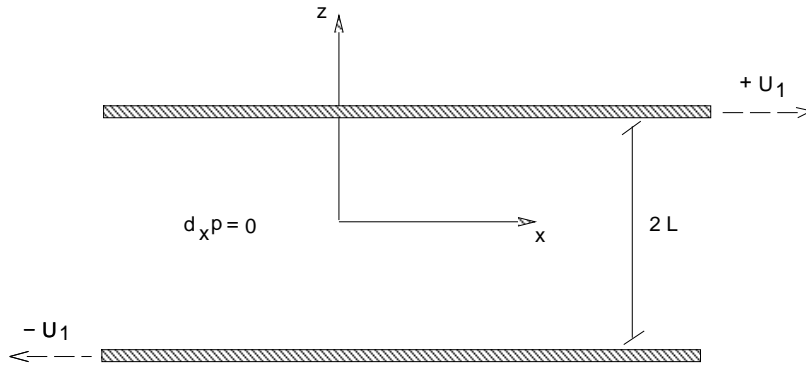

FIGURE 4.1. The planar Couette flows.

Because of symmetry (gravity is neglected), T must be an even function of z and u_1 must be an odd function of z. We assume that the turbulence field vanishes

at the plates and at mid-distance between them. Therefore, we take for boundary conditions:

$$u_1(L) = U_1, \quad \chi_1(L) = 0, \quad T(L) = T_0, \quad \Theta(L) = 0, \tag{4.27}$$

$$u_1(0) = 0, \quad \chi_1(0) = 0, \quad T'(0) = 0, \quad \Theta(0) = 0. \tag{4.28}$$

We show in Appendix B that the solution of the system of ordinary differential equations (4.12)–(4.15) with the boundary conditions (4.27)–(4.28) is given by polynomials in z and $\exp(z)$. See Eqs. (B.29)–(B.32) and (B.33)–(B.40) for the case $\eta_1 = 0$.

Remark 15. *The compressible Navier-Stokes equations may be written as:*

$$\partial_t(\rho h - p) + \nabla \cdot (\mathbf{u}(\rho h - p) - \lambda \nabla T) = \Phi,$$
$$\partial_t(\rho \mathbf{u}) + \partial_j(u_j \rho \mathbf{u} - \mu \partial_j \mathbf{u}) = \rho \mathbf{u} \times 2\mathbf{\Omega} + \rho \mathbf{g} - \nabla p,$$
$$\partial_t \rho + \nabla \cdot (\mathbf{u}\rho) = 0,$$

where $h = c_\mathrm{p} T$ and $\Phi \equiv (\mu \nabla u_i) \cdot \nabla u_i = \mu(\nabla u_i)^2$. For stationary one-dimensional planar Couette flows, these equations reduce to:

$$\upsilon T'' + \nu u_1'^{\,2} = 0, \tag{4.29}$$

$$u_1'' = 0, \tag{4.30}$$

where $f' \equiv d_z f$, $\nu \equiv \mu/\rho$, $\upsilon \equiv \lambda/\rho$. For the boundary conditions

$$u_1(L) = U_1, \quad T(L) = T_0, \tag{4.31}$$

$$u_1(0) = 0, \quad T'(0) = 0, \tag{4.32}$$

we obtain:

$$T = (\nu U_1^2/(2\upsilon))(1 - (z/L)^2) + T_0, \tag{4.33}$$

$$u_1 = U_1 (z/L). \tag{4.34}$$

Notice that (4.33)–(4.34) is also the solution of (4.29)–(4.30) for the boundary conditions

$$u_1(+L) = +U_1, \quad T(+L) = T_0,$$
$$u_1(-L) = -U_1, \quad T(-L) = T_0.$$

Next, we discuss the planar Couette profiles resulting from Eqs. (4.12)–(4.15) with $\eta_1 = 0$, the boundary conditions (4.27)–(4.28) and the scaling $s|U_1|$ of ξ for some constant s. The constants in these profiles are s, $\nu \sim 1.5 \cdot 10^{-5}\ m^2/s$, ν_c, $c_\mathrm{p} \sim 10^3\ J/(kg \cdot K)$, $\upsilon \sim 2.0 \cdot 10^{-2}\ J \cdot m^2/(kg \cdot s \cdot K)$, υ_c, L, U_1 and T_0. The values of s, ν_c and υ_c are determined to obtain the best qualitative fit with the experimental profiles of Reichardt ([17]) shown in Fig. 4.2.
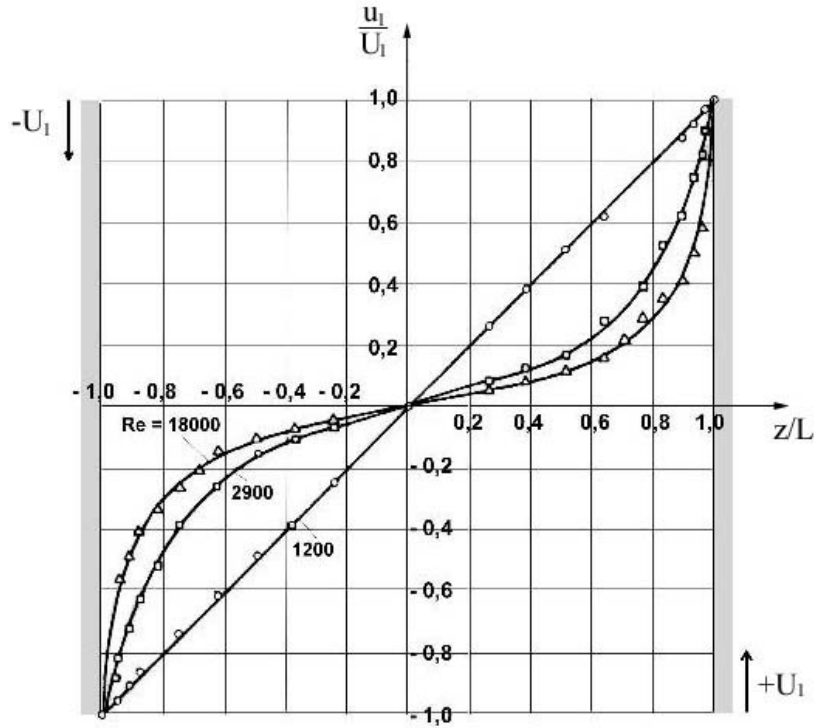
FIGURE 4.2. Experimental profiles of momentum in planar Couette flows, by Reichardt [17].

For comparison, Fig. 4.3.(a) shows the planar Couette momentum profiles given by Navier-Stokes, that is, the profiles of u_1/U_1 resulting from (4.34). We immediatly see that

$$u_1/U_1 = f_1(z/L), \tag{4.35}$$

so the profiles are independent of any parameter, in particular of the Reynolds number

$$\mathrm{Re} \equiv |U_1|(2L)/\nu. \tag{4.36}$$

Let us consider now the planar Couette momentum profiles given by EUE, that is, the profiles of $(u_1 + \chi_1)/U_1$ resulting from Eqs. (4.13) and (4.15) with $\eta_1 = 0$, the boundary conditions (4.27)–(4.28) on u_1 and χ_1, and the scaling $s|U_1|$ of ξ for some constant s. The constants in these profiles are s, $\nu \sim 1.5 \cdot 10^{-5}\ m^2/s$, ν_c, L and U_1.
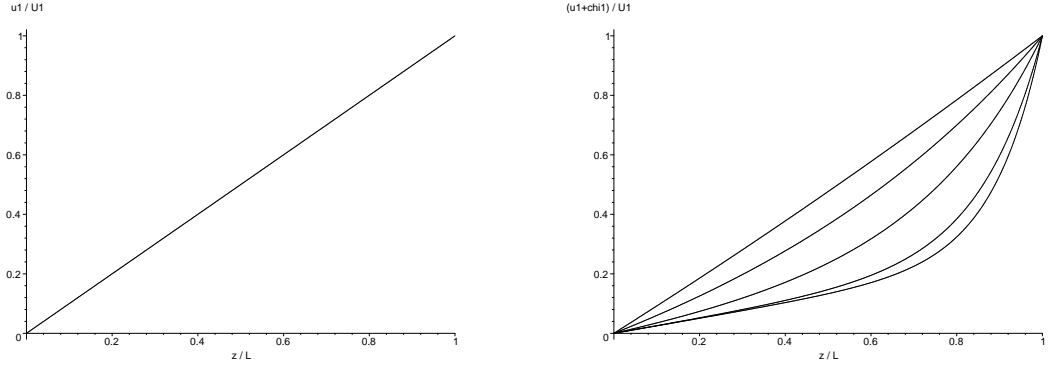
(a) Navier-Stokes profiles: independent of Re.

(b) EUE profiles: Re=$5.0 \cdot 10^2$ or lower values, $3.0 \cdot 10^3$, $7.0 \cdot 10^3$, $1.4 \cdot 10^4$, $1.8 \cdot 10^4$ (curves from top to bottom); $s_0 = 1 \cdot 10^{-3}$; $M_1 = 4$.

FIGURE 4.3. Navier-Stokes and EUE profiles of momentum for planar Couette flows.

One sees from (B.30), (B.32) and (B.33)–(B.36) that

$$u_1/U_1 = f_2(z/L, s\mathrm{Re}), \tag{4.37}$$

$$\chi_1/U_1 = (1/\mathrm{M}_1)f_3(z/L, s\mathrm{Re}), \tag{4.38}$$

where

$$\mathrm{M}_1 \equiv \nu_c/\nu, \tag{4.39}$$

thus

$$(u_1 + \chi_1)/U_1 = f_4(z/L, s\mathrm{Re}, \mathrm{M}_1). \tag{4.40}$$

When plotting the results of our calculations, it is observed that a Re-profile family (that is, a family of profiles parameterized by Re) of the analytical extension of $(u_1+\chi_1)/U_1$ to $z/L \in [-1,+1]$ agrees qualitatively with experimental data provided the following conditions on s and M_1 are satisfied, regardless the sign of U_1:

$$s = +s_0 > 0, \quad \forall z/L \in (0,+1], \tag{4.41}$$

$$s = -s_0 < 0, \quad \forall z/L \in [-1,0), \tag{4.42}$$

$$\mathrm{M}_1 > 1. \tag{4.43}$$

Remark 16. *The conditions* (4.41)–(4.42) *on s imply that a* Re-*profile family of the analytical extension of* $(u_1 + \chi_1)/U_1$ *to* $z/L \in [-1,+1]$ *agrees qualitatively with experimental data only if the following conditions on* $\xi = s|U_1|$ *are satisfied (regardless*

the sign of U_1):

$$\xi > 0, \quad \forall z/L \in (0, +1], \tag{4.44}$$

$$\xi < 0, \quad \forall z/L \in [-1, 0). \tag{4.45}$$

Neither the vorticity nor the shear of **u** *have these properties: both these quantities are single-signed throughout the layer and switch their signs when the sign of U_1 is switched.*

In particular, the analytical extension of $(u_1 + \chi_1)/U_1$ to $z/L \in [-1, +1]$ is an odd function when the conditions (4.41)–(4.43) are satisfied. Therefore, we discuss its restriction to $z/L \in [0, +1]$. For this purpose, we write:

$$(u_1 + \chi_1)/U_1 = f_4(z/L, \mathrm{Re}^*, \mathrm{M}_1), \tag{4.46}$$

where

$$\mathrm{Re}^* \equiv s_0 \mathrm{Re}, \quad s_0 > 0. \tag{4.47}$$

In plots, Re^* controls the boundary layer width of $(u_1 + \chi_1)/U_1$ at $z/L = 1$ (or else, the profile slope at $z/L = 1$), while M_1 controls the shear of $(u_1 + \chi_1)/U_1$ at $z/L = 0$ (that is, the profile slope at $z/L = 0$). Indeed, the boundary layer width at $z/L = 1$ decreases (the profile slope at $z/L = 1$ steepens) for increasing values of Re^*, the shear at $z/L = 0$ decreases for increasing values of M_1. For $s_0 = 0$ or $\mathrm{M}_1 = 1$, the profiles collapse into the Navier-Stokes straight line profile (the case $\mathrm{M}_1 = 1$ can be derived by adding Eqs. (4.13) and (4.15)). The Re-profile family of $(u_1 + \chi_1)/U_1$ that fits best qualitatively the experimental profiles of Reichardt ([17]) is obtained for $s_0 \sim 1 \cdot 10^{-3}$ and $\mathrm{M}_1 \sim 4$. Fig. 4.3.(b) shows some members of this Re-profile family of $(u_1 + \chi_1)/U_1$.

Remark 17. *Notice from (4.46)–(4.47) that s_0 is an amplification factor for the span of a* Re-*profile family of $(u_1 + \chi_1)/U_1$. Therefore, it fixes the critical value of* Re *for the laminar-turbulent threshold occurring in each* Re-*profile family of $(u_1 + \chi_1)/U_1$. Notice from Fig. 4.3.(b) that for $s_0 = 1 \cdot 10^{-3}$ the* Re-*profile family of $(u_1 + \chi_1)/U_1$ starts deviating from the laminar straight line at* Re $\sim 1 \cdot 10^3$. *According to Reichardt ([17]), the experimental critical value of* Re *is $1.5 \cdot 10^3$.*

Like $(u_1 + \chi_1)/U_1$, the analytical extensions of u_1/U_1 and χ_1/U_1 to $z/L \in [-1, +1]$ are observed in plots to be odd functions when the conditions (4.41)–(4.43) are satisfied. Therefore, we discuss their restrictions to $z/L \in [0, +1]$. For this purpose, we write:

$$u_1/U_1 = f_2(z/L, \mathrm{Re}^*), \tag{4.48}$$

$$\chi_1/U_1 = (1/\mathrm{M}_1) f_3(z/L, \mathrm{Re}^*). \tag{4.49}$$

Fig. 4.4 shows the profiles of u_1/U_1 and χ_1/U_1 that give rise to the profiles in figure 4.3.(b). Notice that χ_1/U_1 always reaches its maximum value in the buffer layer of u_1/U_1. Notice also that whenever there is a boundary layer the profile of u_1/U_1

(a) Re $= 5.0 \cdot 10^2$, $3.0 \cdot 10^3$, $7.0 \cdot 10^3$, $1.4 \cdot 10^4$, $1.8 \cdot 10^4$ (curves from top to bottom); $s_0 = 1 \cdot 10^{-3}$.

(b) Re $= 1.8 \cdot 10^4$, $1.4 \cdot 10^4$, $7.0 \cdot 10^3$, $3.0 \cdot 10^3$, $5.0 \cdot 10^2$ (curves from top to bottom); $s_0 = 1 \cdot 10^{-3}$; $M_1 = 4$.
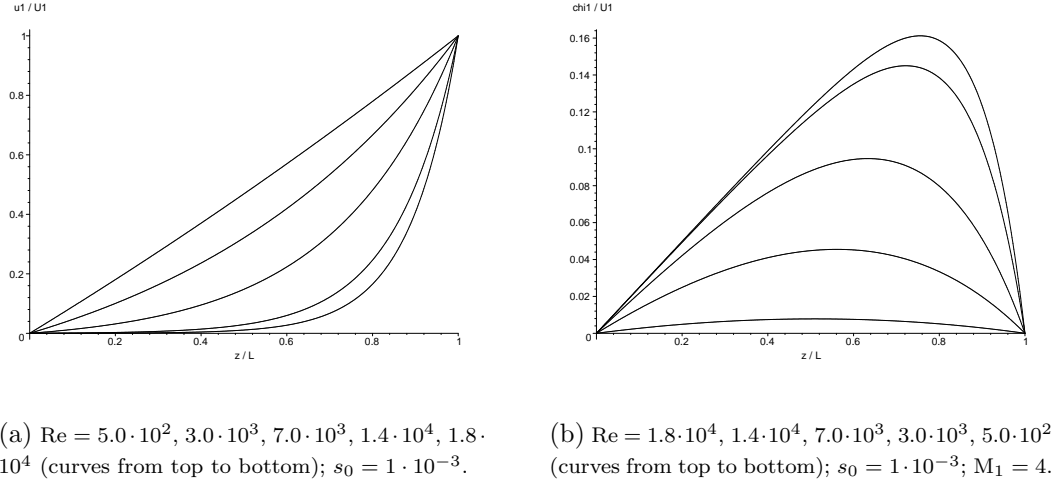
FIGURE 4.4. EUE profiles of u_1/U_1 and χ_1/U_1 for planar Couette flows.

is flat with zero slope in the core layer, while ξ is non-zero: EUE predicts that transverse molecular conduction is dominated by turbulent transfer in a core layer. This is why the shear of $(u_1 + \chi_1)/U_1$ at $z/L = 0$ decreases for increasing values of M_1: one sees from (4.49) that χ_1/U_1 tends to zero, identically, thus $(u_1 + \chi_1)/U_1$ tends to u_1/U_1. In plots, Re* controls the boundary layer width of u_1/U_1 at $z/L = 1$ and the point z_c/L of maximum value of χ_1/U_1 as well as the maximum value of χ_1/U_1: for increasing values of Re*, the boundary layer width of u_1/U_1 at $z/L = 1$ decreases, z_c/L tends to 1 and the maximum value of χ_1/U_1 grows asymptotically to $1/M_1$. For $s_0 = 0$, the profiles of u_1/U_1 collapse into the Navier-Stokes straight line profile and χ_1/U_1 vanishes identically.

For comparison, Fig. 4.5.(a) shows planar Couette temperature profiles given by Navier-Stokes, that is, profiles of $(T - T_0)/(T(0) - T_0)$ resulting from (4.33). We immediatly see that

$$(T - T_0)/(T(0) - T_0) = f_5(z/L). \tag{4.50}$$

Let us consider now planar Couette temperature profiles given by EUE. First, we discuss the profiles of $(T - T_0)/(T(0) - T_0)$ resulting from Eq. (4.21) with $\eta_1 = 0$ and the boundary conditions (4.23)–(4.24). The constants in these profiles are $s_0 \sim 1 \cdot 10^{-3}$, $\nu \sim 1.5 \cdot 10^{-5}\ m^2/s$, $\nu_c \sim 4\nu$, $\upsilon \sim 2.0 \cdot 10^{-2}\ J \cdot m^2/(kg \cdot s \cdot K)$, L, U_1 and T_0. One sees from (4.22) and (4.25)–(4.26) that

$$(T - T_0)/(T(0) - T_0) = f_6(z/L, \mathrm{Re}^*, M_1). \tag{4.51}$$

In plots, it is observed that the analytical extension of $(T - T_0)/(T(0) - T_0)$ to $z/L \in [-1, +1]$ is an even function (as expected, because of symmetry) when the conditions (4.41)–(4.43) are satisfied. Therefore, we discuss its restriction to $z/L \in$

(a) Navier-Stokes profiles: in-dependent of Re.

(b) Eq. (4.21) profiles: Re = $1.8 \cdot 10^4$, $1.4 \cdot 10^4$, $1.0 \cdot 10^4$, $5.0 \cdot 10^2$ or lower values (curves from top to bottom); $s_0 = 1 \cdot 10^{-3}$; $M_1 = 4$.

(c) EUE profiles: Re = $1.8 \cdot 10^4$, $1.4 \cdot 10^4$, $1.0 \cdot 10^4$, $5.0 \cdot 10^2$ or lower values (curves from top to bottom); $s_0 = 1 \cdot 10^{-3}$; Pr = 0.7; $M_1 = 4$; $M_2 = 4$.

FIGURE 4.5. Navier-Stokes and EUE profiles of temperature for planar Couette flows.

$[0, +1]$. Both Re^* and M_1 control the boundary layer width of $(T - T_0)/(T(0) - T_0)$ at $z/L = 1$: the width decreases for increasing values of Re^* or M_1. In addition, when there is a boundary layer, Re^* controls the profile slope of $(T - T_0)/(T(0) - T_0)$ in the core layer: the slope steepens for increasing values of Re^*. Fig. 4.5.(b) shows some members of the Re-profile family of $(T - T_0)/(T(0) - T_0)$ for $s_0 = 1 \cdot 10^{-3}$ and $M_1 = 4$.

Remark 18. *One sees from* (4.22) *and* (4.25)–(4.26) *that for* $\mathrm{Re} \gg 1$,

$$T(0) - T_0 \sim (\nu^3/(8\upsilon L^2))(1/M_1)\,\mathrm{Re}^2. \tag{4.52}$$

Notice that this expression is independent of s_0.

Second, we discuss the profiles of $(T + \Theta - T_0)/(T(0) - T_0)$ resulting from Eqs. (4.12) and (4.14) with $\eta_1 = 0$, the boundary conditions (4.27)–(4.28) on T and Θ, and the scaling $s_0|U_1|$ of ξ for $s_0 = 1 \cdot 10^{-3}$. The constants in these profiles are $s_0 \sim 1 \cdot 10^{-3}$, $\nu \sim 1.5 \cdot 10^{-5}\ m^2/s$, $\nu_c \sim 4\nu$, $c_{\mathrm{p}} \sim 10^3\ J/(kg \cdot K)$, $\upsilon \sim 2.0 \cdot 10^{-2}\ J \cdot m^2/(kg \cdot s \cdot K)$, υ_c, L, U_1 and T_0. One sees from (B.29), (B.31) and (B.37)–(B.40) that

$$(T - T_0)/(T(0) - T_0) = f_7(z/L, \mathrm{Re}^*, \mathrm{Pr}, M_1), \tag{4.53}$$

$$\Theta/(T(0) - T_0) = (1/M_2)f_8(z/L, \mathrm{Re}^*, \mathrm{Pr}, M_1), \tag{4.54}$$

where

$$\mathrm{Pr} \equiv c_{\mathrm{p}}\mu/\lambda = c_{\mathrm{p}}\nu/\upsilon \quad \text{is the Prandtl number,} \tag{4.55}$$

$$M_2 \equiv \upsilon_c/\upsilon, \tag{4.56}$$

thus

$$(T + \Theta - T_0)/(T(0) - T_0) = f_9(z/L, \mathrm{Re}^*, \mathrm{Pr}, M_1, M_2). \tag{4.57}$$

In plots, it is observed that the analytical extension of $(T + \Theta - T_0)/(T(0) - T_0)$ to $z/L \in [-1, +1]$ is an even function (as expected, because of symmetry) when the conditions (4.41)–(4.43) are 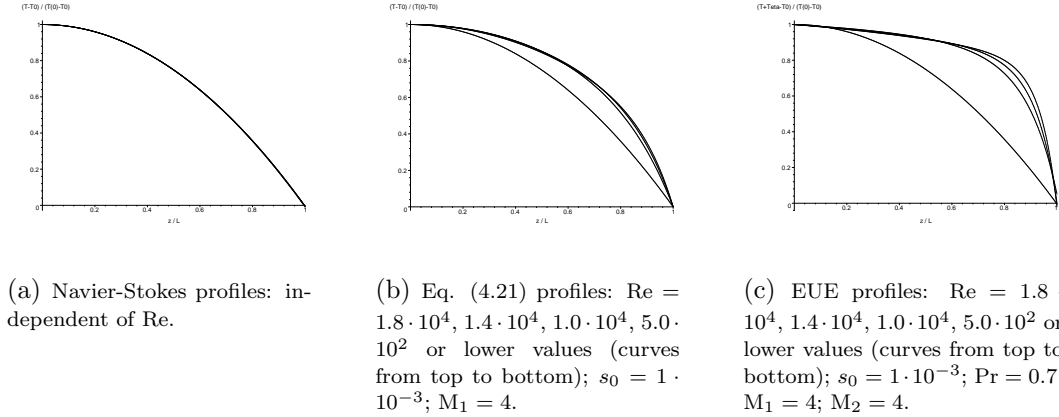satisfied. Therefore, we discuss its restriction to $z/L \in [0, +1]$. The value of M_2 was not determined from qualitative fitting with experimental profiles, because we were unable to find appropriate data. Instead, we assumed $\mathrm{Pr}_c \sim \mathrm{Pr}$ for $\mathrm{Pr}_c \equiv c_p \nu_c / \upsilon_c$ and took $M_2 = M_1(\mathrm{Pr}/\mathrm{Pr}_c) \sim M_1$. While M_1 has little effect on these profiles, Re^* and Pr control the boundary layer width at $z/L = 1$, M_2 controls the slope in the core layer. Indeed, the boundary layer width at $z/L = 1$ decreases for increasing values of Re^* or Pr, the slope in the core layer decreases for increasing values of M_2. Fig. 4.5.(c) shows some members of the Re-profile family of $(T + \Theta - T_0)/(T(0) - T_0)$ for $s_0 = 1 \cdot 10^{-3}$, $M_1 = 4$, $\mathrm{Pr} = 0.7$ (air) and $M_2 = 4$.

Remark 19. *One sees from* (B.29)*,* (B.31) *and* (B.37)–(B.40) *that for* $\mathrm{Re} \gg 1$*,*

$$T(0) - T_0 \sim (\nu^3/(8\upsilon L^2))((M_1 - 1)/M_1)(1/(2 - \mathrm{Pr}))\, \mathrm{Re}^2 \quad \textit{if} \quad \mathrm{Pr} < 1, \tag{4.58}$$

$$T(0) - T_0 \sim (\nu^3/(8\upsilon L^2))(1/M_1)(1/\mathrm{Pr})(1/(\mathrm{Pr} - 1))(4/s_0)\, \mathrm{Re}\, \exp(s_0 \mathrm{Re}(\mathrm{Pr} - 1)/2) \quad \textit{if} \quad \mathrm{Pr} > 1. \tag{4.59}$$

Thus, the one-dimensional EUE *description of planar Couette flows predicts different core flow temperature relationships with* Re *depending on whether* $\mathrm{Pr} < 1$ *or* $\mathrm{Pr} > 1$*. Notice that Eq.* (4.52)*, which is independent of* Pr*, agrees with Eq.* (4.58)*.*
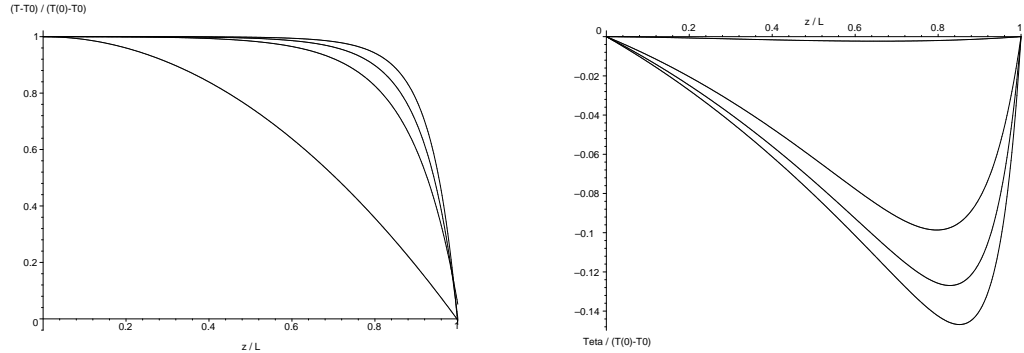
(a) $\mathrm{Re} = 1.8 \cdot 10^4,\ 1.4 \cdot 10^4,\ 1.0 \cdot 10^4,\ 5.0 \cdot 10^2$ (curves from top to bottom); $s_0 = 1 \cdot 10^{-3}$; $\mathrm{Pr} = 0.7$; $M_1 = 4$.

(b) $\mathrm{Re} = 5.0 \cdot 10^2,\ 1.0 \cdot 10^4,\ 1.4 \cdot 10^4,\ 1.8 \cdot 10^4$ (curves from top to bottom); $s_0 = 1 \cdot 10^{-3}$; $\mathrm{Pr} = 0.7$; $M_1 = 4$; $M_2 = 4$.

FIGURE 4.6. EUE profiles of $(T - T_0)/(T(0) - T_0)$ and $\Theta/(T(0) - T_0)$ for planar Couette flows.

Like $(T + \Theta - T_0)/(T(0) - T_0)$, the analytical extensions of $(T - T_0)/(T(0) - T_0)$ and $\Theta/(T(0) - T_0)$ to $z/L \in [-1, +1]$ are observed in plots to be even functions when the conditions (4.41)–(4.43) are satisfied. Therefore, we discuss their restrictions to

$z/L \in [0, +1]$. Fig. 4.6 shows the profiles of $(T - T_0)/(T(0) - T_0)$ and $\Theta/(T(0) - T_0)$ that give rise to the profiles of Fig. 4.5.(c). Notice that $\Theta/(T(0) - T_0)$ always reaches its maximum absolute value in the buffer layer of $(T - T_0)/(T(0) - T_0)$. Notice also that whenever there is a boundary layer the profile of $(T - T_0)/(T(0) - T_0)$ is flat with zero slope in the core layer, while ξ is non-zero: EUE predicts that transverse molecular conduction is dominated by turbulent transfer in a core layer. This is why the profile slope of $(T + \Theta - T_0)/(T(0) - T_0)$ in the core layer decreases for increasing values of M_2: one sees from (4.54) that $\Theta/(T(0) - T_0)$ tends to zero, identically, thus $(T + \Theta - T_0)/(T(0) - T_0)$ tends to $(T - T_0)/(T(0) - T_0)$. While M_1 has little effect on these profiles, Re^* and Pr control the boundary layer width of $(T - T_0)/(T(0) - T_0)$ at $z/L = 1$ and the point z_c/L of maximum absolute value of $\Theta/(T(0) - T_0)$ as well as the maximum absolute value of $\Theta/(T(0) - T_0)$. Indeed, for increasing values of Re^* or Pr, the boundary layer width of $(T - T_0)/(T(0) - T_0)$ at $z/L = 1$ decreases, z_c/L tends to 1 and the maximum absolute value of $\Theta/(T(0) - T_0)$ grows asymptotically to $1/M_2$.

(a) $Re = 1.8 \cdot 10^4$; $s_0 = 1 \cdot 10^{-3}$; $M_1 = 4$.

(b) $Re = 1.8 \cdot 10^4$; $s_0 = 1 \cdot 10^{-3}$; $Pr = 0.7$; $M_1 = 4$; $M_2 = 4$.
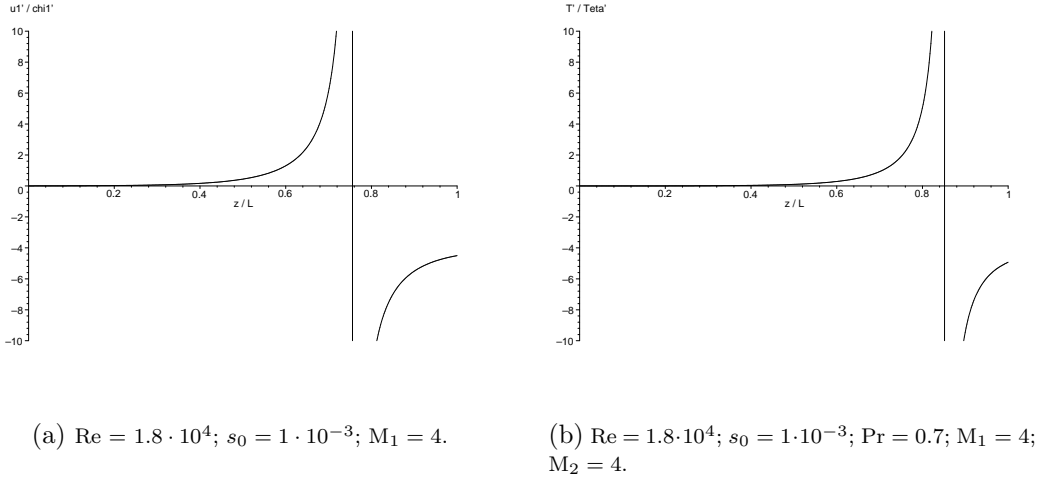
FIGURE 4.7. EUE profiles of u_1'/χ_1' and T'/Θ' for planar Couette flows.

Fig. 4.7 shows EUE profiles of u_1'/χ_1' and T'/Θ' linked to the profiles in 4.4 and 4.6. Notice that the conditions (3.25)–(3.26) are satisfied, therefore the entropy source term (3.24) in the upscaled description is non-negative. The same is true for any other value of Re.

Fig. 4.8 shows EUE profiles of the viscous dissipation functions in the upscaled description and profiles of the entropy source term in the upscaled description, for planar Couette flows. These quantities are defined in (2.68), (3.23) and (3.24).

(a) $\mathrm{Re} = 5.0 \cdot 10^2, 3.0 \cdot 10^3, 7.0 \cdot 10^3, 1.4 \cdot 10^4, 1.8 \cdot 10^4$ (curves from top to bottom); $s_0 = 1 \cdot 10^{-3}$; $M_1 = 4$.

(b) $\mathrm{Re} = 5.0 \cdot 10^2, 3.0 \cdot 10^3, 7.0 \cdot 10^3, 1.4 \cdot 10^4, 1.8 \cdot 10^4$ (curves from top to bottom); $s_0 = 1 \cdot 10^{-3}$; $\mathrm{Pr} = 0.7$; $M_1 = 4$; $M_2 = 4$.

(c) $\mathrm{Re} = 5.0 \cdot 10^2, 3.0 \cdot 10^3, 7.0 \cdot 10^3, 1.4 \cdot 10^4, 1.8 \cdot 10^4$ (curves from top to bottom); $s_0 = 1 \cdot 10^{-3}$; $\mathrm{Pr} = 0.7$; $M_1 = 4$; $M_2 = 4$.
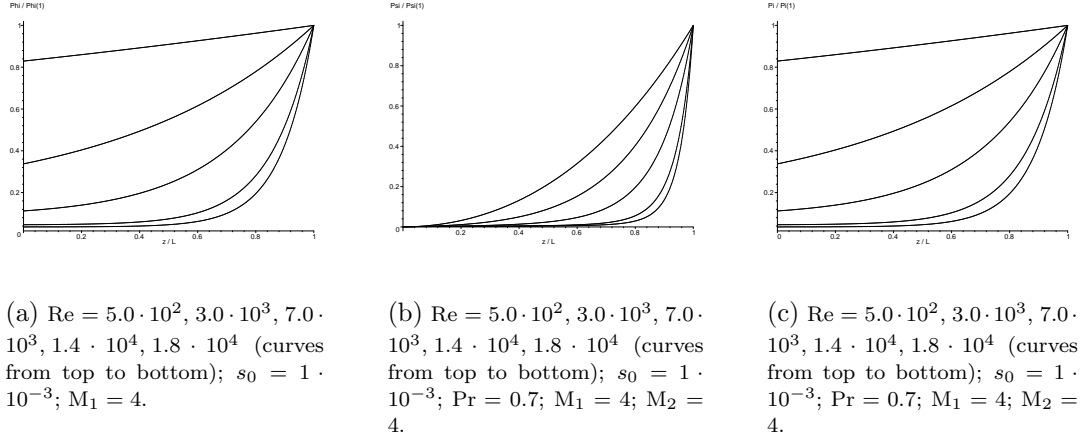
FIGURE 4.8. EUE profiles of the viscous dissipation functions in the upscaled description and profiles of the entropy source term in the upscaled description, for planar Couette flows.

Here, we have $\Phi/\rho = (\nu u_1' + \nu_c \chi_1')(u_1' + \chi_1')$, $\Psi/\rho = (\upsilon T' + \upsilon_c \Theta')(T' + \Theta')$ and $\Pi = (\Phi/\rho)/(T + \Theta) + (\Psi/\rho)/(T + \Theta)^2$. Notice that the three quantities are non-negative (as their values at $z/L = 1$ can be shown to be non-negative) and that non-equilibrium occurs mainly in the boundary layer (whenever the boundary layer exists).

4.2. **The planar Poiseuille flows.** We consider Poiseuille flows between two planar parallel plates. These flows are driven by a constant pressure gradient imposed parallel to the plates. We place the frame of reference at mid-distance between the plates.

FIGURE 4.9. The planar Poiseuille flows.

Because of symmetry (gravity is neglected), T and u_1 must be even functions of z. We assume that the turbulence field vanishes at the plates and at mid-distance between them. Therefore, we take for boundary conditions:
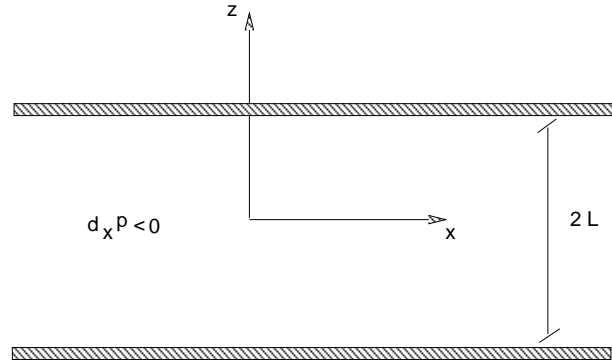
$$u_1(L) = 0, \quad \chi_1(L) = 0, \quad T(L) = T_0, \quad \Theta(L) = 0, \tag{4.60}$$

$$u_1'(0) = 0, \quad \chi_1(0) = 0, \quad T'(0) = 0, \quad \Theta(0) = 0. \tag{4.61}$$

We show in Appendix B that the solution of the system of ordinary differential equations (4.12)–(4.15) with the boundary conditions (4.60)–(4.61) is given by polynomials in z and $\exp(z)$. See Eqs. (B.9)–(B.12) and (B.21)–(B.28).

Remark 20. *The compressible Navier-Stokes equations may be written as:*

$$\partial_t(\rho h - p) + \nabla \cdot (\mathbf{u}(\rho h - p) - \lambda \nabla T) = \Phi,$$

$$\partial_t(\rho \mathbf{u}) + \partial_j(u_j \rho \mathbf{u} - \mu \partial_j \mathbf{u}) = \rho \mathbf{u} \times 2\mathbf{\Omega} + \rho \mathbf{g} - \nabla p,$$

$$\partial_t \rho + \nabla \cdot (\mathbf{u}\rho) = 0,$$

where $h = c_\mathrm{p} T$ and $\Phi \equiv (\mu \nabla u_i) \cdot \nabla u_i = \mu(\nabla u_i)^2$. For stationary one-dimensional planar Poiseuille flows, these equations reduce to:

$$\upsilon T'' + \nu u_1'^2 = 0, \tag{4.62}$$

$$\nu u_1'' = \eta_1, \tag{4.63}$$

where $f' \equiv d_z f$, $\nu \equiv \mu/\rho$, $\upsilon \equiv \lambda/\rho$ and $\eta_1 \equiv \partial_x(p/\rho)$. For the boundary conditions

$$u_1(L) = 0, \quad T(L) = T_0, \tag{4.64}$$

$$u_1'(0) = 0, \quad T'(0) = 0, \tag{4.65}$$

we obtain:

$$T = (\eta_1{}^2 L^4/(12\nu\upsilon))(1 - (z/L)^4) + T_0, \tag{4.66}$$

$$u_1 = (\eta_1 L^2/(2\nu))((z/L)^2 - 1). \tag{4.67}$$

Notice that (4.66)–(4.67) is also the solution of (4.62)–(4.63) for the boundary conditions

$$u_1(+L) = 0, \quad T(+L) = T_0,$$

$$u_1(-L) = 0, \quad T(-L) = T_0.$$

Next, we discuss the planar Poiseuille profiles resulting from Eqs. (4.12)–(4.15) with the boundary conditions (4.60)–(4.61) and the scaling $s(|\eta_1|L^2/(2\nu))$ of ξ for some constant s. The constants in these profiles are s, $\nu \sim 1.5 \cdot 10^{-5}\ m^2/s$, ν_c, $c_\mathrm{p} \sim 10^3\ J/(kg \cdot K)$, $\upsilon \sim 2.0 \cdot 10^{-2}\ J \cdot m^2/(kg \cdot s \cdot K)$, υ_c, L, η_1 and T_0. The values of s, ν_c and υ_c are determined to obtain the best qualitative fit with the experimental profiles of Nikuradse [16] (taken from pipes, thus inadequate) shown in Fig. 4.10.
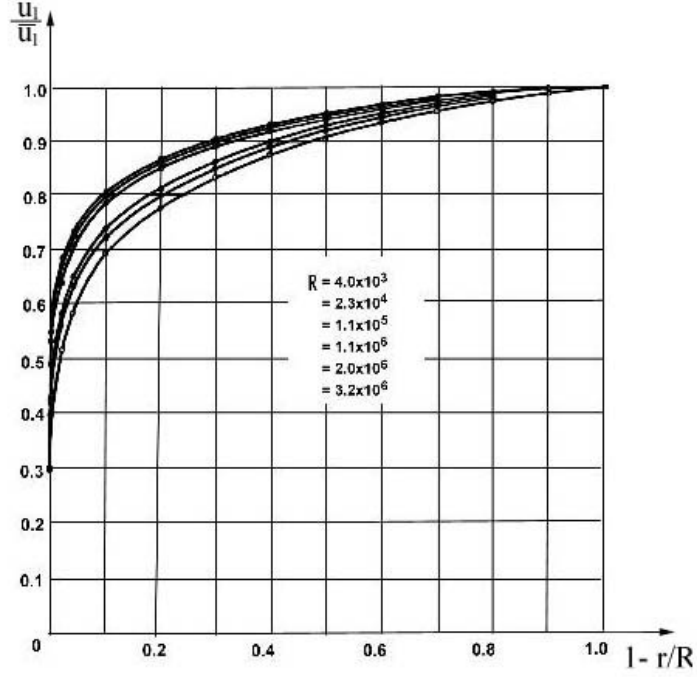
FIGURE 4.10. Experimental profiles of momentum in cylindrical Poiseuille flows, by Nikuradse [16] (permission to reproduce requested). Here, $\bar{u}_1$ is the cross-sectional mean value of u_1 in a pipe.

For comparison, Fig. 4.11.(a) shows the planar Poiseuille momentum profiles given by Navier-Stokes, that is, the profiles of $u_1/u_1(0)$ resulting from (4.67). We immediatly see that

$$u_1/u_1(0) = g_1(z/L), \tag{4.68}$$

so the profiles are independent of any parameter.

Let us consider now the planar Poiseuille momentum profiles given by EUE, that is, the profiles of $(u_1 + \chi_1)/u_1(0)$ resulting from Eqs. (4.13) and (4.15) with the boundary conditions (4.60)–(4.61) on u_1 and χ_1, and the scaling $s(|\eta_1|L^2/(2\nu))$ of ξ for some constant s. The constants in these profiles are s, $\nu \sim 1.5 \cdot 10^{-5} \ m^2/s$, ν_c, L and η_1. One sees from (B.10), (B.12) and (B.21)–(B.24) that

$$u_1/u_1(0) = g_2(z/L, s\mathrm{R}), \tag{4.69}$$

$$\chi_1/u_1(0) = (1/\mathrm{M}_1)g_3(z/L, s\mathrm{R}), \tag{4.70}$$
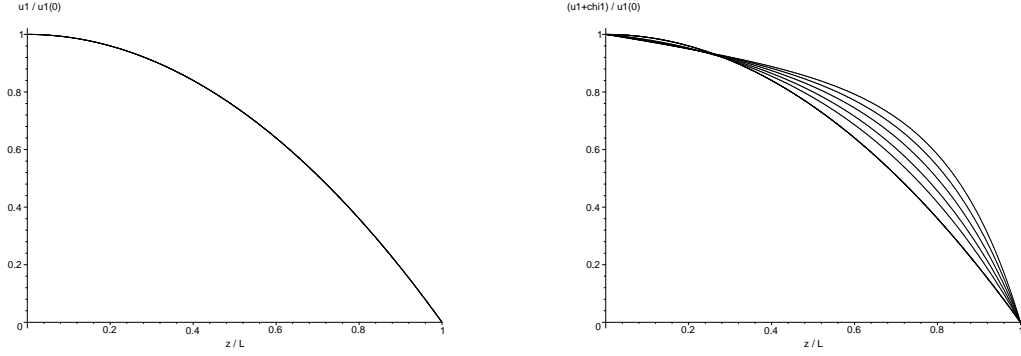
(a) Navier-Stokes profiles: independent of R.

(b) EUE profiles: R [Re] $= 6 \cdot 10^5$ [$1.3 \cdot 10^7$], $5 \cdot$ 10^5 [$5.7 \cdot 10^6$], $4 \cdot 10^5$ [$2.5 \cdot 10^6$], $3 \cdot 10^5$ [$1.1 \cdot 10^6$], $2 \cdot$ 10^5 [$4.4 \cdot 10^5$], $2.2 \cdot 10^3$ [$2.2 \cdot 10^3$] or any lower value (curves from top to bottom); $s_0 = 2 \cdot 10^{-5}$; $M_1 = 4$.

FIGURE 4.11. Navier-Stokes and EUE profiles of momentum for planar Poiseuille flows.

where
$$R \equiv |\eta_1| L^3 / \nu^2, \tag{4.71}$$
thus
$$(u_1 + \chi_1)/u_1(0) = g_4(z/L, sR, M_1). \tag{4.72}$$
When plotting the results of our calculations, it is observed that a R-profile family (that is, a family of profiles parameterized by R) of the analytical extension of $(u_1 + \chi_1)/u_1(0)$ to $z/L \in [-1, +1]$ agrees qualitatively with experimental data provided the following conditions on s and M_1 are satisfied, regardless the sign of η_1:
$$s = +s_0 > 0, \quad \forall z/L \in (0, +1], \tag{4.73}$$
$$s = -s_0 < 0, \quad \forall z/L \in [-1, 0), \tag{4.74}$$
$$M_1 > 1. \tag{4.75}$$

Remark 21. *The conditions (4.73)–(4.74) on s imply that a R-profile family of the analytical extension of $(u_1 + \chi_1)/u_1(0)$ to $z/L \in [-1, +1]$ agrees qualitatively with experimental data only if the following conditions on $\xi = s(|\eta_1| L^2 / (2\nu))$ are satisfied (regardless the sign of η_1):*
$$\xi > 0, \quad \forall z/L \in (0, +1], \tag{4.76}$$
$$\xi < 0, \quad \forall z/L \in [-1, 0). \tag{4.77}$$
Neither the vorticity nor the shear of **u** *have these properties: both these quantities switch their signs when the sign of η_1 is switched.*

In particular, the analytical extension of $(u_1 + \chi_1)/u_1(0)$ to $z/L \in [-1, +1]$ is an even function when the conditions (4.73)–(4.75) are satisfied. Therefore, we discuss its restriction to $z/L \in [0, +1]$. For this purpose, we write:

$$(u_1 + \chi_1)/u_1(0) = g_4(z/L, \mathrm{R}^*, \mathrm{M}_1), \qquad (4.78)$$

where

$$\mathrm{R}^* \equiv s_0 \mathrm{R}, \quad s_0 > 0. \qquad (4.79)$$

In plots, R^* controls the boundary layer width of $(u_1+\chi_1)/u_1(0)$ at $z/L = 1$ (or else, the profile slope at $z/L = 1$), while M_1 controls the profile slope of $(u_1 + \chi_1)/u_1(0)$ in the core layer. Indeed, the boundary layer width at $z/L = 1$ decreases (the profile slope at $z/L = 1$ steepens) for increasing values of R^*, the slope in the core layer decreases for increasing values of M_1. For $s_0 = 0$ or $\mathrm{M}_1 = 1$, the profiles collapse into the Navier-Stokes parabolic profile (the case $\mathrm{M}_1 = 1$ can be derived by adding Eqs. (4.13) and (4.15)). The R-profile family of $(u_1+\chi_1)/u_1(0)$ that fits best qualitatively the experimental profiles of Nikuradse ([16]) is obtained for $s_0 \sim 2 \cdot 10^{-5}$ and $\mathrm{M}_1 \sim 4$. Fig. 4.11.(b) shows some members of this R-profile family of $(u_1 + \chi_1)/u_1(0)$.

Remark 22. *Notice from (4.78)–(4.79) that s_0 is an amplification factor for the span of a R-profile family of $(u_1+\chi_1)/u_1(0)$. Therefore, it fixes the critical value of R for the laminar-turbulent threshold occurring in each R-profile family of $(u_1+\chi_1)/u_1(0)$. Notice from Fig. 4.11.(b) that for $s_0 = 2 \cdot 10^{-5}$ the R-profile family of $(u_1 + \chi_1)/U_1$ starts deviating from the laminar parabola at $\mathrm{R} \sim 2.2 \cdot 10^3$, which corresponds to $\mathrm{Re} \equiv |u_1(0)|(2L)/\nu \sim 2.2 \cdot 10^3$. According to Nikuradse ([16]), the experimental lower limit for the critical value of $\mathrm{Re} \equiv |\bar{u}_1|(2L)/\nu$, where $\bar{u}_1$ is the cross-sectional mean value of u_1 in a pipe, is $2.3 \cdot 10^3$.*

Remark 23. *One sees from (B.10), (B.12) and (B.21)–(B.24) that for $\mathrm{R} \gg 1$,*

$$u_1(0) \sim (\nu/L)(4/s_0^2)(1/\mathrm{R}) \exp(s_0 \mathrm{R}/2). \qquad (4.80)$$

This core flow velocity relationship with pressure gradient (see the definition (4.71) of R) is rather different from the experimental relationship for pipe flows, which states that $\bar{u}_1$ (the cross-sectional mean value of u_1 in a pipe) is proportional to $|\eta_1|^{1/2}$ in turbulent regimes ([19]).

Like $(u_1 + \chi_1)/u_1(0)$, the analytical extensions of $u_1/u_1(0)$ and $\chi_1/u_1(0)$ to $z/L \in [-1, +1]$ are observed in plots to be even functions when the conditions (4.73)–(4.75) are satisfied. Therefore, we discuss their restrictions to $z/L \in [0, +1]$. For this purpose, we write:

$$u_1/u_1(0) = g_2(z/L, \mathrm{R}^*), \qquad (4.81)$$

$$\chi_1/u_1(0) = (1/\mathrm{M}_1)g_3(z/L, \mathrm{R}^*). \qquad (4.82)$$

Fig. 4.12 shows the profiles of $u_1/u_1(0)$ and $\chi_1/u_1(0)$ that give rise to the profiles in figure 4.11.(b). Notice that $\chi_1/u_1(0)$ always reaches its maximum absolute value in the buffer layer of $u_1/u_1(0)$. Notice also that whenever there is a boundary layer the
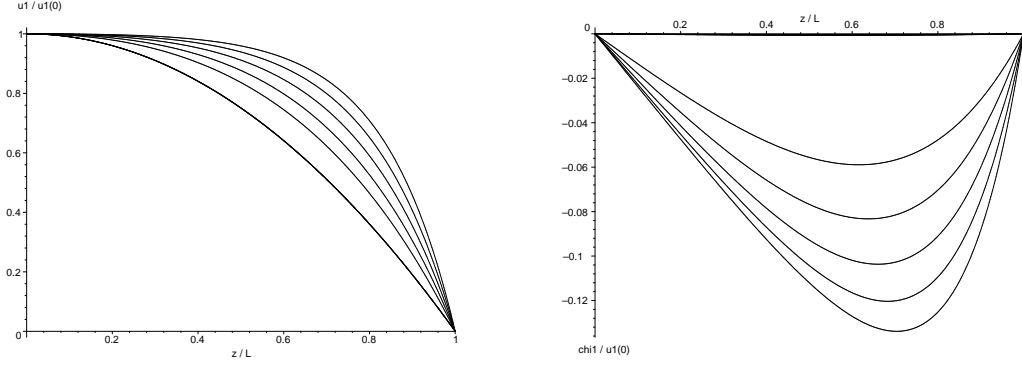
(a) R [Re] = $6 \cdot 10^5$ [$1.3 \cdot 10^7$], $5 \cdot 10^5$ [$5.7 \cdot 10^6$], $4 \cdot 10^5$ [$2.5 \cdot 10^6$], $3 \cdot 10^5$ [$1.1 \cdot 10^6$], $2 \cdot 10^5$ [$4.4 \cdot 10^5$], $2.2 \cdot 10^3$ [$2.2 \cdot 10^3$] (curves from top to bottom); $s_0 = 2 \cdot 10^{-5}$.

(b) R [Re] = $2.2 \cdot 10^3$ [$2.2 \cdot 10^3$] (vanished curve), $2 \cdot 10^5$ [$4.4 \cdot 10^5$], $3 \cdot 10^5$ [$1.1 \cdot 10^6$], $4 \cdot 10^5$ [$2.5 \cdot 10^6$], $5 \cdot 10^5$ [$5.7 \cdot 10^6$], $6 \cdot 10^5$ [$1.3 \cdot 10^7$] (curves from top to bottom); $s_0 = 2 \cdot 10^{-5}$; $M_1 = 4$.

FIGURE 4.12. EUE profiles of $u_1/u_1(0)$ and $\chi_1/u_1(0)$ for planar Poiseuille flows.

profile of $u_1/u_1(0)$ is flat with zero slope in the core layer, while ξ is non-zero: EUE predicts that transverse molecular conduction is dominated by turbulent transfer in a core layer. This is why the profile slope of $(u_1 + \chi_1)/u_1(0)$ in the core layer decreases for increasing values of M_1: one sees from (4.82) that $\chi_1/u_1(0)$ tends to zero, identically, thus $(u_1 + \chi_1)/u_1(0)$ tends to $u_1/u_1(0)$. In plots, R^* controls the boundary layer width of $u_1/u_1(0)$ at $z/L = 1$ and the point z_c/L of maximum absolute value of $\chi_1/u_1(0)$ as well as the maximum absolute value of $\chi_1/u_1(0)$: for increasing values of R^*, the boundary layer width of $u_1/u_1(0)$ at $z/L = 1$ decreases, z_c/L tends to 1 and the maximum value of $\chi_1/u_1(0)$ grows asymptotically to $1/M_1$. For $s_0 = 0$, the profiles of $u_1/u_1(0)$ collapse into the Navier-Stokes parabolic profile and $\chi_1/u_1(0)$ vanishes identically.

For comparison, Fig. 4.13.(a) shows planar Poiseuille temperature profiles given by Navier-Stokes, that is, profiles of $(T - T_0)/(T(0) - T_0)$ resulting from (4.66). We immediatly see that

$$(T - T_0)/(T(0) - T_0) = g_5(z/L). \tag{4.83}$$

Let us consider now planar Poiseuille temperature profiles given by EUE. First, we discuss the profiles of $(T - T_0)/(T(0) - T_0)$ resulting from Eq. (4.21) with the boundary conditions (4.23)–(4.24). The constants in these profiles are $s_0 \sim 2 \cdot 10^{-5}$, $\nu \sim 1.5 \cdot 10^{-5}\ m^2/s$, $\nu_c \sim 4\nu$, $\upsilon \sim 2.0 \cdot 10^{-2}\ J \cdot m^2/(kg \cdot s \cdot K)$, L, η_1 and T_0. One

(a) Navier-Stokes profiles: independent of R.

(b) Eq. (4.21) profiles: R [Re] = $6 \cdot 10^5$ [$1.3 \cdot 10^7$], $5 \cdot 10^5$ [$5.7 \cdot 10^6$], $4 \cdot 10^5$ [$2.5 \cdot 10^6$], $3 \cdot 10^5$ [$1.1 \cdot 10^6$], $2 \cdot 10^5$ [$4.4 \cdot 10^5$], $2.2 \cdot 10^3$ [$2.2 \cdot 10^3$] or any lower value (curves from top to bottom); $s_0 = 2 \cdot 10^{-5}$; $M_1 = 4$.

(c) EUE profiles: R [Re] = $6 \cdot 10^5$ [$1.3 \cdot 10^7$], $5 \cdot 10^5$ [$5.7 \cdot 10^6$], $4 \cdot 10^5$ [$2.5 \cdot 10^6$], $3 \cdot 10^5$ [$1.1 \cdot 10^6$], $2 \cdot 10^5$ [$4.4 \cdot 10^5$], $2.2 \cdot 10^3$ [$2.2 \cdot 10^3$] or any lower value (curves from top to bottom); $s_0 = 2 \cdot 10^{-5}$; Pr = 0.7; $M_1 = 4$; $M_2 = 4$.
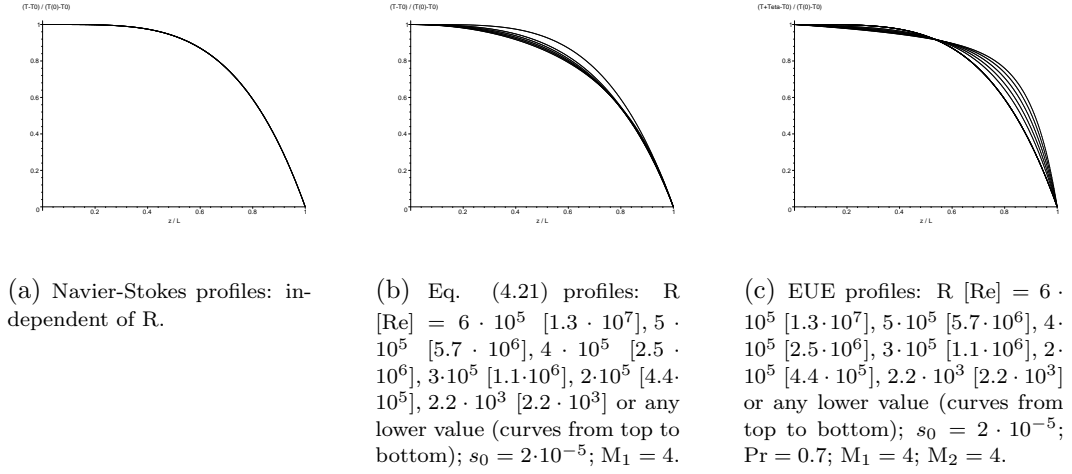
FIGURE 4.13. Navier-Stokes and EUE profiles of temperature for planar Poiseuille flows.

sees from (4.22) and (4.25)–(4.26) that

$$(T - T_0)/(T(0) - T_0) = g_6(z/L, R^*, M_1). \qquad (4.84)$$

In plots, it is observed that the analytical extension of $(T - T_0)/(T(0) - T_0)$ to $z/L \in [-1, +1]$ is an even function (as expected, because of symmetry) when the conditions (4.73)–(4.75) are satisfied. Therefore, we discuss its restriction to $z/L \in [0, +1]$. Both R^* and M_1 control the boundary layer width of $(T - T_0)/(T(0) - T_0)$ at $z/L = 1$: the width decreases for increasing values of R^* or M_1. In addition, when there is a boundary layer, R^* controls the profile slope of $(T - T_0)/(T(0) - T_0)$ in the core layer: the slope steepens for increasing values of R^*. Fig. 4.13.(b) shows some members of the R-profile family of $(T - T_0)/(T(0) - T_0)$ for $s_0 = 2 \cdot 10^{-5}$ and $M_1 = 4$.

Remark 24. *One sees from* (4.22) *and* (4.25)–(4.26) *that for* R $\gg$ 1,

$$T(0) - T_0 \sim (\nu^3/(\upsilon L^2))(1/M_1)(8/s_0^4)\,(1/R^2)\exp(s_0 R). \qquad (4.85)$$

Second, we discuss the profiles of $(T + \Theta - T_0)/(T(0) - T_0)$ resulting from Eqs. (4.12) and (4.14) with the boundary conditions (4.60)–(4.61) on T and Θ, and the scaling $s_0(|\eta_1|L^2/(2\nu))$ of ξ for $s_0 = 2 \cdot 10^{-5}$. The constants in these profiles are $s_0 \sim 2 \cdot 10^{-5}$, $\nu \sim 1.5 \cdot 10^{-5}\ m^2/s$, $\nu_c \sim 4\nu$, $c_{\rm p} \sim 10^3\ J/(kg \cdot K)$, $\upsilon \sim 2.0 \cdot 10^{-2}\ J \cdot m^2/(kg \cdot s \cdot K)$, υ_c, L, η_1 and T_0. One sees from (B.9), (B.11) and (B.25)–(B.28) that

$$(T - T_0)/(T(0) - T_0) = g_7(z/L, R^*, Pr, M_1), \qquad (4.86)$$

$$\Theta/(T(0) - T_0) = (1/M_2)g_8(z/L, R^*, Pr, M_1), \qquad (4.87)$$

thus

$$(T + \Theta - T_0)/(T(0) - T_0) = g_9(z/L, \mathrm{R}^*, \mathrm{Pr}, \mathrm{M}_1, \mathrm{M}_2). \qquad (4.88)$$

In plots, it is observed that the analytical extension of $(T + \Theta - T_0)/(T(0) - T_0)$ to $z/L \in [-1, +1]$ is an even function (as expected, because of symmetry) when the conditions (4.73)–(4.75) are satisfied. Therefore, we discuss its restriction to $z/L \in [0, +1]$. The value of M_2 was not determined from qualitative fitting with experimental profiles, because we were unable to find appropriate data. Instead, we assumed $\mathrm{Pr}_c \sim \mathrm{Pr}$ for $\mathrm{Pr}_c \equiv c_\mathrm{p} \nu_c / \upsilon_c$ and took $\mathrm{M}_2 = \mathrm{M}_1(\mathrm{Pr}/\mathrm{Pr}_c) \sim \mathrm{M}_1$. While M_1 has little effect on these profiles, R^* and Pr control the boundary layer width at $z/L = 1$, M_2 controls the slope in the core layer. Indeed, the boundary layer width at $z/L = 1$ decreases for increasing values of R^* or Pr, the slope in the core layer decreases for increasing values of M_2. Fig. 4.13.(c) shows some members of the R-profile family of $(T + \Theta - T_0)/(T(0) - T_0)$ for $s_0 = 2 \cdot 10^{-5}$, $\mathrm{M}_1 = 4$, $\mathrm{Pr} = 0.7$ (air) and $\mathrm{M}_2 = 4$.

Remark 25. *One sees from* (B.9), (B.11) *and* (B.25)–(B.28) *that for* $\mathrm{R} \gg 1$,

$$T(0) - T_0 \sim (\nu^3/(\upsilon L^2))((\mathrm{M}_1 - 1)/\mathrm{M}_1)(1/(2 - \mathrm{Pr}))(8/s_0^4)\,(1/\mathrm{R}^2)\exp(s_0\mathrm{R}) \quad if \quad \mathrm{Pr} < 1, \qquad (4.89)$$

$$T(0) - T_0 \sim (\nu^3/(\upsilon L^2))(1/\mathrm{M}_1)(1/\mathrm{Pr}^2)(1/(\mathrm{Pr} - 1))(32/s_0^5)\,(1/\mathrm{R}^3)\exp(s_0\mathrm{R}(\mathrm{Pr} + 1)/2) \quad if \quad \mathrm{Pr} > 1. \qquad (4.90)$$

Thus, the one-dimensional EUE *description of planar Poiseuille flows predicts different core flow temperature relationships with* R *depending on whether* $\mathrm{Pr} < 1$ *or* $\mathrm{Pr} > 1$. *Notice that Eq.* (4.85), *which is independent of* Pr, *agrees with Eq.* (4.89).
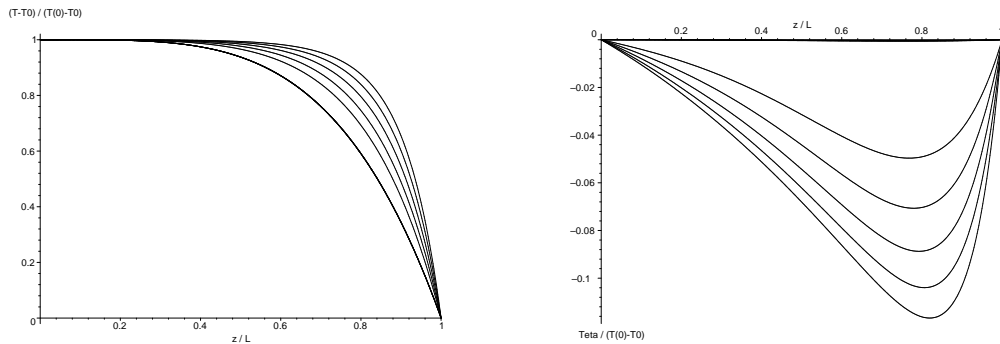
(a) R [Re] = $6 \cdot 10^5$ [$1.3 \cdot 10^7$], $5 \cdot 10^5$ [$5.7 \cdot 10^6$], $4 \cdot 10^5$ [$2.5 \cdot 10^6$], $3 \cdot 10^5$ [$1.1 \cdot 10^6$], $2 \cdot 10^5$ [$4.4 \cdot 10^5$], $2.2 \cdot 10^3$ [$2.2 \cdot 10^3$] (curves from top to bottom); $s_0 = 2 \cdot 10^{-5}$; Pr = 0.7; $\mathrm{M}_1 = 4$.

(b) R [Re] = $2.2 \cdot 10^3$ [$2.2 \cdot 10^3$] (vanished curve), $2 \cdot 10^5$ [$4.4 \cdot 10^5$], $3 \cdot 10^5$ [$1.1 \cdot 10^6$], $4 \cdot 10^5$ [$2.5 \cdot 10^6$], $5 \cdot 10^5$ [$5.7 \cdot 10^6$], $6 \cdot 10^5$ [$1.3 \cdot 10^7$] (curves from top to bottom); $s_0 = 2 \cdot 10^{-5}$; Pr = 0.7; $\mathrm{M}_1 = 4$; $\mathrm{M}_2 = 4$.

FIGURE 4.14. EUE profiles of $(T - T_0)/(T(0) - T_0)$ and $\Theta/(T(0) - T_0)$ for planar Poiseuille flows.

Like $(T+\Theta-T_0)/(T(0)-T_0)$, the analytical extensions of $(T-T_0)/(T(0)-T_0)$ and $\Theta/(T(0)-T_0)$ to $z/L \in [-1,+1]$ are observed in plots to be even functions when the conditions (4.73)–(4.75) are satisfied. Therefore, we discuss their restrictions to $z/L \in [0,+1]$. Fig. 4.14 shows the profiles of $(T-T_0)/(T(0)-T_0)$ and $\Theta/(T(0)-T_0)$ that give rise to the profiles of Fig. 4.13.(c). Notice that $\Theta/(T(0)-T_0)$ always reaches its maximum absolute value in the buffer layer of $(T-T_0)/(T(0)-T_0)$. Notice also that whenever there is a boundary layer the profile of $(T-T_0)/(T(0)-T_0)$ is flat with zero slope in the core layer, while ξ is non-zero: EUE predicts that transverse molecular conduction is dominated by turbulent transfer in a core layer. This is why the profile slope of $(T+\Theta-T_0)/(T(0)-T_0)$ in the core layer decreases for increasing values of M_2: one sees from (4.87) that $\Theta/(T(0)-T_0)$ tends to zero, identically, thus $(T+\Theta-T_0)/(T(0)-T_0)$ tends to $(T-T_0)/(T(0)-T_0)$. While M_1 has little effect on these profiles, R^* and Pr control the boundary layer width of $(T-T_0)/(T(0)-T_0)$ at $z/L = 1$ and the point z_c/L of maximum absolute value of $\Theta/(T(0)-T_0)$ as well as the maximum absolute value of $\Theta/(T(0)-T_0)$. Indeed, for increasing values of R^* or Pr, the boundary layer width of $(T-T_0)/(T(0)-T_0)$ at $z/L = 1$ decreases, z_c/L tends to 1 and the maximum absolute value of $\Theta/(T(0)-T_0)$ grows asymptotically to $1/M_2$.
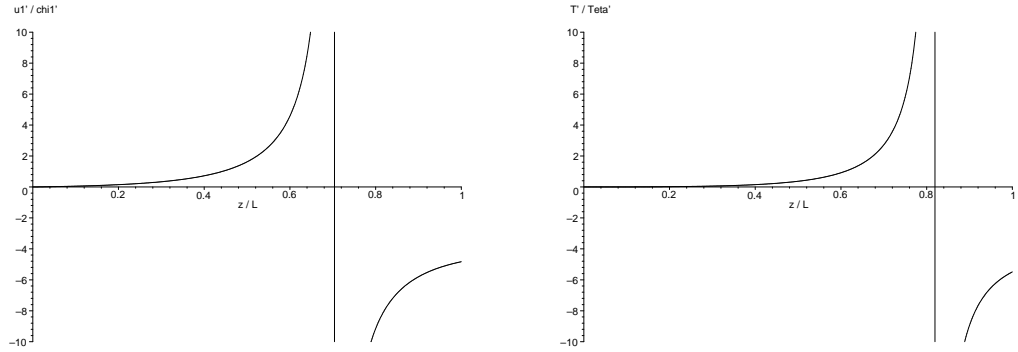
(a) R [Re] $= 6 \cdot 10^5$ [$1.3 \cdot 10^7$]; $s_0 = 2 \cdot 10^{-5}$; $M_1 = 4$.

(b) R [Re] $= 6 \cdot 10^5$ [$1.3 \cdot 10^7$]; $s_0 = 2 \cdot 10^{-5}$; Pr $= 0.7$; $M_1 = 4$; $M_2 = 4$.

FIGURE 4.15. EUE profiles of u_1'/χ_1' and T'/Θ' for planar Poiseuille flows.

Fig. 4.15 shows EUE profiles of u_1'/χ_1' and T'/Θ' linked to the profiles in 4.12 and 4.14. Notice that the conditions (3.25)–(3.26) are satisfied, therefore the entropy source term (3.24) in the upscaled description is non-negative. The same is true for any other value of R.

(a) R [Re] = $2.2 \cdot 10^3$ [$2.2 \cdot 10^3$], $2 \cdot 10^5$ [$4.4 \cdot 10^5$], $3 \cdot 10^5$ [$1.1 \cdot 10^6$], $4 \cdot 10^5$ [$2.5 \cdot 10^6$], $5 \cdot 10^5$ [$5.7 \cdot 10^6$], $6 \cdot 10^5$ [$1.3 \cdot 10^7$] (curves from top to bottom); $s_0 = 2 \cdot 10^{-5}$; $M_1 = 4$.

(b) R [Re] = $2.2 \cdot 10^3$ [$2.2 \cdot 10^3$], $2 \cdot 10^5$ [$4.4 \cdot 10^5$], $3 \cdot 10^5$ [$1.1 \cdot 10^6$], $4 \cdot 10^5$ [$2.5 \cdot 10^6$], $5 \cdot 10^5$ [$5.7 \cdot 10^6$], $6 \cdot 10^5$ [$1.3 \cdot 10^7$] (curves from top to bottom); $s_0 = 2 \cdot 10^{-5}$; Pr = 0.7; $M_1 = 4$; $M_2 = 4$.

(c) R [Re] = $2.2 \cdot 10^3$ [$2.2 \cdot 10^3$], $2 \cdot 10^5$ [$4.4 \cdot 10^5$], $3 \cdot 10^5$ [$1.1 \cdot 10^6$], $4 \cdot 10^5$ [$2.5 \cdot 10^6$], $5 \cdot 10^5$ [$5.7 \cdot 10^6$], $6 \cdot 10^5$ [$1.3 \cdot 10^7$] (curves from top to bottom); $s_0 = 2 \cdot 10^{-5}$; Pr = 0.7; $M_1 = 4$; $M_2 = 4$.
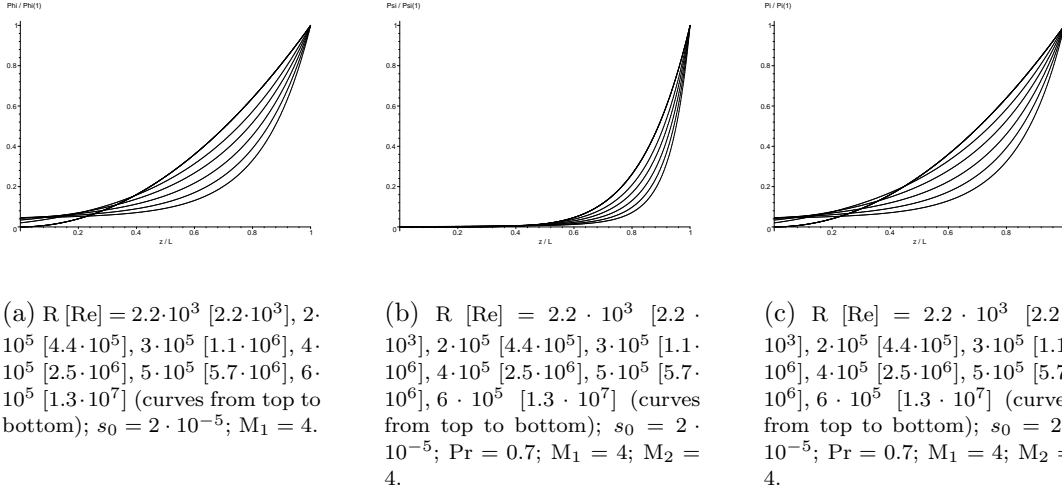
FIGURE 4.16. EUE profiles of the viscous dissipation functions in the upscaled description and profiles of the entropy source term in the upscaled description, for planar Poiseuille flows.

Fig. 4.16 shows EUE profiles of the viscous dissipation functions in the upscaled description and profiles of the entropy source term in the upscaled description, for planar Poiseuille flows. These quantities are defined in (2.68), (3.23) and (3.24). Here, we have $\Phi/\rho = (\nu u_1' + \nu_c \chi_1')(u_1' + \chi_1')$, $\Psi/\rho = (\upsilon T' + \upsilon_c \Theta')(T' + \Theta')$ and $\Pi = (\Phi/\rho)/(T + \Theta) + (\chi_1 \eta_1)/(T + \Theta) + (\Psi/\rho)/(T + \Theta)^2$. Notice that the three quantities are non-negative (as their values at $z/L = 1$ can be shown to be non-negative) and that non-equilibrium occurs mainly in the boundary layer (whenever the boundary layer exists).

5. CONCLUSION

We propose a model for underresolved predictions of the large scale evolution of flows, the Extended Upscaled Euler model (EUE). The model stands for a statistical upscaling of the Euler equations onto a local equilibrium mechanism that satisfies the total energy conservation principle and is phenomenologically extended to describe irreversible processes in finite-time transformations of bulk elements of fluid. The closure assumptions apply to both the enthalpy and the internal energy representations of heat balance. The pressure gradient arises as an affinity ([7, 11]) of the entropy source term in the upscaled description. The turbulence mechanism has a curl formulation. The model can be readily extended to comprise a compressible

turbulent mixing mechanism for passive species, namely:

$$\partial_t(\rho c_i) + \nabla \cdot (\mathbf{u}\rho c_i + \boldsymbol{\chi}\rho c_i - \mathrm{k}\nabla c_i) = 0, \tag{5.1}$$

$$\partial_t(\rho\Xi) + \nabla \cdot (\mathbf{u}\rho\Xi - \boldsymbol{\chi}\rho c_i - \mathrm{k}_c\nabla\Xi) = 0, \tag{5.2}$$

where

$$\Xi \equiv \langle \rho' c_i' \rangle / \langle \rho \rangle. \tag{5.3}$$

We tested the one-dimensional EUE qualitative description of planar Couette, planar Poiseuille and Ekman flows. This was done by scaling the variable χ_3, a procedure that does not fully validate the model for these flows. The main results are the following. The viscous dissipation functions and the entropy source term have non-negative values in the upscaled description of planar Couette and planar Poiseuille flows. The viscous dissipation function Φ has non-negative values in the upscaled description of Ekman flows (the enthalpy equation was not solved for these flows, therefore the viscous dissipation function Ψ and the entropy source term were not discussed). Qualitative agreement with experimental profiles is found for a wide range of the Reynolds number, including the transition ranges to turbulence. This agreement occurs for strongly underresolved solutions (stationary one-dimensional solutions) despite using constant values of μ_c and λ_c (this constancy reflects scale-independence) and, remarkably, the same values for the three case studies. For undercritical values of the Reynolds number, EUE profiles overlap with Navier-Stokes profiles. In the supercritical solutions of EUE, molecular conduction is dominated by turbulent transfer in the core layers, the variables of turbulence reach their maximum values in the buffer layers and non-equilibrium occurs mainly in the boundary layers. The supercritical solutions of EUE for planar Poiseuille flows exhibit a much higher frictional heating than the corresponding Navier-Stokes solutions, especially for values of the Prandtl number larger than one. The same is true for planar Couette flows provided the Prandtl number is larger than one. When Θ is replaced by zero, these effects of the Prandtl number are lost. The core flow velocity relationship with pressure gradient obtained in the supercritical solutions of EUE for planar Poiseuille flows is rather different from the experimental relationship for turbulent pipe flows. Therefore, we expect the same to be true about the core flow temperature relationship with pressure gradient.

Appendix A. The Ekman flows

We consider frictional flows driven by a geostrophic core flow and a planar differentially rotating plate ([1]), and describe them as stationary flows in the upscaled description that depend only on the direction z orthogonal to the plate. This includes describing the exact (that is, in all scales) stationary states of these flows, that occur in laminar regimes, given by the corresponding Navier-Stokes description.

We employ the constant ρ thermodynamic limit, where p is treated as a dynamic pressure through the substitution of the state equation by $\nabla \cdot \mathbf{u} = 0$, and disregard the balances of enthalpy. Therefore, the EUE model (2.70)–(2.76) becomes:

$$\partial_j(u_j\mathbf{u} + \chi_j\mathbf{u} - \nu\partial_j\mathbf{u}) = \mathbf{u} \times 2\mathbf{\Omega} - \nabla(p/\rho + \phi), \tag{A.1}$$

$$\nabla \cdot \mathbf{u} = 0, \tag{A.2}$$

$$\partial_j(u_j\boldsymbol{\chi} - \chi_j\mathbf{u} - \nu_c\partial_j\boldsymbol{\chi}) = \boldsymbol{\chi} \times 2\mathbf{\Omega}, \tag{A.3}$$

$$\nabla \cdot \boldsymbol{\chi} = 0, \tag{A.4}$$

where

$$\nabla(-\phi) \equiv \mathbf{g}, \quad \nu \equiv \mu/\rho, \quad \nu_c \equiv \mu_c/\rho. \tag{A.5}$$

We take $\Omega \equiv |\mathbf{\Omega}|$ sufficiently small for centrifugal effects to be negligible, therefore $\mathbf{g} = \mathbf{g}_0$. We assume that $\mathbf{g}_0$ is constant and orthogonal to the plate (as it is in a tank experiment). Under these conditions and for solutions that depend only on the direction z orthogonal to the boundary, Eqs. (A.1)–(A.4) read:

$$d_z(u_3u_1 + \chi_3u_1 - \nu\, d_zu_1) = +2\Omega u_2 - \partial_x(p/\rho), \tag{A.6}$$

$$d_z(u_3u_2 + \chi_3u_2 - \nu\, d_zu_2) = -2\Omega u_1 - \partial_y(p/\rho), \tag{A.7}$$

$$d_z(u_3u_3 + \chi_3u_3 - \nu\, d_zu_3) = -g_0 - \partial_z(p/\rho), \tag{A.8}$$

$$d_zu_3 = 0, \tag{A.9}$$

$$d_z(u_3\chi_1 - \chi_3u_1 - \nu_c\, d_z\chi_1) = +2\Omega\chi_2, \tag{A.10}$$

$$d_z(u_3\chi_2 - \chi_3u_2 - \nu_c\, d_z\chi_2) = -2\Omega\chi_1, \tag{A.11}$$

$$d_z(-\nu_c\, d_z\chi_3) = 0, \tag{A.12}$$

$$d_z\chi_3 = 0, \tag{A.13}$$

where d_z stands for the derivative of a function that depends only on z.

From (A.9), u_3 is constant. Hence, $u_3 = 0$ for an impermeable boundary. In this case, Eq. (A.8) reduces to $\partial_z(p/\rho) = -g_0$. Consequently $\partial_z\partial_x(p/\rho) = \partial_x\partial_z(p/\rho) = 0$ and $\partial_z\partial_y(p/\rho) = \partial_y\partial_z(p/\rho) = 0$, that is $\partial_x(p/\rho)$ and $\partial_y(p/\rho)$ must be constant. From Eq. (A.13), χ_3 is constant. With $u_3 = 0$ and χ_3 constant, Eq. (A.7) and Eq. (A.11) become linear. Thus, for $\partial_y(p/\rho) = 0$ and for homogeneous boundary conditions on u_2 and χ_2 we obtain $u_2 = 0$ and $\chi_2 = 0$. Therefore, the system (A.6)–(A.13) reduces to:

$$\nu u_1'' - \xi u_1' + 2\Omega u_2 = \eta_1, \tag{A.14}$$

$$\nu u_2'' - \xi u_2' - 2\Omega u_1 = \eta_2, \tag{A.15}$$

$$\nu_c\chi_1'' + \xi u_1' + 2\Omega\chi_2 = 0, \tag{A.16}$$

$$\nu_c\chi_2'' + \xi u_2' - 2\Omega\chi_1 = 0, \tag{A.17}$$

where

$$f' \equiv d_z f, \tag{A.18}$$

$$\xi \equiv \chi_3, \tag{A.19}$$

$$\eta_1 \equiv \partial_x(p/\rho), \tag{A.20}$$

$$\eta_2 \equiv \partial_y(p/\rho). \tag{A.21}$$

Remark 26. *For $\xi = 0$, the solution of Eqs. (A.16)–(A.17) with the homogeneous boundary conditions $\chi_1 = 0$ and $\chi_2 = 0$ at $z = 0$ and $z = L$ is zero. This means that the turbulence mechanism (2.73)–(2.75) does not take place in one-dimensional frictional flows. Thus, the strictly one-dimensional approximation of* EUE *is inadequate to describe frictional flows. Therefore, in this study our goal will be limited to finding the* EUE *qualitative description of Ekman flows by providing some scaling of ξ.*

We assume that the turbulence field vanishes at the plate and at some fixed height $z = L$ where the flow is geostrophic ([1]). Therefore, we take for boundary conditions:

$$u_1(0) = \ 0 \ , \ \ \chi_1(0) = 0, \ \ u_2(0) \ = \ 0 \ , \ \ \chi_2(0) = 0, \tag{A.22}$$

$$u_1(L) = U_1, \ \ \chi_1(L) = 0, \ \ u_2(L) = U_2, \ \ \chi_2(L) = 0, \tag{A.23}$$

where

$$U_1 = -\eta_2/(2\Omega), \tag{A.24}$$

$$U_2 = +\eta_1/(2\Omega). \tag{A.25}$$

We show in Appendix C that the solution of the linear system of ordinary differential equations (A.14)–(A.17) with the boundary conditions (A.22)–(A.23) is given by polynomials in $\cos(z)$ and $\exp(z)$. See Eqs. (C.9)–(C.12) and (C.29)–(C.36).

Remark 27. *The compressible Navier-Stokes equations may be written as:*

$$\partial_t(\rho h - p) + \nabla \cdot (\mathbf{u}(\rho h - p) - \lambda \nabla T) = \Phi,$$

$$\partial_t(\rho \mathbf{u}) + \partial_j(u_j \rho \mathbf{u} - \mu \partial_j \mathbf{u}) = \rho \mathbf{u} \times 2\mathbf{\Omega} + \rho \mathbf{g} - \nabla p,$$

$$\partial_t \rho + \nabla \cdot (\mathbf{u}\rho) = 0,$$

where $h = c_{\mathrm{p}}T$ and $\Phi \equiv (\mu \nabla u_i) \cdot \nabla u_i = \mu(\nabla u_i)^2$. For Ekman flows, these equations reduce to:

$$\nu u_1'' + 2\Omega u_2 = \eta_1, \tag{A.26}$$

$$\nu u_2'' - 2\Omega u_1 = \eta_2, \tag{A.27}$$

where $f' \equiv d_z f$, $\nu \equiv \mu/\rho$, $\eta_1 \equiv \partial_x(p/\rho)$ and $\eta_2 \equiv \partial_y(p/\rho)$. With the boundary conditions

$$u_1(0) = \ 0 \ , \ \ u_2(0) \ = \ 0, \tag{A.28}$$

$$u_1(L) = U_1, \ \ u_2(L) = 0, \tag{A.29}$$

we obtain:

$$u_1 = U_1(1 - \cos(z/\delta_E) \ e^{-z/\delta_E}), \tag{A.30}$$

$$u_2 = U_1 \ \text{sen}(z/\delta_E) \ e^{-z/\delta_E}, \tag{A.31}$$
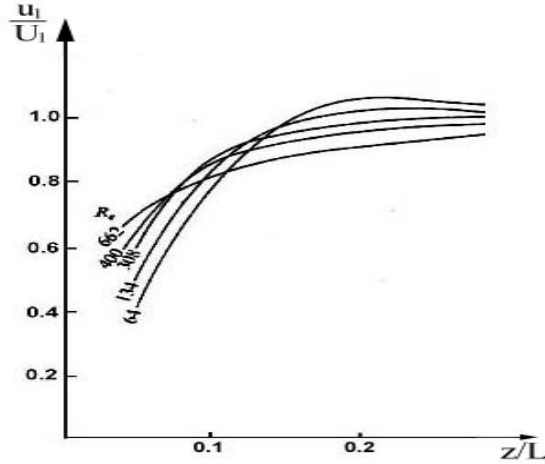
where

$$\delta_E \equiv (\nu/\Omega)^{1/2}. \tag{A.32}$$

FIGURE A.1. Experimental profiles of momentum in Ekman flows, by Caldwell and van Atta [3] (permission to reproduce requested). Here, Re is defined by $U_1/(\nu\Omega)^{1/2}$. This number is 10 times smaller than the Reynolds number $|U_1|L/\nu$ we employ in EUE figures, where $\Omega \sim \nu/(0.1L)^2$.

Next, we show the Ekman profiles resulting from Eqs. (A.14)–(A.17) with the boundary conditions (A.22)–(A.23) and the scaling $s|U_1|$ of ξ for some constant s. Without loss of generality, we take $U_2 = 0$. One sees from (C.13), (C.15) and (C.27) that $r_1 \sim +(\Omega/\nu)^{1/2}$ and $r_2 \sim -(\Omega/\nu)^{1/2}$ for $\xi^2 \ll 8\nu\Omega$. Hence, from (C.9), the boundary layer width of u_1 is $\delta \sim (\nu/\Omega)^{1/2} = \delta_E$. Therefore we take $\Omega \sim \nu/(0.1L)^2$, so that $\delta \sim 0.1L$ (where L is a fixed height where we want the flow to be geostrophic). The constants in these profiles are s, $\nu \sim 1.5 \cdot 10^{-5} \ m^2/s$, ν_c, L and U_1. The family of $(u_1 + \chi_1)/U_1$ profiles parameterized by the Reynolds number $\text{Re} \equiv |U_1|L/\nu$ that fit best qualitatively the experimental profiles of Caldwell and

van Atta ([3]), shown in Fig. A.1, is obtained for $s \sim -2 \cdot 10^{-3}$ and $\nu_c \sim 4\nu$. The conditions $\xi^2/(8\nu\Omega) \ll 1$ and Ro $\ll 1$, where Ro $\equiv |U_1|/(2\Omega L)$ is the Rossby number (which must be small for the core flows to be geostrophic [1]), imply the conditions Re $\ll (L/|s|)(8\Omega/\nu)^{1/2}$ and Re $\ll L^2(2\Omega/\nu)$. For $\Omega \sim \nu/(0.1L)^2$ and $s \sim -2 \cdot 10^{-3}$, they become Re $\ll 1 \cdot 10^4$ and Re $\ll 2 \cdot 10^2$ respectively. In the Ekman profiles soon to be shown and resulting from Eqs. (A.14)–(A.17), we explore Re values that strongly violate the second of these conditions. Therefore, we expect the profiles for these Re values to be non-physical. According to Caldwell, van Atta ([3]) and Faller ([8]), the onset of fluctuations in the flow velocity is observed for $U_1/(\nu\Omega)^{1/2} \sim 1 \cdot 10^2$; for $\Omega \sim \nu/(0.1L)^2$, this value corresponds to Re $\sim 1 \cdot 10^3$. Notice from Fig. A.6.(b) that the sufficient condition (3.25) is violated; this occurs for any value of the Reynolds number. Still, one sees from Fig. A.7 that the viscous dissipation function Φ is non-negative.
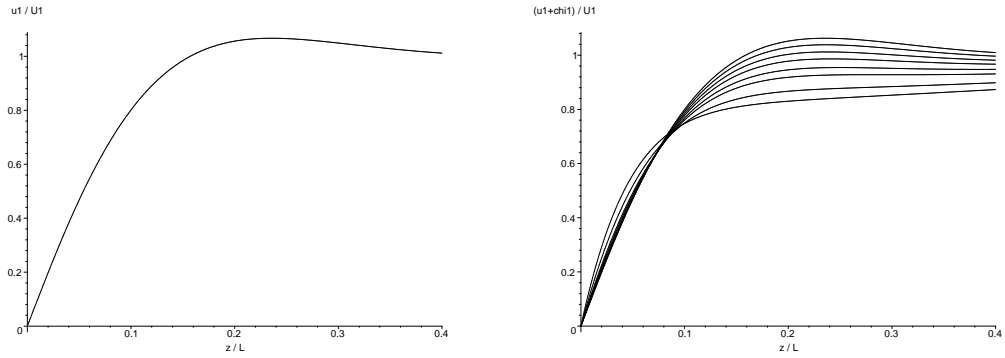
(a) Navier-Stokes profiles: independent of Re; $\Omega \sim \nu/(0.1L)^2$.

(b) EUE profiles: Re $= 1.0 \cdot 10^2, 6.5 \cdot 10^2, 1.3 \cdot 10^3, 2.0{\cdot}10^3, 3.0{\cdot}10^3, 4.0{\cdot}10^3, 6.6{\cdot}10^3, 1.0{\cdot}10^4, 1.5{\cdot} 10^4, 2.0 \cdot 10^4, 2.5 \cdot 10^4$ (curves from top to bottom at $z/L = 0.2$); $s = -2 \cdot 10^{-3}$; $\nu_c = 4\nu$; $\Omega \sim \nu/(0.1L)^2$.

FIGURE A.2. Navier-Stokes and EUE profiles of the first component of momentum for Ekman flows.
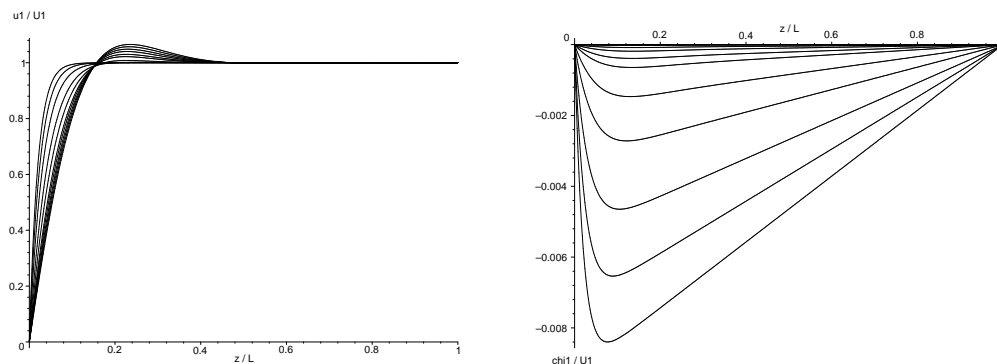
(a) Re $= 1.0 \cdot 10^2$, $6.5 \cdot 10^2$, $1.3 \cdot 10^3$, $2.0 \cdot 10^3$, $3.0 \cdot 10^3$, $4.0 \cdot 10^3$, $6.6 \cdot 10^3$, $1.0 \cdot 10^4$, $1.5 \cdot 10^4$, $2.0 \cdot 10^4$, $2.5 \cdot 10^4$ (curves from top to bottom at $z/L = 0.2$); $s = -2 \cdot 10^{-3}$; $\Omega \sim \nu/(0.1L)^2$.

(b) Re $= 1.0 \cdot 10^2$, $6.5 \cdot 10^2$, $1.3 \cdot 10^3$, $2.0 \cdot 10^3$, $3.0 \cdot 10^3$, $4.0 \cdot 10^3$, $6.6 \cdot 10^3$, $1.0 \cdot 10^4$, $1.5 \cdot 10^4$, $2.0 \cdot 10^4$, $2.5 \cdot 10^4$ (curves from top to bottom); $s = -2 \cdot 10^{-3}$; $\nu_c = 4\nu$; $\Omega \sim \nu/(0.1L)^2$.

FIGURE A.3. EUE profiles of u_1/U_1 and χ_1/U_1 for Ekman flows.

(a) Navier-Stokes profiles: independent of Re; $\Omega \sim \nu/(0.1L)^2$.

(b) EUE profiles: $1.0 \cdot 10^2$, $6.5 \cdot 10^2$, $1.3 \cdot 10^3$, $2.0 \cdot 10^3$, $3.0 \cdot 10^3$, $4.0 \cdot 10^3$, $6.6 \cdot 10^3$, $1.0 \cdot 10^4$, $1.5 \cdot 10^4$, $2.0 \cdot 10^4$, $2.5 \cdot 10^4$ (curves from top to bottom at $z/L = 0.1$); $s = -2 \cdot 10^{-3}$; $\nu_c = 4\nu$; $\Omega \sim \nu/(0.1L)^2$.
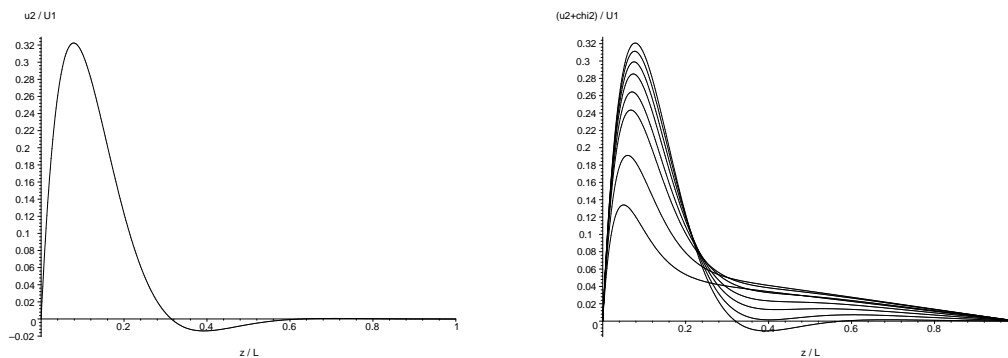
FIGURE A.4. Navier-Stokes and EUE profiles of the second component of momentum for Ekman flows.
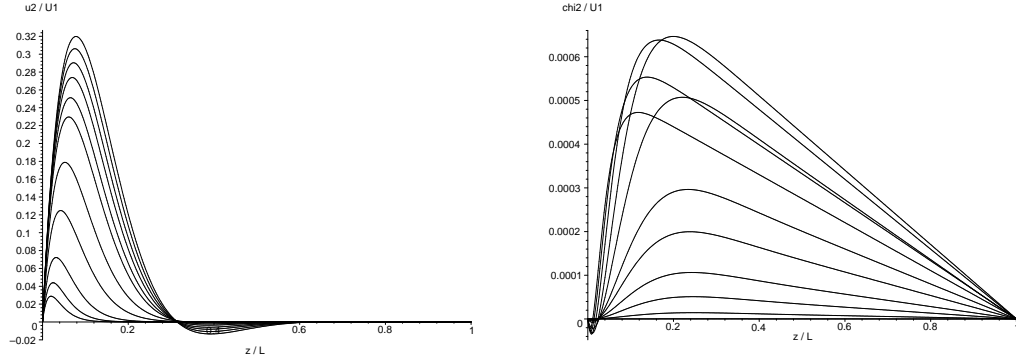
(a) $\text{Re} = 1.0 \cdot 10^2, 6.5 \cdot 10^2, 1.3 \cdot 10^3, 2.0 \cdot 10^3, 3.0 \cdot 10^3, 4.0 \cdot 10^3, 6.6 \cdot 10^3, 1.0 \cdot 10^4, 1.5 \cdot 10^4, 2.0 \cdot 10^4, 2.5 \cdot 10^4$ (curves from top to bottom at $z/L = 0.1$); $s = -2 \cdot 10^{-3}$; $\Omega \sim \nu/(0.1L)^2$.

(b) $\text{Re} = 1.0 \cdot 10^2, 6.5 \cdot 10^2, 1.3 \cdot 10^3, 2.0 \cdot 10^3, 3.0 \cdot 10^3, 4.0 \cdot 10^3, 6.6 \cdot 10^3, 1.0 \cdot 10^4, 1.5 \cdot 10^4, 2.0 \cdot 10^4, 2.5 \cdot 10^4$ (curves with amplitudes $\sim$ vanish., $1 \cdot 10^{-5}, 5 \cdot 10^{-5}, 1 \cdot 10^{-4}, 2 \cdot 10^{-4}, 3 \cdot 10^{-4}, 5 \cdot 10^{-4}, 6.6 \cdot 10^{-4}, 6.4 \cdot 10^{-4}, 5.5 \cdot 10^{-4}, 4.7 \cdot 10^{-4}$); $s = -2 \cdot 10^{-3}$; $\nu_c = 4\nu$; $\Omega \sim \nu/(0.1L)^2$.

FIGURE A.5. EUE profiles of u_2/U_1 and χ_2/U_1 for Ekman flows.
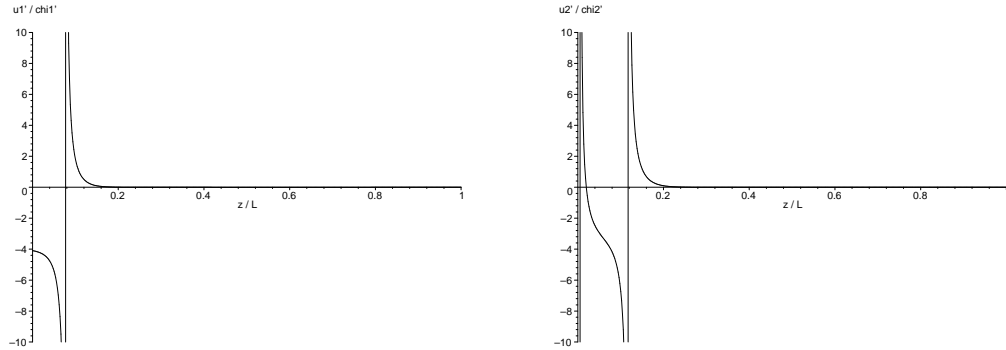
(a) $\text{Re} = 2.5 \cdot 10^4$; $s = -2 \cdot 10^{-3}$; $\nu_c = 4\nu$; $\Omega \sim \nu/(0.1L)^2$.

(b) $\text{Re} = 2.5 \cdot 10^4$; $s = -2 \cdot 10^{-3}$; $\nu_c = 4\nu$; $\Omega \sim \nu/(0.1L)^2$.

FIGURE A.6. EUE profiles of u_1'/χ_1' and u_2'/χ_2' for Ekman flows.
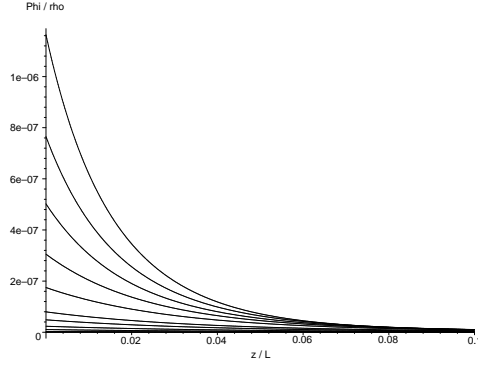
FIGURE A.7. EUE profiles of the viscous dissipation function Φ/ρ: Re $= 2.5 \cdot 10^4$, $2.0 \cdot 10^4$, $1.5 \cdot 10^4$, $1.0 \cdot 10^4$, $6.6 \cdot 10^3$, $4.0 \cdot 10^3$, $3.0 \cdot 10^3$, $2.0 \cdot 10^3$, $1.3 \cdot 10^3$ (curves from top to bottom); $s = -2 \cdot 10^{-3}$; $\nu_c = 4\nu$.

APPENDIX B. DERIVATION OF THE STATIONARY ONE-DIMENSIONAL EUE SOLUTION FOR PLANAR COUETTE AND PLANAR POISEUILLE FLOWS

The non-linear system (4.12)–(4.15) has a general solution: following the order (4.13), (4.15), (4.12) and (4.14), the equations can be solved one by one as linear equations with constant coefficients. Here, we derive this general solution.

Rearranged, the system reads:

$$\nu u_1'' - \xi u_1' = \eta_1, \tag{B.1}$$

$$\nu_c \chi_1'' + \xi u_1' = 0, \tag{B.2}$$

$$\upsilon T'' - \xi c_{\mathrm{p}} T' = -(\nu u_1')(u_1' + \chi_1'), \tag{B.3}$$

$$\upsilon_c \Theta'' + \xi c_{\mathrm{p}} T' = -(\nu_c \chi_1')(u_1' + \chi_1') - \chi_1 \eta_1. \tag{B.4}$$

The linear equation with constant coefficients (B.1) is non-homogeneous for $\eta_1 \neq 0$, in which case $u_{1p} \equiv az$ is a particular solution of this equation for $a \equiv -\eta_1/\xi$. $A_r e^{rz}$ is a non-trivial solution of $\nu u_1'' - \xi u_1' = 0$ only if $\nu r^2 - \xi r = 0$ *i.e.* $r = 0$, ξ/ν. Hence, the general solution of the homogeneous part of (B.1) reads $u_{1h} \equiv A_1 + A_2 \, e^{r_2 z}$, with $r_2 \equiv \xi/\nu$. As $u_1 = u_{1p} + u_{1h}$, we obtain:

$$u_1 = az + A_1 + A_2 \, e^{r_2 z}. \tag{B.5}$$

Taking into account (B.5), the linear equation with constant coefficients (B.2) is equivalent to

$$\chi_1' = -(\xi/\nu_c)u_1 + B_1 = -(\xi/\nu_c)(az + A_1 + A_2\, e^{r_2 z}) + B_1,$$

or else, to

$$\chi_1 = -(\xi/\nu_c)(a/2)z^2 - (\xi/\nu_c)A_1 z - (\xi/\nu_c)(A_2/r_2)\, e^{r_2 z} + B_1 z + B_0. \qquad (B.6)$$

Taking into account (B.5) and (B.6), Eq. (B.3) is non-homogeneous linear with constant coefficients, where $-(\nu u_1')(u_1' + \chi_1')$ is the source term. $T_p \equiv c_2 z^2 + c_1 z + (d_1 z + d_0)\, e^{r_2 z} + d\, e^{2r_2 z}$ is a particular solution of this equation if, and only if:

$$c_1 = \nu a(\nu a - a\nu_c c_{\mathrm{p}} - B_1 \nu_c c_{\mathrm{p}} + \xi A_1 c_{\mathrm{p}})\,/\,(-\xi c_{\mathrm{p}}^2 \nu_c),$$

$$c_2 = \nu a^2\,/\,(-2c_{\mathrm{p}}\nu_c),$$

$$d_0 = (\nu A_2/\nu_c)(-2ar_2\nu_c\nu + 2a\nu_c\xi c_{\mathrm{p}} - \nu a\xi + r_2\xi A_1\nu - \xi^2 A_1 c_{\mathrm{p}}$$
$$\qquad - r_2 B_1 \nu_c\nu + B_1\nu_c\xi c_{\mathrm{p}})\,/\,(\nu^2 r_2^2 - 2\nu r_2\xi c_{\mathrm{p}} + \xi^2 c_{\mathrm{p}}^2),$$

$$d_1 = (\nu a A_2 \xi/\nu_c)\,/\,(\nu r_2 - \xi c_{\mathrm{p}}),$$

$$d\ = (\nu A_2^2/\nu_c)(\xi - r_2\nu_c)/(4\nu r_2 - 2\xi c_{\mathrm{p}}).$$

$A_s e^{sz}$ is a non-trivial solution of $\nu T'' - \xi c_{\mathrm{p}} T' = 0$ only if $\nu s^2 - \xi c_{\mathrm{p}} s = 0$ *i.e.* $s = 0,\ \xi c_{\mathrm{p}}/\nu$. Hence, the general solution of the homogeneous part of (B.3) reads $T_h \equiv E_1 + E_2\, e^{s_2 z}$, with $s_2 \equiv \xi c_{\mathrm{p}}/\nu$. As $T = T_p + T_h$, we obtain:

$$T \equiv c_2 z^2 + c_1 z + (d_1 z + d_0)\, e^{r_2 z} + d\, e^{2r_2 z} + E_1 + E_2\, e^{s_2 z}. \qquad (B.7)$$

Taking into account (B.5), (B.6) and (B.7), Eq. (B.4) reads

$$\begin{aligned}
\Theta'' = &((24r_2^3\xi^2 a^2 s_2 - 12r_2^3\xi a s_2\eta_1)z^2 + (24r_2^3 s_2\eta_1 B_1\nu_c - 24r_2^3 s_2\eta_1\xi A_1 \\
&- 48r_2^3 s_2\xi a B_1\nu_c + 48r_2^3 s_2\xi c_{\mathrm{p}}\nu_c c_2 - 24r_2^3 s_2 a^2\nu_c\xi + 48r_2^3 s_2\xi^2 a A_1)z \\
&+ (24r_2^3 s_2\xi^2 A_1^2 + 24r_2^3 s_2 a\nu_c^2 B_1 + 24r_2^3 s_2\eta_1 B_0\nu_c + 24r_2^3 s_2 B_1^2\nu_c^2 \\
&+ 24r_2^3 s_2\xi c_{\mathrm{p}}\nu_c c_1 - 48r_2^3 s_2\xi A_1 B_1\nu_c - 24r_2^3 s_2 a\nu_c\xi A_1) + (24\xi c_{\mathrm{p}}\nu_c s_2 r_2^3 E_2)\, e^{s_2 z} \\
&+ ((24s_2\xi r_2^2 c_{\mathrm{p}}\nu_c d_1 - 24s_2\xi r_2^2 A_2\nu_c a + 48s_2\xi^2 r_2 a A_2)(1 + r_2 z) + 48s_2 r_2^2\xi^2 A_1 A_2 \\
&- 48s_2 r_2^2\xi A_2 B_1\nu_c - 24s_2\xi c_{\mathrm{p}}\nu_c r_2^2 d_1 + 24s_2\xi c_{\mathrm{p}}\nu_c r_2^3 d_0 - 24s_2 A_2 r_2^3\nu_c\xi A_1 \\
&+ 24s_2 A_2 r_2^3\nu_c^2 B_1 + 24s_2 r_2^2 a\nu_c\xi A_2 - 24s_2 r_2\eta_1\xi A_2 - 96s_2 r_2\xi^2 a A_2)\, e^{r_2 z} \\
&+ (24\xi r_2^3 s_2 c_{\mathrm{p}}\nu_c d + 12\xi^2 r_2^3 s_2 A_2^2 - 12\xi r_2^3 s_2 A_2^2\nu_c)\, e^{2r_2 z})\,/\,(-24s_2 r_2^3\nu_c\nu_c).
\end{aligned}$$

thus we obtain:

$$
\begin{aligned}
\Theta = & ((2r_2^3\xi^2 a^2 s_2 - r_2^3\xi a s_2\eta_1)z^4 + (4r_2^3 s_2\eta_1 B_1\nu_c - 4r_2^3 s_2\eta_1\xi A_1 \\
& - 8r_2^3 s_2\xi a B_1\nu_c + 8r_2^3 s_2\xi c_\mathrm{p}\nu_c c_2 - 4r_2^3 s_2 a^2\nu_c\xi + 8r_2^3 s_2\xi^2 a A_1)z^3 \\
& + (12r_2^3 s_2\xi^2 A_1^2 + 12r_2^3 s_2 a\nu_c^2 B_1 + 12r_2^3 s_2\eta_1 B_0\nu_c + 12r_2^3 s_2 B_1^2\nu_c^2 \\
& + 12r_2^3 s_2\xi c_\mathrm{p}\nu_c c_1 - 24r_2^3 s_2\xi A_1 B_1\nu_c - 12r_2^3 s_2 a\nu_c\xi A_1)z^2 + (12F_1 s_2 r_2^2)z \\
& + 12F_0 s_2 r_2^2 + (24\xi c_\mathrm{p}\nu_c r_2^3 E_2)\, e^{s_2 z} + ((24 s_2\xi r_2^2 c_\mathrm{p}\nu_c d_1 - 24 s_2\xi r_2^2 A_2\nu_c a \\
& + 48 s_2\xi^2 r_2 a A_2)z + 48 s_2 r_2\xi^2 A_1 A_2 - 48 s_2 r_2\xi A_2 B_1\nu_c - 24 s_2\xi c_\mathrm{p}\nu_c r_2 d_1 \\
& + 24 s_2\xi c_\mathrm{p}\nu_c r_2^2 d_0 - 24 s_2 A_2 r_2^2\nu_c\xi A_1 + 24 s_2 A_2 r_2^2\nu_c^2 B_1 + 24 s_2 r_2 a\nu_c\xi A_2 \\
& - 24 s_2\eta_1\xi A_2 - 96 s_2\xi^2 a A_2)\, e^{r_2 z} + (12\xi r_2^2 s_2 c_\mathrm{p}\nu_c d + 6\xi^2 r_2 s_2 A_2^2 \\
& - 6\xi r_2^2 s_2 A_2^2\nu_c)\, e^{2r_2 z}) \,/\, (-24 s_2 r_2^3\nu_c\upsilon_c).
\end{aligned}
\tag{B.8}
$$

Therefore, the general one-dimensional EUE solution for planar Poiseuille flows is:

$$
T = c_2 z^2 + c_1 z + (d_1 z + d_0)\, e^{r_2 z} + d\, e^{2r_2 z} + E_1 + E_2\, e^{s_2 z},
\tag{B.9}
$$

$$
u_1 = az + A_1 + A_2\, e^{r_2 z},
\tag{B.10}
$$

$$
\begin{aligned}
\Theta = & ((2r_2^3\xi^2 a^2 s_2 - r_2^3\xi a s_2\eta_1)z^4 + (4r_2^3 s_2\eta_1 B_1\nu_c - 4r_2^3 s_2\eta_1\xi A_1 \\
& - 8r_2^3 s_2\xi a B_1\nu_c + 8r_2^3 s_2\xi c_\mathrm{p}\nu_c c_2 - 4r_2^3 s_2 a^2\nu_c\xi + 8r_2^3 s_2\xi^2 a A_1)z^3 \\
& + (12r_2^3 s_2\xi^2 A_1^2 + 12r_2^3 s_2 a\nu_c^2 B_1 + 12r_2^3 s_2\eta_1 B_0\nu_c + 12r_2^3 s_2 B_1^2\nu_c^2 \\
& + 12r_2^3 s_2\xi c_\mathrm{p}\nu_c c_1 - 24r_2^3 s_2\xi A_1 B_1\nu_c - 12r_2^3 s_2 a\nu_c\xi A_1)z^2 + (12F_1 s_2 r_2^2)z \\
& + 12F_0 s_2 r_2^2 + (24\xi c_\mathrm{p}\nu_c r_2^3 E_2)\, e^{s_2 z} + ((24 s_2\xi r_2^2 c_\mathrm{p}\nu_c d_1 - 24 s_2\xi r_2^2 A_2\nu_c a \\
& + 48 s_2\xi^2 r_2 a A_2)z + 48 s_2 r_2\xi^2 A_1 A_2 - 48 s_2 r_2\xi A_2 B_1\nu_c - 24 s_2\xi c_\mathrm{p}\nu_c r_2 d_1 \\
& + 24 s_2\xi c_\mathrm{p}\nu_c r_2^2 d_0 - 24 s_2 A_2 r_2^2\nu_c\xi A_1 + 24 s_2 A_2 r_2^2\nu_c^2 B_1 + 24 s_2 r_2 a\nu_c\xi A_2 \\
& - 24 s_2\eta_1\xi A_2 - 96 s_2\xi^2 a A_2)\, e^{r_2 z} + (12\xi r_2^2 s_2 c_\mathrm{p}\nu_c d + 6\xi^2 r_2 s_2 A_2^2 \\
& - 6\xi r_2^2 s_2 A_2^2\nu_c)\, e^{2r_2 z}) \,/\, (-24 s_2 r_2^3\nu_c\upsilon_c),
\end{aligned}
\tag{B.11}
$$

$$
\chi_1 = -(\xi/\nu_c)(a/2)z^2 - (\xi/\nu_c)A_1 z - (\xi/\nu_c)(A_2/r_2)\, e^{r_2 z} + B_1 z + B_0,
\tag{B.12}
$$

where

$$r_2 \equiv \xi/\nu, \tag{B.13}$$

$$s_2 \equiv \xi c_{\mathrm{p}}/\nu, \tag{B.14}$$

$$a \equiv -\eta_1/\xi, \tag{B.15}$$

$$c_1 \equiv \nu a(\nu a - a\nu_c c_{\mathrm{p}} - B_1\nu_c c_{\mathrm{p}} + \xi A_1 c_{\mathrm{p}}) \, / \, (-\xi c_{\mathrm{p}}^2 \nu_c), \tag{B.16}$$

$$c_2 \equiv \nu a^2 \, / \, (-2c_{\mathrm{p}}\nu_c), \tag{B.17}$$

$$d_0 \equiv (\nu A_2/\nu_c)(-2ar_2\nu_c\nu + 2a\nu_c\xi c_{\mathrm{p}} - \nu a\xi + r_2\xi A_1\nu - \xi^2 A_1 c_{\mathrm{p}} - r_2 B_1\nu_c\nu + B_1\nu_c\xi c_{\mathrm{p}})$$
$$\, / \, (\nu^2 r_2^2 - 2\nu r_2\xi c_{\mathrm{p}} + \xi^2 c_{\mathrm{p}}^2), \tag{B.18}$$

$$d_1 \equiv (\nu a A_2\xi/\nu_c) \, / \, (\nu r_2 - \xi c_{\mathrm{p}}), \tag{B.19}$$

$$d \equiv (\nu A_2^2/\nu_c)(\xi - r_2\nu_c)/(4\nu r_2 - 2\xi c_{\mathrm{p}}) \tag{B.20}$$

and A_1, A_2, B_0, B_1, E_1, E_2, F_0, F_1 are the constants to be determined by the boundary conditions.

From $u_1'(0) = 0$ and $u_1(L) = 0$, we obtain:

$$A_1 = (-a/r_2)(r_2L - e^{r_2L}), \tag{B.21}$$

$$A_2 = (-a/r_2). \tag{B.22}$$

From $\chi_1(0) = 0$ and $\chi_1(L) = 0$, we obtain:

$$B_0 = \xi A_2/(\nu_c r_2), \tag{B.23}$$

$$B_1 = \xi(2A_1 L r_2 + 2A_2 e^{r_2L} + aL^2 r_2 - 2A_2)/(2L\nu_c r_2). \tag{B.24}$$

From $T'(0) = 0$ and $T(L) = T_0$, we obtain:

$$E_1 = (-1/s_2)(c_1 L s_2 + c_2 L^2 s_2 - T_0 s_2 - (c_1 + d_1 + d_0 r_2 + 2dr_2)\, e^{s_2L}$$
$$+ (d_0 s_2 + d_1 L s_2)\, e^{r_2L} + (ds_2)\, e^{2r_2L}), \tag{B.25}$$

$$E_2 = (-1/s_2)(c_1 + d_1 + d_0 r_2 + 2dr_2). \tag{B.26}$$

From $\Theta(0) = 0$ and $\Theta(L) = 0$, we obtain:

$$
\begin{aligned}
F_0 = (&-4\xi c_\mathrm{p}\nu_c r_2^3 E_2 - 8s_2 r_2 \xi^2 A_1 A_2 + 8s_2 r_2 \xi A_2 B_1 \nu_c + 4s_2 \xi c_\mathrm{p}\nu_c r_2 d_1 \\
&- 4s_2 \xi c_\mathrm{p}\nu_c r_2^2 d_0 + 4s_2 A_2 r_2^2 \nu_c \xi A_1 - 4s_2 A_2 r_2^2 \nu_c^2 B_1 - 4s_2 r_2 a\nu_c \xi A_2 \\
&+ 4s_2 \eta_1 \xi A_2 + 16 s_2 \xi^2 a A_2 - 2\xi r_2^2 s_2 c_\mathrm{p}\nu_c d - \xi^2 r_2 s_2 A_2^2 + \xi r_2^2 s_2 A_2^2 \nu_c) \\
&/ (2s_2 r_2^2),
\end{aligned}
\tag{B.27}
$$

$$
\begin{aligned}
F_1 = (&48 s_2 r_2 \xi A_2 B_1 \nu_c + 24 s_2 \xi c_\mathrm{p}\nu_c r_2 d_1 - 48 s_2 r_2 \xi^2 A_1 A_2 - 24 \xi c_\mathrm{p}\nu_c r_2^3 E_2 \\
&+ 6\xi r_2^2 s_2 A_2^2 \nu_c - 12 \xi r_2^2 s_2 c_\mathrm{p}\nu_c d - 24 s_2 r_2 a\nu_c \xi A_2 + 24 s_2 A_2 r_2^2 \nu_c \xi A_1 \\
&- 24 s_2 \xi c_\mathrm{p}\nu_c r_2^2 d_0 - 24 s_2 A_2 r_2^2 \nu_c^2 B_1 + 96 s_2 \xi^2 a A_2 + 24 s_2 \eta_1 \xi A_2 - 6\xi^2 r_2 s_2 A_2^2 \\
&- 24 r_2^3 L^2 s_2 \xi A_1 B_1 \nu_c - 12 r_2^3 L^2 s_2 a\nu_c \xi A_1 + 12 r_2^3 L^2 s_2 \xi c_\mathrm{p}\nu_c c_1 + 12 r_2^3 L^2 s_2 B_1^2 \nu_c^2 \\
&+ 12 r_2^3 L^2 s_2 a\nu_c^2 B_1 + 12 r_2^3 L^2 s_2 \eta_1 B_0 \nu_c + 12 r_2^3 L^2 s_2 \xi^2 A_1^2 + 8r_2^3 L^3 s_2 \xi^2 a A_1 \\
&- 4r_2^3 L^3 s_2 a^2 \nu_c \xi - r_2^3 \xi a L^4 s_2 \eta_1 - 4r_2^3 L^3 s_2 \eta_1 \xi A_1 + 4r_2^3 L^3 s_2 \eta_1 B_1 \nu_c \\
&- 8r_2^3 L^3 s_2 \xi a B_1 \nu_c + 2r_2^3 \xi^2 a^2 L^4 s_2 + 8r_2^3 L^3 s_2 \xi c_\mathrm{p}\nu_c c_2 + (24\xi c_\mathrm{p}\nu_c r_2^3 E_2)\, e^{s_2 L} \\
&+ (24 s_2 A_2 r_2^2 \nu_c^2 B_1 - 24 s_2 A_2 r_2^2 \nu_c \xi A_1 - 96 s_2 \xi^2 a A_2 - 24 s_2 \eta_1 \xi A_2 \\
&+ 24 s_2 r_2 a\nu_c \xi A_2 + 24 s_2 \xi r_2^2 L c_\mathrm{p}\nu_c d_1 - 24 s_2 \xi r_2^2 L A_2 \nu_c a + 48 s_2 \xi^2 r_2 L a A_2 \\
&- 24 s_2 \xi c_\mathrm{p}\nu_c r_2 d_1 + 48 s_2 r_2 \xi^2 A_1 A_2 + 24 s_2 \xi c_\mathrm{p}\nu_c r_2^2 d_0 - 48 s_2 r_2 \xi A_2 B_1 \nu_c)\, e^{r_2 L} \\
&+ (12 \xi r_2^2 s_2 c_\mathrm{p}\nu_c d + 6\xi^2 r_2 s_2 A_2^2 - 6\xi r_2^2 s_2 A_2^2 \nu_c)\, e^{2r_2 L}) / (-12 L s_2 r_2^2).
\end{aligned}
\tag{B.28}
$$

The case $\eta_1 = 0$ implies $a = c_1 = c_2 = d_1 = 0$ in (B.13)–(B.20), therefore (B.9)–(B.12) simplifies to:

$$
T = d_0\, e^{r_2 z} + d\, e^{2r_2 z} + E_1 + E_2\, e^{s_2 z},
\tag{B.29}
$$

$$
u_1 = A_1 + A_2\, e^{r_2 z},
\tag{B.30}
$$

$$
\begin{aligned}
\Theta = -(&(12 r_2^3 s_2 \xi^2 A_1^2 + 12 r_2^3 s_2 B_1^2 \nu_c^2 - 24 r_2^3 s_2 \xi A_1 B_1 \nu_c) z^2 + (12 F_1 s_2 r_2^2) z \\
&+ (12 F_0 s_2 r_2^2) + (24\xi c_\mathrm{p}\nu_c r_2^3 E_2)\, e^{s_2 z} + (48 s_2 r_2 \xi^2 A_1 A_2 - 48 s_2 r_2 \xi A_2 B_1 \nu_c \\
&+ 24 s_2 \xi c_\mathrm{p}\nu_c r_2^2 d_0 - 24 s_2 A_2 r_2^2 \nu_c \xi A_1 + 24 s_2 A_2 r_2^2 \nu_c^2 B_1)\, e^{r_2 z} \\
&+ (12 \xi r_2^2 s_2 c_\mathrm{p}\nu_c d + 6\xi^2 r_2 s_2 A_2^2 - 6\xi r_2^2 s_2 A_2^2 \nu_c)\, e^{2r_2 z}) / (24 s_2 r_2^3 \nu_c \upsilon_c),
\end{aligned}
\tag{B.31}
$$

$$
\chi_1 = -(\xi/\nu_c) A_1 z - (\xi/\nu_c)(A_2/r_2)\, e^{r_2 z} + B_1 z + B_0,
\tag{B.32}
$$

where

$$
r_2 \equiv \xi/\nu,
$$
$$
s_2 \equiv \xi c_\mathrm{p}/\upsilon,
$$
$$
d_0 \equiv (\nu A_2/\nu_c)(r_2 \xi A_1 \upsilon - \xi^2 A_1 c_\mathrm{p} - r_2 B_1 \nu_c \upsilon + B_1 \nu_c \xi c_\mathrm{p}) / (\upsilon^2 r_2^2 - 2\upsilon r_2 \xi c_\mathrm{p} + \xi^2 c_\mathrm{p}^2),
$$
$$
d \equiv -(\nu A_2^2/\nu_c)(r_2 \nu_c - \xi) / (4\upsilon r_2 - 2\xi c_\mathrm{p})
$$

and A_1, A_2, B_0, B_1, E_1, E_2, F_0, F_1 are the constants to be determined by the boundary conditions. This is the general one-dimensional EUE solution for planar Couette flows.

From $u_1(0) = 0$ and $u_1(L) = U_1$, we obtain:

$$A_1 = +U_1/(1 - e^{r_2 L}), \tag{B.33}$$
$$A_2 = -U_1/(1 - e^{r_2 L}). \tag{B.34}$$

From $\chi_1(0) = 0$ and $\chi_1(L) = 0$, we obtain:

$$B_0 = \xi A_2/(\nu_c r_2), \tag{B.35}$$
$$B_1 = \xi(A_1 L r_2 + A_2\, e^{r_2 L} - A_2)/(L\nu_c r_2). \tag{B.36}$$

From $T'(0) = 0$ and $T(L) = T_0$, we obtain:

$$E_1 = (1/s_2)(T_0 s_2 - d_0 s_2\, e^{r_2 L} - d s_2\, e^{2r_2 L} + (r_2 d_0 + 2r_2 d)\, e^{s_2 L}), \tag{B.37}$$
$$E_2 = (-r_2/s_2)(d_0 + 2d). \tag{B.38}$$

From $\Theta(0) = 0$ and $\Theta(L) = 0$, we obtain:

$$\begin{aligned}
F_0 = &(-4\xi c_{\mathrm{p}}\nu_c r_2^3 E_2 - 8s_2 r_2 \xi^2 A_1 A_2 + 8s_2 r_2 \xi A_2 B_1 \nu_c - 4s_2 \xi c_{\mathrm{p}}\nu_c r_2^2 d_0 \\
&+ 4s_2 A_2 r_2^2 \nu_c \xi A_1 - 4s_2 A_2 r_2^2 \nu_c^2 B_1 - 2\xi r_2^2 s_2 c_{\mathrm{p}}\nu_c d - \xi^2 r_2 s_2 A_2^2 + \xi r_2^2 s_2 A_2^2 \nu_c) \\
&/ (2s_2 r_2^2),
\end{aligned} \tag{B.39}$$

$$\begin{aligned}
F_1 = &(-24\xi c_{\mathrm{p}}\nu_c r_2^3 E_2 + 12 r_2^3 L^2 s_2 \xi^2 A_1^2 + 12 r_2^3 L^2 s_2 B_1^2 \nu_c^2 - 24 r_2^3 L^2 s_2 \xi A_1 B_1 \nu_c \\
&- 12\xi r_2^2 s_2 c_{\mathrm{p}}\nu_c d - 24 s_2 \xi c_{\mathrm{p}}\nu_c r_2^2 d_0 + 24 s_2 A_2 r_2^2 \nu_c \xi A_1 - 24 s_2 A_2 r_2^2 \nu_c^2 B_1 \\
&+ 48 s_2 r_2 \xi A_2 B_1 \nu_c - 48 s_2 r_2 \xi^2 A_1 A_2 + 6\xi r_2^2 s_2 A_2^2 \nu_c - 6\xi^2 r_2 s_2 A_2^2 \\
&+ (24\xi c_{\mathrm{p}}\nu_c r_2^3 E_2)\, e^{s_2 L} + (24 s_2 \xi c_{\mathrm{p}}\nu_c r_2^2 d_0 - 48 s_2 r_2 \xi A_2 B_1 \nu_c + 48 s_2 r_2 \xi^2 A_1 A_2 \\
&+ 24 s_2 A_2 r_2^2 \nu_c^2 B_1 - 24 s_2 A_2 r_2^2 \nu_c \xi A_1)\, e^{r_2 L} + (12\xi r_2^2 s_2 c_{\mathrm{p}}\nu_c d - 6\xi r_2^2 s_2 A_2^2 \nu_c \\
&+ 6\xi^2 r_2 s_2 A_2^2)\, e^{2r_2 L}) / (-12 L s_2 r_2^2).
\end{aligned} \tag{B.40}$$

Appendix C. Derivation of the stationary one-dimensional EUE solution for Ekman flows

We derive the general solution of the linear system with constant coefficients (A.14)–(A.17).

In terms of the deviation $\tilde{\mathbf{u}} \equiv \mathbf{u} - \mathbf{U}$ from the geostrophic field $\mathbf{U} \equiv (-\frac{\eta_2}{2\Omega}, +\frac{\eta_1}{2\Omega}, 0)$, the system reads:

$$\nu\tilde{u}_1'' - \xi\tilde{u}_1' + 2\Omega\tilde{u}_2 = 0, \tag{C.1}$$

$$\nu\tilde{u}_2'' - \xi\tilde{u}_2' - 2\Omega\tilde{u}_1 = 0, \tag{C.2}$$

$$\nu_c\chi_1'' + \xi\tilde{u}_1' + 2\Omega\chi_2 = 0, \tag{C.3}$$

$$\nu_c\chi_2'' + \xi\tilde{u}_2' - 2\Omega\chi_1 = 0. \tag{C.4}$$

Eqs. (C.1) and (C.2) give an homogeneous linear system with constant coefficients. $\boldsymbol{\alpha}_k e^{kz}$ is a non-trivial solution of this system only if $\nu k^2 - \xi k + 2\Omega\,\mathrm{i} = 0$ (in which case $\alpha_{k,2} = +\mathrm{i}\,\alpha_{k,1}$) or $\nu k^2 - \xi k - 2\Omega\,\mathrm{i} = 0$ (in which case $\alpha_{k,2} = -\mathrm{i}\,\alpha_{k,1}$). That is, only if:

$$k = \left(\xi \pm (\xi^2 - \mathrm{i}\,8\nu\Omega)^{1/2}\right) / (2\nu) = \left(\xi \pm (\xi^4 + (8\nu\Omega)^2)^{1/4}\,e^{-\mathrm{i}\,\mathrm{arc\,tan}(8\nu\Omega/\xi^2)/2}\right) / (2\nu)$$

or

$$k = \left(\xi \pm (\xi^2 + \mathrm{i}\,8\nu\Omega)^{1/2}\right) / (2\nu) = \left(\xi \pm (\xi^4 + (8\nu\Omega)^2)^{1/4}\,e^{+\mathrm{i}\,\mathrm{arc\,tan}(8\nu\Omega/\xi^2)/2}\right) / (2\nu).$$

Let

$$k_1 \equiv \left(\xi + (\xi^4 + (8\nu\Omega)^2)^{1/4}\,e^{-\mathrm{i}\,\mathrm{arc\,tan}(8\nu\Omega/\xi^2)/2}\right) / (2\nu) = r_1 + \mathrm{i}\,m_1,$$

$$k_2 \equiv \left(\xi + (\xi^4 + (8\nu\Omega)^2)^{1/4}\,e^{+\mathrm{i}\,\mathrm{arc\,tan}(8\nu\Omega/\xi^2)/2}\right) / (2\nu) = r_1 - \mathrm{i}\,m_1,$$

$$k_3 \equiv \left(\xi - (\xi^4 + (8\nu\Omega)^2)^{1/4}\,e^{-\mathrm{i}\,\mathrm{arc\,tan}(8\nu\Omega/\xi^2)/2}\right) / (2\nu) = r_2 + \mathrm{i}\,m_2,$$

$$k_4 \equiv \left(\xi - (\xi^4 + (8\nu\Omega)^2)^{1/4}\,e^{+\mathrm{i}\,\mathrm{arc\,tan}(8\nu\Omega/\xi^2)/2}\right) / (2\nu) = r_2 - \mathrm{i}\,m_2,$$

where

$$r_1 \equiv \left(\xi + (\xi^4 + (8\nu\Omega)^2)^{1/4}\,\cos(\mathrm{arc\,tan}(8\nu\Omega/\xi^2)/2)\right) / (2\nu),$$

$$m_1 \equiv \;\; -(\xi^4 + (8\nu\Omega)^2)^{1/4}\,\mathrm{sen}(\mathrm{arc\,tan}(8\nu\Omega/\xi^2)/2)\; / (2\nu),$$

$$r_2 \equiv \left(\xi - (\xi^4 + (8\nu\Omega)^2)^{1/4}\,\cos(\mathrm{arc\,tan}(8\nu\Omega/\xi^2)/2)\right) / (2\nu),$$

$$m_2 \equiv \;\; +(\xi^4 + (8\nu\Omega)^2)^{1/4}\,\mathrm{sen}(\mathrm{arc\,tan}(8\nu\Omega/\xi^2)/2)\; / (2\nu).$$

Here, one has $k_2 = \bar{k}_1$ and $k_4 = \bar{k}_3$. These numbers are distinct $(\nu, \Omega, \xi \neq 0)$, thus the functions $e_i \equiv e^{k_i z}$ are linearly independent, and therefore $\boldsymbol{\alpha}_{k_1} e^{k_1 z} + \boldsymbol{\alpha}_{k_2} e^{k_2 z} + \boldsymbol{\alpha}_{k_3} e^{k_3 z} + \boldsymbol{\alpha}_{k_4} e^{k_4 z}$ is the general solution of (C.1)–(C.2). Taking into account that $e_2 = \bar{e}_1$ and $e_4 = \bar{e}_3$, one has that $\tilde{\mathbf{u}} \equiv \boldsymbol{\alpha}_{k_1} e^{k_1 z} + \boldsymbol{\alpha}_{k_2} e^{k_2 z} + \boldsymbol{\alpha}_{k_3} e^{k_3 z} + \boldsymbol{\alpha}_{k_4} e^{k_4 z}$ is real only if $\boldsymbol{\alpha}_{k_2} = \bar{\boldsymbol{\alpha}}_{k_1}$ and $\boldsymbol{\alpha}_{k_4} = \bar{\boldsymbol{\alpha}}_{k_3}$. Therefore, we write $\alpha_{k_1,1} \equiv (a_1 - \mathrm{i}\,b_1)/2$, $\alpha_{k_3,1} \equiv (a_2 - \mathrm{i}\,b_2)/2$, and use $\alpha_{k_1,2} = +\mathrm{i}\,\alpha_{k_1,1}$, $\alpha_{k_3,2} = +\mathrm{i}\,\alpha_{k_3,1}$, to obtain:

$$\tilde{u}_1 = (a_1\cos(m_1 z) + b_1\,\mathrm{sen}(m_1 z))\,e^{r_1 z} + (a_2\cos(m_2 z) + b_2\,\mathrm{sen}(m_2 z))\,e^{r_2 z}, \tag{C.5}$$

$$\tilde{u}_2 = (b_1\cos(m_1 z) - a_1\,\mathrm{sen}(m_1 z))\,e^{r_1 z} + (b_2\cos(m_2 z) - a_2\,\mathrm{sen}(m_2 z))\,e^{r_2 z}. \tag{C.6}$$

Taking into account (C.5) and (C.6), Eqs. (C.3) and (C.4) give a non-homogeneous linear system with constant coefficients. We write

$$-\xi\tilde{u}_1' = (c_1 \cos(m_1 z) + d_1 \,\mathrm{sen}(m_1 z))\, e^{r_1 z} + (c_2 \cos(m_2 z) + d_2 \,\mathrm{sen}(m_2 z))\, e^{r_2 z},$$
$$-\xi\tilde{u}_2' = (d_1 \cos(m_1 z) - c_1 \,\mathrm{sen}(m_1 z))\, e^{r_1 z} + (d_2 \cos(m_2 z) - c_2 \,\mathrm{sen}(m_2 z))\, e^{r_2 z},$$

with $c_i \equiv -\xi(a_i r_i + b_i m_i)$ and $d_i \equiv -\xi(b_i r_i - a_i m_i)$, and use that

$$(e \cos(mz) + f \,\mathrm{sen}(mz))e^{rz},$$
$$(f \cos(mz) - e \,\mathrm{sen}(mz))e^{rz},$$

is a particular solution of the system

$$\nu_c \chi_1'' + 2\Omega \chi_2 = (c \cos(mz) + d \,\mathrm{sen}(mz))e^{rz},$$
$$\nu_c \chi_2'' - 2\Omega \chi_1 = (d \cos(mz) - c \,\mathrm{sen}(mz))e^{rz},$$

if, and only if,

$$e = (c\nu_c r^2 - 2md\nu_c r - m^2 c\nu_c - 2d\Omega) \,/\, (\nu_c^2 r^4 + 2\nu_c^2 m^2 r^2 + 4\Omega^2 + 8\nu_c rm\Omega + \nu_c^2 m^4),$$
$$f = (2c\Omega - \nu_c m^2 d + 2c\nu_c rm + \nu_c r^2 d) \,/\, (\nu_c^2 r^4 + 2\nu_c^2 m^2 r^2 + 4\Omega^2 + 8\nu_c rm\Omega + \nu_c^2 m^4),$$

to obtain that

$$\chi_{1p} \equiv (e_1 \cos(m_1 z) + f_1 \,\mathrm{sen}(m_1 z))\, e^{r_1 z} + (e_2 \cos(m_2 z) + f_2 \,\mathrm{sen}(m_2 z))\, e^{r_2 z},$$
$$\chi_{2p} \equiv (f_1 \cos(m_1 z) - e_1 \,\mathrm{sen}(m_1 z))\, e^{r_1 z} + (f_2 \cos(m_2 z) - e_2 \,\mathrm{sen}(m_2 z))\, e^{r_2 z},$$

is a particular solution of (C.3)–(C.4) if, and only if,

$$e_i = (c_i \nu_c r_i^2 - 2m_i d_i \nu_c r_i - m_i^2 c_i \nu_c - 2d_i \Omega) \,/\, (\nu_c^2 r_i^4 + 2\nu_c^2 m_i^2 r_i^2 + 4\Omega^2 + 8\nu_c r_i m_i \Omega + \nu_c^2 m_i^4),$$
$$f_i = (2c_i \Omega - \nu_c m_i^2 d_i + 2c_i \nu_c r_i m_i + \nu_c r_i^2 d_i) \,/\, (\nu_c^2 r_i^4 + 2\nu_c^2 m_i^2 r_i^2 + 4\Omega^2 + 8\nu_c r_i m_i \Omega + \nu_c^2 m_i^4).$$

$\boldsymbol{\alpha}_k e^{kz}$ is a non-trivial solution of the homogeneous part of the system (C.3)–(C.4) only if $\nu_c k^2 + 2\Omega\,\mathrm{i} = 0$ (in which case $\alpha_{k,2} = +\mathrm{i}\,\alpha_{k,1}$) or $\nu_c k^2 - 2\Omega\,\mathrm{i} = 0$ (in which case $\alpha_{k,2} = -\mathrm{i}\,\alpha_{k,1}$), that is, only if

$$k = \pm(-\mathrm{i}\,2\Omega/\nu_c)^{1/2} = \pm(2\Omega/\nu_c)^{1/2}\, e^{-\mathrm{i}\,\pi/4}$$

or

$$k = \pm(+\mathrm{i}\,2\Omega/\nu_c)^{1/2} = \pm(2\Omega/\nu_c)^{1/2}\, e^{+\mathrm{i}\,\pi/4}.$$

One proceeds as for $\tilde{\mathbf{u}}$ to obtain that the general solution of the homogeneous part of (C.3)–(C.4) reads:

$$\chi_{1h} = (g_1 \cos(n_1 z) + h_1 \,\mathrm{sen}(n_1 z))\, e^{s_1 z} + (g_2 \cos(n_2 z) + h_2 \,\mathrm{sen}(n_2 z))\, e^{s_2 z},$$
$$\chi_{2h} = (h_1 \cos(n_1 z) - g_1 \,\mathrm{sen}(n_1 z))\, e^{s_1 z} + (h_2 \cos(n_2 z) - g_2 \,\mathrm{sen}(n_2 z))\, e^{s_2 z},$$

where

$$s_1 \equiv +(2\Omega/\nu_c)^{1/2} \cos(\pi/4) = +(4\Omega/\nu_c)^{1/2}/2,$$
$$n_1 \equiv -(2\Omega/\nu_c)^{1/2} \operatorname{sen}(\pi/4) = -(4\Omega/\nu_c)^{1/2}/2,$$
$$s_2 \equiv -(2\Omega/\nu_c)^{1/2} \cos(\pi/4) = -(4\Omega/\nu_c)^{1/2}/2,$$
$$n_2 \equiv +(2\Omega/\nu_c)^{1/2} \operatorname{sen}(\pi/4) = +(4\Omega/\nu_c)^{1/2}/2.$$

As $\chi_i = \chi_{ip} + \chi_{ih}$, we obtain:

$$
\begin{aligned}
\chi_1 &= (e_1 \cos(m_1 z) + f_1 \operatorname{sen}(m_1 z))\, e^{r_1 z} + (e_2 \cos(m_2 z) + f_2 \operatorname{sen}(m_2 z))\, e^{r_2 z} \\
&\quad + (g_1 \cos(n_1 z) + h_1 \operatorname{sen}(n_1 z))\, e^{s_1 z} + (g_2 \cos(n_2 z) + h_2 \operatorname{sen}(n_2 z))\, e^{s_2 z}, \quad \text{(C.7)} \\
\chi_2 &= (f_1 \cos(m_1 z) - e_1 \operatorname{sen}(m_1 z))\, e^{r_1 z} + (f_2 \cos(m_2 z) - e_2 \operatorname{sen}(m_2 z))\, e^{r_2 z} \\
&\quad + (h_1 \cos(n_1 z) - g_1 \operatorname{sen}(n_1 z))\, e^{s_1 z} + (h_2 \cos(n_2 z) - g_2 \operatorname{sen}(n_2 z))\, e^{s_2 z}. \quad \text{(C.8)}
\end{aligned}
$$

Therefore, the general one-dimensional EUE solution for Ekman flows is:

$$u_1 = U_1 + (a_1 \cos(m_1 z) + b_1 \operatorname{sen}(m_1 z)) e^{r_1 z} + (a_2 \cos(m_2 z) + b_2 \operatorname{sen}(m_2 z)) e^{r_2 z}, \quad \text{(C.9)}$$
$$u_2 = U_2 + (b_1 \cos(m_1 z) - a_1 \operatorname{sen}(m_1 z)) e^{r_1 z} + (b_2 \cos(m_2 z) - a_2 \operatorname{sen}(m_2 z)) e^{r_2 z}, \quad \text{(C.10)}$$

$$
\begin{aligned}
\chi_1 &= (e_1 \cos(m_1 z) + f_1 \operatorname{sen}(m_1 z))\, e^{r_1 z} + (e_2 \cos(m_2 z) + f_2 \operatorname{sen}(m_2 z))\, e^{r_2 z} \\
&\quad + (g_1 \cos(n_1 z) + h_1 \operatorname{sen}(n_1 z))\, e^{s_1 z} + (g_2 \cos(n_2 z) + h_2 \operatorname{sen}(n_2 z))\, e^{s_2 z}, \quad \text{(C.11)} \\
\chi_2 &= (f_1 \cos(m_1 z) - e_1 \operatorname{sen}(m_1 z))\, e^{r_1 z} + (f_2 \cos(m_2 z) - e_2 \operatorname{sen}(m_2 z))\, e^{r_2 z} \\
&\quad + (h_1 \cos(n_1 z) - g_1 \operatorname{sen}(n_1 z))\, e^{s_1 z} + (h_2 \cos(n_2 z) - g_2 \operatorname{sen}(n_2 z))\, e^{s_2 z}, \quad \text{(C.12)}
\end{aligned}
$$

where

$$r_1 \equiv \left(\xi + (\xi^4 + (8\nu\Omega)^2)^{1/4} \cos(\text{arc tan}(8\nu\Omega/\xi^2)/2)\right) / (2\nu), \tag{C.13}$$

$$m_1 \equiv \quad -(\xi^4 + (8\nu\Omega)^2)^{1/4} \text{ sen}(\text{arc tan}(8\nu\Omega/\xi^2)/2) \; / \; (2\nu), \tag{C.14}$$

$$r_2 \equiv \left(\xi - (\xi^4 + (8\nu\Omega)^2)^{1/4} \cos(\text{arc tan}(8\nu\Omega/\xi^2)/2)\right) / (2\nu), \tag{C.15}$$

$$m_2 \equiv \quad +(\xi^4 + (8\nu\Omega)^2)^{1/4} \text{ sen}(\text{arc tan}(8\nu\Omega/\xi^2)/2) \; / \; (2\nu), \tag{C.16}$$

$$c_i \equiv -\xi(a_i r_i + b_i m_i), \tag{C.17}$$

$$d_i \equiv -\xi(b_i r_i - a_i m_i), \tag{C.18}$$

$$e_i \equiv (c_i \nu_c r_i^2 - 2m_i d_i \nu_c r_i - m_i^2 c_i \nu_c - 2d_i\Omega)$$
$$/ \; (\nu_c^2 r_i^4 + 2\nu_c^2 m_i^2 r_i^2 + 4\Omega^2 + 8\nu_c r_i m_i \Omega + \nu_c^2 m_i^4), \tag{C.19}$$

$$f_i \equiv (2c_i\Omega - \nu_c m_i^2 d_i + 2c_i \nu_c r_i m_i + \nu_c r_i^2 d_i)$$
$$/ \; (\nu_c^2 r_i^4 + 2\nu_c^2 m_i^2 r_i^2 + 4\Omega^2 + 8\nu_c r_i m_i \Omega + \nu_c^2 m_i^4), \tag{C.20}$$

$$s_1 \equiv +(4\Omega/\nu_c)^{1/2}/2, \tag{C.21}$$

$$n_1 \equiv -(4\Omega/\nu_c)^{1/2}/2, \tag{C.22}$$

$$s_2 \equiv -(4\Omega/\nu_c)^{1/2}/2, \tag{C.23}$$

$$n_2 \equiv +(4\Omega/\nu_c)^{1/2}/2 \tag{C.24}$$

and a_1, b_1, a_2, b_2, g_1, h_1, g_2, h_2 are the constants to be determined by the boundary conditions. Here, we remind that

$$\cos(\text{arc tan}(x)) = 1/(1 + x^2)^{1/2}, \tag{C.25}$$

$$\text{sen}(\text{arc tan}(x)) = x/(1 + x^2)^{1/2}, \tag{C.26}$$

and that

$$\cos(\text{arc tan}(x)/2) = ((1 + \cos(\text{arc tan}(x)))/2)^{1/2}, \tag{C.27}$$

$$\text{sen}(\text{arc tan}(x)/2) = \text{sen}(\text{arc tan}(x))/(2\cos(\text{arc tan}(x)/2)). \tag{C.28}$$

From $u_1(0) = 0$, $u_2(0) = 0$, $u_1(L) = U_1$ and $u_2(L) = U_2$, we obtain:

$$a_1 = +\big(U_1\, e^{L(r_1+r_2)} - (U_1 \tan(m_2L)^2 - 2U_2 \tan(m_2L))\, e^{L(r_1+r_2)} - U_1(\tan(m_2L)^2 + 1)\, e^{2r_2L}\big)$$
$$/\ (2(\tan(m_2L)^2 - 1)\, e^{L(r_1+r_2)} + (\tan(m_2L)^2 + 1)(e^{2r_1L} + e^{2r_2L})), \tag{C.29}$$

$$b_1 = +\big(U_2\, e^{L(r_1+r_2)} - (U_2\tan(m_2L)^2 + 2U_1\tan(m_2L))\, e^{L(r_1+r_2)} - U_2(\tan(m_2L)^2 + 1)\, e^{2r_2L}\big)$$
$$/\ (2(\tan(m_2L)^2 - 1)\, e^{L(r_1+r_2)} + (\tan(m_2L)^2 + 1)(e^{2r_1L} + e^{2r_2L})), \tag{C.30}$$

$$a_2 = -\big(U_1(\tan(m_2L)^2 + 1)\, e^{r_1L} + (U_1 \tan(m_2L)^2 + 2U_2 \tan(m_2L) - U_1)\, e^{r_2L}\big)\, e^{r_1L}$$
$$/\ (2(\tan(m_2L)^2 - 1)\, e^{L(r_1+r_2)} + (\tan(m_2L)^2 + 1)(e^{2r_1L} + e^{2r_2L})), \tag{C.31}$$

$$b_2 = -\big(U_2(\tan(m_2L)^2 + 1)\, e^{r_1L} + (U_2 \tan(m_2L)^2 - 2U_1 \tan(m_2L) - U_2)\, e^{r_2L}\big)\, e^{r_1L}$$
$$/\ (2(\tan(m_2L)^2 - 1)\, e^{L(r_1+r_2)} + (\tan(m_2L)^2 + 1)(e^{2r_1L} + e^{2r_2L})), \tag{C.32}$$

where $r_1 + r_2 = \xi/\nu$.

From $\chi_1(0) = 0$, $\chi_2(0) = 0$, $\chi_1(L) = 0$ and $\chi_2(L) = 0$, we obtain:

$$g_1 = (e_1 + e_2 - 2(e_1 + e_2)\cos(nL)^2 - 2(f_1 + f_2)\cos(nL)\mathrm{sen}(nL) + (e_1 + e_2)\, e^{-2sL}$$
$$+ (e_1\cos((m-n)L) - f_1\mathrm{sen}((m-n)L))\, e^{L(s+r_1)} + (f_1\mathrm{sen}((m+n)L) - e_1\cos((m+n)L))\, e^{L(r_1-s)}$$
$$+ (e_2\cos((m+n)L) + f_2\mathrm{sen}((m+n)L))\, e^{L(s+r_2)} - (e_2\cos((m-n)L) + f_2\mathrm{sen}((m-n)L))\, e^{L(r_2-s)})e^{-2sL}$$
$$/\ (-1 - e^{-4sL} - 2(1 - 2\cos(nL)^2)\, e^{-2sL}), \tag{C.33}$$

$$h_1 = (f_1 + f_2 - 2(f_1 + f_2)\cos(nL)^2 + 2(e_1 + e_2)\cos(nL)\mathrm{sen}(nL) + (f_1 + f_2)\, e^{-2sL}$$
$$+ (e_1\mathrm{sen}((m-n)L) + f_1\cos((m-n)L))\, e^{L(s+r_1)} - (e_1\mathrm{sen}((m+n)L) + f_1\cos((m+n)L))\, e^{L(r_1-s)}$$
$$+ (f_2\cos((m+n)L) - e_2\mathrm{sen}((m+n)L))\, e^{L(s+r_2)} + (e_2\mathrm{sen}((m-n)L) - f_2\cos((m-n)L))\, e^{L(r_2-s)})e^{-2sL}$$
$$/\ (-1 - e^{-4sL} - 2(1 - 2\cos(nL)^2)\, e^{-2sL}), \tag{C.34}$$

$$g_2 = (e_1 + e_2 + (e_1 + e_2 + 2(f_1 + f_2)\cos(nL)\mathrm{sen}(nL) - 2(e_1 + e_2)\cos(nL)^2)\, e^{-2sL}$$
$$+ (f_1\mathrm{sen}((m-n)L) - e_1\cos((m-n)L))\, e^{L(r_1-s)} + (e_1\cos((m+n)L) - f_1\mathrm{sen}((m+n)L))\, e^{L(r_1-3s)}$$
$$- (e_2\cos((m+n)L) + f_2\mathrm{sen}((m+n)L))\, e^{L(r_2-s)} + (e_2\cos((m-n)L) + f_2\mathrm{sen}((m-n)L))\, e^{L(r_2-3s)})$$
$$/\ (-1 - e^{-4sL} - 2(1 - 2\cos(nL)^2)\, e^{-2sL}), \tag{C.35}$$

$$h_2 = (f_1 + f_2 + (f_1 + f_2 - 2(e_1 + e_2)\cos(nL)\mathrm{sen}(nL) - 2(f_1 + f_2)\cos(nL)^2)\, e^{-2sL}$$
$$- (e_1\mathrm{sen}((m-n)L) + f_1\cos((m-n)L))\, e^{L(r_1-s)} + (e_1\mathrm{sen}((m+n)L) + f_1\cos((m+n)L))\, e^{L(r_1-3s)}$$
$$+ (e_2\mathrm{sen}((m+n)L) - f_2\cos((m+n)L))\, e^{L(r_2-s)} + (f_2\cos((m-n)L) - e_2\mathrm{sen}((m-n)L))\, e^{L(r_2-3s)})$$
$$/\ (-1 - e^{-4sL} - 2(1 - 2\cos(nL)^2)\, e^{-2sL}), \tag{C.36}$$

where $m \equiv m_2$, $n \equiv n_2$ and $s \equiv s_1$.

References

[1] D.J. ACHESON, *Elementary fluid dynamics*, Oxford, 1990

[2] P. BRADSHAW, *Understanding and prediction of turbulent flow - 1996*, Int. J. of Heat and Fluid Flow, 18 (1997) 45-54

[3] D.R. CALDWELL, C.W. VAN ATTA, *Characteristics of Ekman boundary layer instabilities*, J. of Fluid Mechanics, 44 (1970) 79-90

[4] A.J. CHORIN, O.H. HALD, R. KUPFERMAN, *Optimal prediction with memory*, Physica D, 166:3-4 (2002) 239-257

[5] A.J. CHORIN, A.P. KAST, R. KUPFERMAN, *Unresolved computation and optimal predictions*, Comm. Pure App. Math., 52:10 (1999) 1231-1254

[6] A.J. CHORIN, A.P. KAST, R. KUPFERMAN, *Optimal prediction of underresolved dynamics*, Proc. Nat. Acad. Sci. USA, 95:8 (1998) 4094-4098

[7] S.R. DE GROOT, P. MAZUR, *Non-equilibrium thermodynamics*, Dover, 1984

[8] A.J. FALLER, *An experimental study of the instability of the laminar Ekman boundary layer*, J. of Fluid Mechanics, 15:4 (1962) 560-576

[9] U. FRISCH, *Turbulence*, Cambridge Univ. Press, 1995

[10] P. GLANSDORFF, I. PRIGOGINE, *Thermodynamic theory of structure, stability and fluctuations*, Wiley, 1971

[11] D. KONDEPUDI, I. PRIGOGINE, *Modern thermodynamics: from heat engines to dissipative structures*, Wiley, 1999

[12] P.R. KRAMER, A.J. MAJDA, E. EIJNDEN, *Closure approximations for passive scalar turbulence: a comparative study on an exactly solvable model with complex features*, 2002, to appear in J. of Stat. Phys.

[13] L.D. LANDAU, E.M. LIFSHITZ, *Fluid mechanics*, Butterworth-Heinemann, 2000, 2nd ed.

[14] W.D. MCCOMB, *The physics of fluid turbulence*, Oxford Univ. Press, 1990

[15] F.R. MENTER, *A comparison of some recent eddy-viscosity turbulence models*, Trans. of ASME, 118 (1996), 514-519

[16] J. NIKURADSE, *Strömungsgesetze in rauhen Rohren*, Forschg. Arb. Ing.-Wes., 361 (1933)

[17] H. REICHARDT, *Über die Geschwindigkeitsverteilung in einer geradlinigen turbulenten Couette-Strömung*, ZAMM, 36 (1956), S26-S29

[18] P. SAGAUT, *Large Eddy Simulation for incompressible flows*, Springer-Verlag, 2001

[19] H. SCHLICHTING, *Boundary-layer theory*, McGraw-Hill, 1979

[20] J.C.R. HUNT, N.D. SANDHAM, J.C. VASSILICOS, B.E. LAUNDER, P.A. MONKEWITZ, G.F. HEWITT, *Developments in turbulence research: a review based on the 1999 Programme of the Isaac Newton Institute, Cambridge*, J. of Fluid Mechanics, 436 (2001), 353-391

[21] G.B. WHITHAM, *Linear and nonlinear waves*, Wiley, 1974

IMPA-OS, ESTR. DONA CASTORINA 110, RIO DE JANEIRO/RJ, 22460-320 (BRAZIL)
E-mail address: krause@fluid.impa.br